ASSESSMENT OF THE RELATIONSHIP BETWEEN THE SPILLED LNAPL VOLUME AND ITS THICKNESS IN MONITORING WELLS CONSIDERING THE WATER TABLE FLUCTUATION HISTORY

BY

Muhammad Saleem

A Dissertation Presented to the

DEANSHIP OF GRADUATE STUDIES

KING FAHD UNIVERSITY OF PETROLEUM & MINERALS

DHAHRAN, SAUDI ARABIA

In Partial Fulfillment of the

Requirements for the Degree of

DOCTOR OF PHILOSOPHY

In

CIVIL ENGINEERING

March, 2005

KING FAHD UNIVERSITY OF PETROLEUM AND MINERALS
DHAHRAN, SAUDI ARABIA

COLLEGE OF GRADUATE STUDIES

This dissertation, written by **Muhammad Saleem** under the direction of his dissertation advisor, and approved by his dissertation committee, has been presented to and accepted by the Dean of the College of Graduate Studies, in partial fulfillment of the requirements for the degree of

Doctor of Philosophy in Civil Engineering

(Water Resources & Environmental Engineering)

Dissertation Committee

Dr. Mohammad S. Al-Suwaiyan (Chairman)

Dr. Saad Ali Aiban (Member)

Dr. Rashid I. Allayla (Member)

Dr. M.H. Al-Malack (Member)

Dr. Mahbub Hussain (Member)

Prof. H. I. Al-Abdul Wahhab
Chairman, Dept. of Civil Engineering

Dr. M. Abdulaziz Al-Ohali
Dean, College of Graduate Studies

Date 1427/2/17

24-5-2005

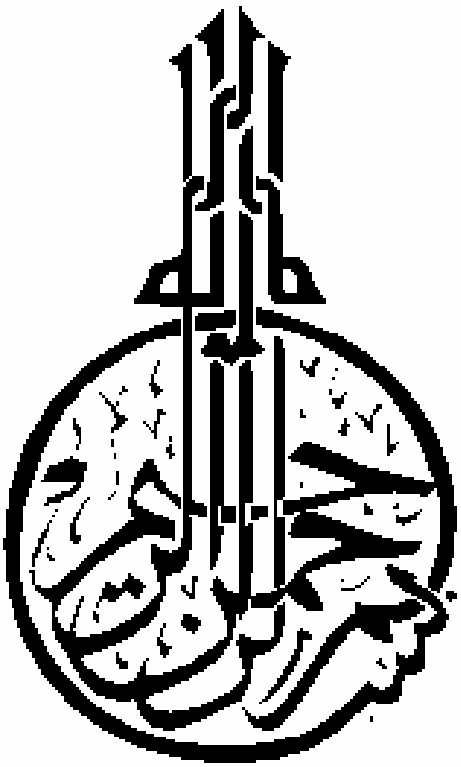

This dissertation is dedicated to

My Beloved Parents, Wife and Sons

ACKNOWLEDGMENTS

All praise and thanks be to **ALLAH**, the Almighty, the Most Gracious, the Most Merciful, for all the blessings and mercies He has bestowed upon me and Peace be upon His Prophet.

I would like to express my gratitude and appreciation to my advisor Dr. Mohamad S. Al-Suwaiyan for his invaluable guidance, support and encouragement during the course of this work. I highly acknowledge the cooperation, encouragement and useful suggestions from my dissertation committee members Dr. Saad A. Aiban, Dr. Muhammad H. Al-Malack, Dr. Rashid I. Allayla, and Dr. Mahbub Hussain.

Acknowledgement is due to the Department of Civil Engineering, King Fahd University of Petroleum and Minerals for providing me with a warm atmosphere and continuous support to carry out this research. I am also grateful to King AbdulAziz City for Science and Technology (KACST) for the financial support provided under Project No. AR-22-91. I should acknowledge the Pakistan Atomic Energy Commission (PAEC) for granting me leave for higher studies.

My sincere thanks are due to Dr. Hammad I. Al-AbdulWahhab, Chairman of the Department for his enlightening advice and support. I would like to extend my thanks to the faculty and staff of the Civil Engineering Department for their help in making my stay during this research a memorable one.

Sincere thanks are due to Mr. Muhammad Fareed Kandlawala for his support and help throughout this work. I should like to thank Mr. Saad bin Mansoor for his help in the programming part. Special thanks are due to Mr. Mohammad H. Essa for his help which was available to me round the clock. I sincerely thank all my friends and well-wishers for their support and encouragement during my studies at KFUPM.

Profound thanks are due to my mother, wife and children for their never ending love, support, understanding and encouragement. Praise be to **ALLAH** for blessing me with such a family.

TABLE OF CONTENT

LIST OF TABLES

LIST OF FIGURES

LIST OF PLATES

الخلاصة

أسم الطالب : محمد سليم

عنوان الرسالة : دراسة العلاقة بين كمية المركبات العضوية الخفيفة غير الذائبة (LNAPL) وسماكتها داخل آبار المراقبة مع أخذ تغير منسوب المياه في الاعتبار.

القسم : الهندسة المدنية

التخصص : هندسة مصادر مياه وبيئة

تاريخ التخرج : مارس ٢٠٠٥م

تعتبر عملية تقدير كمية الهيدروكربونات غير الذائبة في البيئة المسامية هي الخطوة الأولى في سلسلة عملية معالجة التربة والمياه الجوفية، وبما أن منسوب المياه وسمك الهيدروكربونات في آبار المراقبة هما البيانان المتوفران في الحقل لتقييم مدى التلوث، ونظراً لعدم وجود علاقة بين كمية الهيدروكربونات المنسكبة وسمكها في آبار المراقبة التي تكون مناسيب المياه فيها غير مستقرة، فإن هناك حاجة ماسة لدراسة تأثير تغير منسوب المياه على سمك الهيدروكربونات المنسكبة، ولذا تم تطوير نموذج رياضي لتمثيل هذه الظاهرة يدمج تغير مناسيب المياه و التخلف والانحباس، كما أجريت تجارب مخبرية للحصول على بيانات سمك الهيدروكربونات في آبار المراقبة تحت تأثير منسوب مياه متغير. فقد أجريت أربعة تجارب باستخدام نوعين من البيئة المسامية مع الكيروسين والديزل، واستخدمت هذه النتائج لمعايرة النموذج الرياضي. كما قورنت النتائج المتحصلة من المحاكاة بتلك المتحصلة من التجارب المخبرية والمنشورة.

ولقد أظهرت التجارب الأربعة أحجام انسكاب حرجة قدرت بـ ٤,٨و٤,٣و٤,١٥و٣,٩سم٣/سم٢ على التوالي، كما قورنت نتائج الاختبارات على أساس هيدروستاتيكي مع النتائج المنشورة المقدرة من نماذج مختلفة. وأظهرت نتائج المقارنة على أساس الخطأ المئوي أن النموذج الرياضي المطور هو أفضل متنبئ لجميع التجارب (حيث بلغت نسبة الخطأ المئوي ٥,٨% إلى ١٠,٧% و ٣,٧ % إلى ١٩,٧% و ٠,٦% إلى ٦,١% و ١,٦% إلى ١٠% على التوالي)، وأن إدماج تغير منسوب المياه في نموذج الانحباس المتخلف له تأثير كبير على التنبؤات، كما أن تغير السطح البيني للهيدروكربونات والمياه الأرضية يرتبط عكسياً مع سمك الهيدروكربونات في آبار المراقبة، كما وجد أن أعلى كمية للهيدروكربونات تكون مع أدنى مستوى لمنسوب المياه والعكس صحيح، وأظهرت النتائج أن تنبؤات النموذج متوافقة مع القياسات المخبرية كما أعطت النموذج نتائج عالية في مدى ١٦,٢% إلى ٨٥,١% و ٧,٩% إلى ٤٧,٢% و ٦,٤% إلى ٧٠,٣% و ٦,٧% إلى ٤٣,٤% في جميع الحالات الأربعة على التوالي، كما وجد أن حساسية النموذج لمسامية الرمل وكثافة الـ (LNAPL) متدنية جداً مما يجعل استخدام النموذج موثوقاً.

درجة الدكتوراه في العلوم الهندسية
جامعة الملك فهد للبترول والمعادن
الظهران- المملكة العربية السعودية

DISSERTATION ABSTRACT

NAME: MUHAMMAD SALEEM

TITLE: ASSESSMENT OF THE RELATIONSHIP BETWEEN THE SPILLED LNAPL VOLUME AND ITS THICKNESS IN MONITORING WELLS CONSIDERING THE WATER TABLE FLUCTUATION HISTORY

MAJOR FIELD: CIVIL ENGINEERING (WATER RESOURCES & ENVIRONMENTAL ENGINEERING)

DATE OF DEGREE: MARCH 2005

The quantification of spilled hydrocarbon is of vital importance and is a first step in the remediation hierarchy. In most cases, watertable elevation and hydrocarbon thickness are the primary field data available to enable the evaluation of the extent of hydrocarbon contamination. However, because of the unavailability of relationship between the spilled hydrocarbon and its thickness in the monitoring wells under dynamic water table conditions, there is a marked paucity of research considering fluctuating water table conditions. A mathematical model was developed to predict the extent of hydrocarbon contamination. Developed model incorporates the water table fluctuation history, hysteresis, and entrapment. An experimental setup was utilized to obtain data on hydrocarbon thickness with the fluctuated water table conditions. The data obtained from the study were used to validate the mathematical model. In the experimental program four runs were performed: Uniform sand and well-graded sand were used with diesel and kerosene. Simulation results using the developed model were compared with experimental as well as results reported in the literature.

Critical spilled volumes noted for all four runs were 4.8, 4.3, 4.15, and 3.9 cm^3/cm^2, respectively. Comparison of experimental results based on hydrostatic conditions with the results predicted by different models reported in the literature were also performed. Comparison on the basis of percentage error shows that the developed mathematical model is the best predictor in all four cases (with percentage error of 5.8 to 10.7%, 3.7 to 19.7%, 0.6 to 6.1%, and 1.6 to 10.0% respectively). Inclusion of water table fluctuation history in a hysteretic entrapment model was shown to have an impact on the predictions. Hydrocarbon/groundwater interface fluctuations correlate inversely with the hydrocarbon thickness in monitoring wells. It was noted that the amount of hydrocarbon in the monitoring well was at a maximum when the water table elevation was at its historically low value, and vice versa. Comparison with experimental results results shows that the model predictions are in close agreement with the experimental data. The model over predicted the results in the range of 16.2 to 85.1%, 7.9 to 47.2%, 6.4 to 70.3%, and 6.7 to 43.4% in all four cases respectively. It was found that the sensitivity of the developed model with sand porosity and LNAPL density is quite low. Making the use of the model more reliable.

DOCTOR OF PHILOSOPHY DEGREE
KING FAHD UNIVERSITY OF PETROLEUM AND MINERALS
DHAHRAN, SAUDI ARABIA

CHAPTER 1

INTRODUCTION

Intentional and unintentional release of hydrocarbons into the soil and subsurface pose a great threat to the biosphere environment. Some of the most common and most damaging types of groundwater contaminants are immiscible liquids. Nonaqueous Phase Liquids (NAPLs), the hydrocarbons which are the major source of contamination, that exist as a separate, immiscible phase when they come into contact with water and/or air. Nonaqueous phase liquids (NAPL) are typically classified as either: 1) Light Nonaqueous Phase Liquids (LNAPLs; such as common fuels) have densities less than that of water, or 2) Dense Nonaqueous Phase Liquids (DNAPLs; such as heavy crude oil) have densities greater than that of water. Seepage of these contaminants into the vadose zone poses a great threat to the environment especially to groundwater quality. Serious contamination of groundwater and soil leads to health, economical, and social problems (Hoag and Marley 1986; Borden and Kao, 1992).

1.1 Hazards Associated with Hydrocarbon Contamination

The major environmental health and safety problems associated with hydrocarbon discharge to the subsurface environment are soil and groundwater pollution and fire and explosion hazards (Hall and Quam, 1976)). Hydrocarbon products are typically multi-

component organic mixtures composed of chemicals with varying degree of water solubility. Some additives such as methyl tertiary-butyl ether and alcohols are highly soluble (Hoag and Marley 1986; Ali 2002). On the other hand, components such as benzene, toluene, ethylbenzene, and xylenes are slightly soluble in water. In general, NAPLs represent potential long-term sources for continued groundwater contamination at many sites (Osgood, 1974). Almost all of the components are carcinogenic and some at least have some adverse health effects (Haskell 1997; Ali 2002). In addition, contaminated water may not be used for human and animal consumption. Furthermore, this water may not be suitable even for irrigation purposes. The contaminated soil and groundwater pose a constant aesthetic problem and decrease the economic value of land (Rubin *et al.* 1998).

In may parts of the world, especially in oil producing countries, soil and groundwater contamination due to hydrocarbon spills is increasing at an alarming rate (Osgood 1974; Nodak 1998; Ahmad *et al* 2002). An example of intentional spill of hydrocarbon is shown in plate 1.1 (Aiban 1998), where crude oil is being used for soil stabilization in the Dammam area, which may eventually contaminate the subsurface.

In the Kingdom of Saudi Arabia a large number of underground fuel storage tanks were installed during the massive development of the past three decades. Most of the fuel storage tanks have exceeded their design life or have started leaking because of improper installation. These underground storage tanks are a potential source of soil and groundwater contamination in the Kingdom (Al-Suwaiyan *et al*. 2003). An example of a

Plate 1.1 An example of crude oil spraying to stabilize the embankment near Dammam city (Aiban 1998)

Plate 1.2 A photograph showing contaminated ground water and soil due to a leaking underground fuel storage tank in Dammam, Saudi Arabia (source Dr. Aiban, special collection)

leaking underground storage tank is presented in plate 1.2 where gasoline and diesel are leaking from an underground storage tank in the Dammam city area.

1.2 Importance of the Quantification of Spilled Hydrocarbon Volume

Once a spill of LNAPL is discovered, it is required that an estimate is made of magnitude and extent of the contamination caused. The quantification of spilled volume is of primary importance in the remediation work and considered as the first step in the remediation hierarchy. Installation of monitoring wells across the spill site is a common practice. If the volume of LNAPL appearing in the monitoring well and the vertical hydraulic gradients are not large, the accumulated thickness of LNAPL can be a reasonable source of information for estimating the actual spilled volume. However, the ground water table is always in a transient state and under transient conditions, physical equilibrium may never be reached. In fluctuating water table conditions one may not be able to relate the LNAPL thickness in the monitoring well with the actual spilled volume.

1.3 Problem Definition and Objectives

The primary objective of this study was to assess the relationship between LNAPL thickness in the observation wells and specific spilled volume taking into account the history of water table fluctuation. Though different analytical and quantitative methods have been developed for free product estimate in spills under constant water table conditions, there has been a marked paucity of research regarding fluctuating water table conditions. Therefore, this study focuses on the development and

verification of a model, based on well-established theories, which can help in studying the relationship between LNAPL thickness in observation wells and LNAPL in the adjacent formation taking into account the history of water table fluctuation. The developed model will help to predict the extent of hydrocarbon contamination more accurately and reliably. An experimental program was designed as shown in figure 1.1, to predict the experimental estimates of spilled hydrocarbon and its thickness in monitoring wells in relation to water table fluctuations. Data obtained was utilized to compare with the simulated results obtained from the developed model predictions. Data reported in the literature was also utilized for comparison and verification of model predictions. More specifically, the objectives of the study were:

1. To develop a model that incorporates the aquifer hydrostatics and porous media properties. Established theories of LNAPL transport in porous media will also be utilized wherever needed.
2. To incorporate the water table fluctuations history, hysteresis and entrapment in the developed model to obtain a better estimate of spilled LNAPL volumes.
3. To utilize a laboratory experimental set-up and the obtained data on LNAPL product thickness under the influence of water table fluctuation. The data obtained from the laboratory study will be used to validate the analytical model.
4. To compare the simulation results and experimental data with the results reported in the literature.

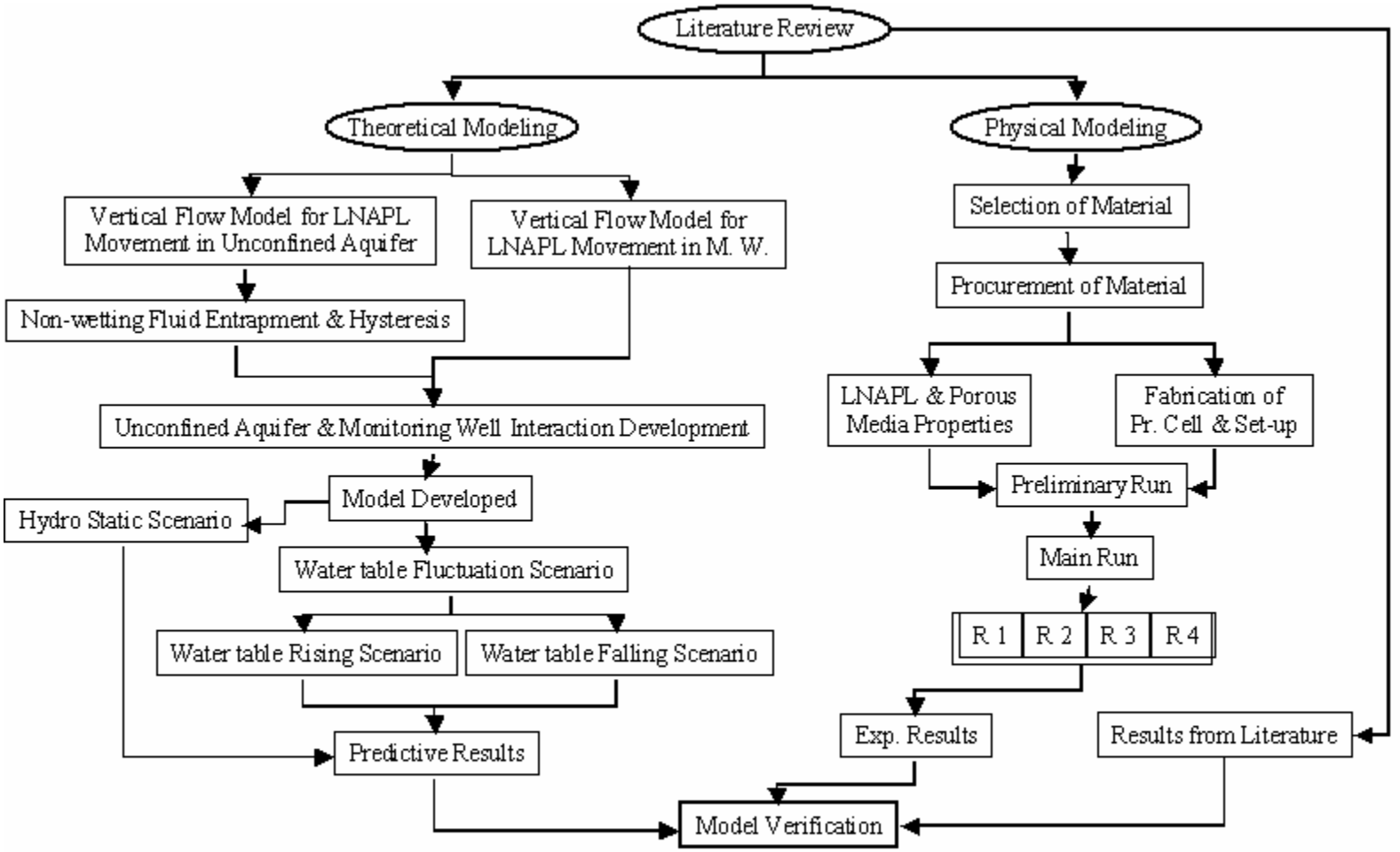

Figure 1.1 Different phases and tasks of the study.

CHAPTER 2

LITERATURE REVIEW

2.1 General

Estimation of Light Nonaqueous Phase Liquid (LNAPL) volumes in the soil and groundwater is the first and most crucial step in the remediation hierarchy. Usually this step dictates the type and extent of the recovery and remediation techniques that can be efficiently utilized. Inaccurate volume estimates can lead to unrealistic expectations of recoverable contamination, poor determination of liability and inaccurate cost estimation for the remediation work (Lundegard and Mudford, 1998; Sharma, 2000).

2.2 Quantification of Spilled Hydrocarbon Volume

Generally, one of the most important variables to be determined at any hydrocarbon spill site is the amount of product lost. This quantity largely governs whether the site needs remediation or not. Quantification of the original amount of spilled hydrocarbon requires knowledge of several concepts such as two and three phase relations, aquifer hydraulics, porous media properties (e.g. texture, pore size distribution, heterogeneity, and the presence of other fluids). A clear understanding of the phase distribution and movement of contaminants is critical to evaluate remedial decisions and volume quantification (Huling and Weaver, 1991).

In general, two methods are used to determine the spilled hydrocarbon volume: direct measurement in the field and prediction models employed by researchers. Exhaustive field measurements are not only costly but also tedious and time consuming. These methods require considerable effort in order to collect field data at regular intervals in space and time. Furthermore, precision of the measurement is limited by the precision of field instruments, and by degree of human error (Wickramanayake, *et al.* 1990b; Jaynes, 1992; Mualem, 1992). Therefore, in brief, current field measurement technology is time consuming, expensive, and often yields parameter estimates for only a narrow range of field conditions. However, the utilization of indirect approaches does not obviate the need for continued research toward improved direct methods.

In sharp contrast to direct measurement, relatively more attention is being paid to the development of indirect methods which predict the spilled volume from more easily measured data, including saturation pressure data, and hydrocarbon thickness data in the monitoring wells. It is fortunate that indirect methods are generally more convenient and far less costly to implement. Moreover, indirect methods often give estimates which may well be accurate enough, or are close to being accurate enough, for many applications.

2.2.1 Direct Methods

The most reliable way of estimating the large spills of hydrocarbon could be collecting soil samples at various points in space from various depths. The laboratory analysis will give the spatial hydrocarbon distribution. Integration of such hydrocarbon distribution gives the total spilled volume. Special consideration must be given to the

design of the monitoring wells and the collection of groundwater samples (Fetter 1992; Hess *et al.* 1992).

In the past, most of the field studies were based on direct measurements (Williams and Wilder, 1971; Hult, 1984; EPA, 1987). In several other studies, the purpose of direct measurement was the calibration of predictive models (Ostendorf *et al.,* 1993; Steffy, 1997; Aral and Liao, 2000; and Darnault *et al.*, 2001). In order to understand the phenomena more clearly laboratory experimental studies have been conducted on various vertical columns containing water and spilled oil. Water and oil content were measured at different elevations and time in order to determine the fluid profile in porous media. Results were compared with calculated distribution based on two-phase capillary pressure versus saturation data (Eckberg and Sunada, 1984; and Wickramanayake *et al.*, 1991).

Other methods include bail-down testing, extrapolation of free hydrocarbon thickness between monitoring points, contouring of thickness maps, extrapolation of geologic information, planimetering, and estimation of porosity, specific yield and retention. All of these are key factors used in ultimately determining the hydrocarbon volume determination in place (Testa and Paczkowski, 1989; Blake and Fryberger, 1983; Dragun, 1988; Kramer, 1981). However, there is potential hazard of increase in the vertical extent of contamination during drilling and well installation programs. Furthermore, hydrocarbon, contaminated soil and aquifer material, and vapors brought to the surface because of drilling operations, may lead to conditions which are potentially an ignition hazard. These operations may also expose drilling and sampling crews to the hazard of chemical exposure (Newell *et al.* 1995). Literature review shows that

researchers are more interested in indirect methods than direct methods. This may be due to the reasons mentioned earlier.

2.2.2 Indirect Methods

As there are difficulties involved in field measurements, considerable efforts have been made to develop simple algorithms for predicting spilled hydrocarbon volumes based on indirect methods. These approaches fall into two broad categories: first, physically based models that rely on some conceptual model of the properties of the porous media and hydrocarbons, second, empirical approaches that make no assumptions regarding the mechanisms of existing fluids and porous media.

The modeling of all processes involved in the contamination and reclamation of soil and groundwater is based on the appropriate quantification of the processes mentioned in previous sections. The ability to predict reliably and quantitatively the spilled volume of hydrocarbons in soil and groundwater is of vital importance. The incorporation of all phenomena and processes associated with hydrocarbon contamination and quantification is an extremely complicated task (Schuckman et al, 1997).

A number of researchers have used indirect approaches to determine hydraulic properties of unsaturated porous media, probably starting with Krumbein and Monk (1942). Some researchers used porous media and hydrocarbon properties to predict hydraulic properties of soils (Gupta and Larson, 1979; Arya and Paris, 1981). These

approaches were tested several times by other researchers according to their requirements (Haverkamp and Parlange, 1986; Mishra *et al.*, 1989; and Arya and Dierolf, 1992).

Mayer and Miller (1992) used porous media particle size properties to determine spilled hydrocarbon distribution in porous media. Similarly, Ryan and Dhir (1993), Huntley *et al.* (1994a, 1994b) and Parcher *et al.* (1995) extended research in this area. Busby *et al.* (1995) used hydrocarbon properties and studied their influence in their saturation-pressure relationship investigation. The literature survey revealed that most of the work on indirect approaches was done during the last two decades (table 1). The use of indirect methods for the determination of spilled hydrocarbon is still a promising area for interested researchers (Darnault *et al.*, 2001; Aral and Lio, 2002).

In most cases, water-table elevations and hydrocarbon thickness are the primary field data which are available at (almost) every field and may be used to evaluate the extent of hydrocarbon contamination (Farr *et al.,* 1990; Ballestero *et al.,* 1994; Marinelli and Durnford, 1996).

2.3 Quantification Based on the Measurement of LNAPL Thickness and Water Table Elevation in the Field

Historically, great efforts have been made to develop a relationship, which can predict the specific spill volume of hydrocarbon(s) in the porous media by using a readily available parameter in the field. Different empirical and theoretical models were developed to achieve this objective.

In estimating the spilled hydrocarbon volume in a formation, it is often assumed that there is a linear relationship between hydrocarbon thickness in the monitoring well and in the formation. This hypothesis is based on the key assumption that there is some sort of a physical equilibrium between these two phases (Parker 1987; Lenhard and Parker 1988; 1997; Kemblowski and Chiang, 1990; Liao and Aral 1999). Interpretation of hydrocarbon thickness data from observation wells, however, presents a number of difficulties. Since there is no capillary fringe in a monitoring well, hydrocarbon thickness in the well is usually larger than that in the formation, under equilibrium conditions (Van Dam, 1967; Testa and Winegardner, 1991). de Pastrovich *et al.* (1979) used a simple force balance subject to a number of simplifying assumptions and proposed that the measured LNAPL thickness in monitoring wells is approximately four times the thickness of the soil zone in which free hydrocarbon is observable.

Blake and Hall (1984) presented a simple relationship based on field observations as:

$$T_w = T_f + (x + h_a) \qquad (2.1)$$

Where T_w and T_f are the LNAPL thickness in the monitoring well and in the formation, respectively. Similarly x is the interface distance below the groundwater table, within the well and h_a is the free product distance to the groundwater table, within the formation.

Hall *et al.* (1984) investigated the relationship between oil thickness in porous media to the thickness of oil in an observation well by adding oil incrementally to sandy porous media packed in large scale laboratory boxes. Coarse, medium, and fine textured

sands were employed. After addition of a critical oil volume which increased as soil grain size diminished, a 1:1 relationship between soil hydrocarbon thickness and well hydrocarbon thickness was observed. Their observations did not agree with the relationship developed by de Pastrovich *et al.* (1979). Consequently, Hall *et al.* (1984) proposed that hydrocarbon thickness in soils could be estimated from well hydrocarbon thickness after applying a porous media dependent correction factor. They did not, however, propose any technique to evaluate the correction factor from basic soil properties.

In another laboratory investigation of the relationship between soil and well hydrocarbon thickness, Hampton and Miller (1988) found the relationship proposed by de Pastrovich *et al.* (1979) and Hall *et al.* (1984) to be inadequate for describing their experimental observations. The Equation developed by de Pastrovich *et al.* (1979) was found to yield crude order-of-magnitude approximations of mobile hydrocarbon thickness. Several other researchers (e.g. Schiegg, 1995; Testa and Paczkowski, 1989) also presented different relationships but found these inadequate for explaining the experimental results (Kramer, 1982; Hampton and Miller, 1988; Darnault *et al*., 2001).

Wagner *et al.* (1989) compared estimates using various techniques including simple and complex relationships, bail-down tests, and chemical analysis of soil samples. The study indicated that estimates from bail-down tests, analysis of soil samples from a test pit, a developmental hydrocarbon-sensing probe, and the relationship proposed by de Pastrovich *et al.* (1979) yielded comparable results at only one field site.

2.3.1 Study on Nonhysteretic Model

It is now well-established that the drying and imbibition curves for a soil will not be the same (A typical hysteretic fluid retention curve is presented in figure. 2.1.) because of the hysteresis which is a function of hydrocarbon and porous media properties such as grain geometry, contact angle between fluid and particles and entrapped air (Fetter, 1992). Farr *et al.* (1990) and Lenhard and Parker (1990) developed methods for evaluating the LNAPL volume in porous media under static conditions based on fluid and porous media properties and apparent LNAPL thickness. They, however, neglected the effect of hysteresis in their model. Farr et al (1990) gave the relationship as,

$$T_f = \phi(1 - S_r)D\left(T_w / D - 1\right) \tag{2.2}$$

$$\text{and} \quad D = h^{ow}{}_d / \Delta\rho - h^{ao}{}_d / \rho_o \tag{2.3}$$

Where ϕ is the porosity, S_r is the residual saturation, ρ_o is the density of LNAPL, $\Delta\rho$ is the difference in density between water and LNAPL, and $h^{ow}{}_d$ and $h^{ao}{}_d$ are the displacement heads of nonwetting to wetting fluids, respectively.

Based on the LNAPL thickness in the well these two studies developed similar analytical models for predicting the vertical saturation distribution of LNAPL in a homogeneous porous media. The major assumptions made by the above authors are:

1. Oil and water pressure distributions are assumed to be hydrostatic and air pressure is assumed to be atmospheric everywhere, implying that all fluids are in a static equilibrium.

2. Relationships between capillary pressure and saturation are nonhysteretic and described by the main drainage curves.
3. The effects of air entrapped by water, oil entrapped by water, and air entrapped by oil are negligible.

The zones delineated as a, b, and c in figure 2.2 pertain to air, oil, and water saturations, respectively and there is no entrapped phase. Thus, the figure indicates that the oil saturation at a particular elevation is equal to the difference between total liquid saturation and water saturation. Neglecting hysteresis and entrapment eliminates the effects of the previous saturation history and leads to a unique relationship between LNAPL thickness in a well (T_w) and the specific oil volume in the porous media (V_o).

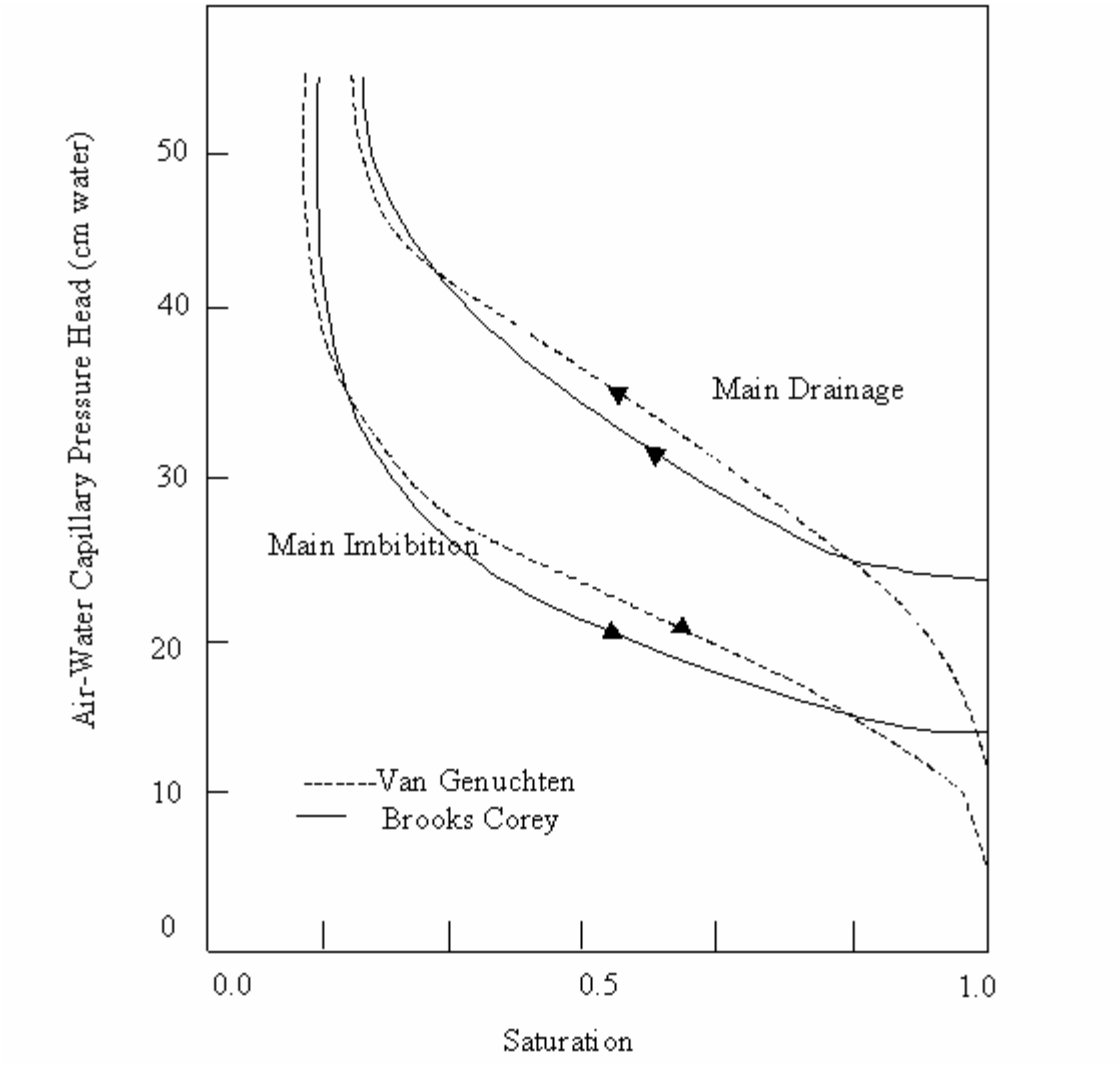

Figure 2.1. Typical hysteretic fluid retention curves (Marinelli and Durnford, 1996)

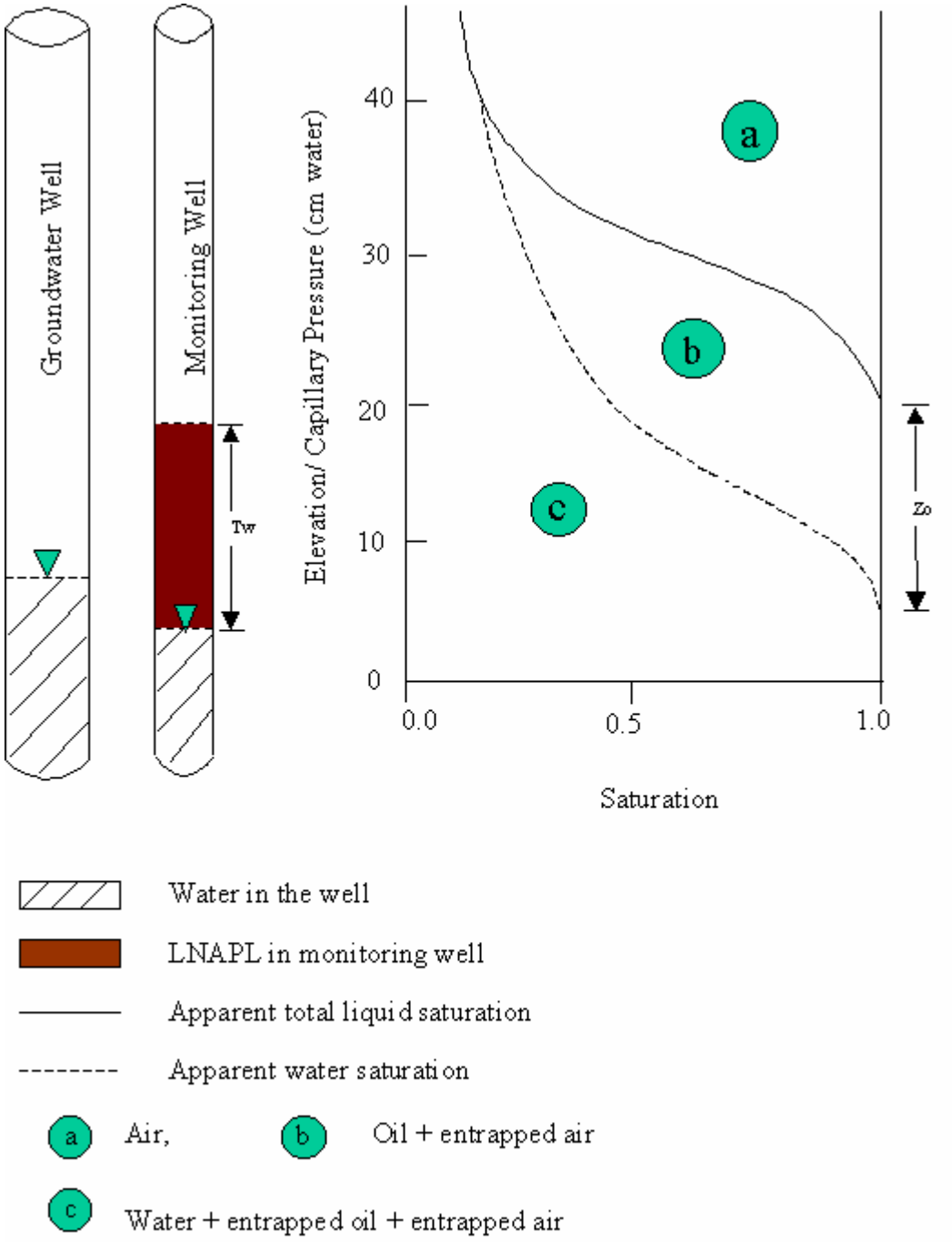

Fig. 2.2. Three phase fluid saturation versus elevation relationships (modified from Marinelli and Durnford, 1996)

The specific oil volume is the total volume of vertically distributed oil per unit planimetric area of the aquifer. Because specific oil volume has units of length, it is referred to in some literature as the LNAPL thickness or product thickness in the formation (Marinelli and Durnford, 1996). However, V_o is more properly thought of as an oil volume per unit area and does not represent the physical thickness of the formation over which oil is distributed.

In a controlled study, Wickramanayake *et al.* (1991) compared the methods proposed by de Pastrovich *et al.*, (1979), Hall *et al.* (1984), and Lenhard and Parker (1990) to estimate LNAPL volume from a known release. In this study the method proposed by Lenhard and Parker (1990) provided the best estimate of LNAPL release after the system had reached equilibrium. However, all estimates were within an order of magnitude of the actual release volume. Huntly *et al.* (1994a; 1994b) studied the relationship between the LNAPL thickness in the monitoring well and specific spilled volume in the formation and reported uncertainty in this method.

Liao and Aral (1999) developed a model based on the analytical solution of volumetric equilibrium equations for constant residual saturation levels. Therefore, the model represented only estimates of hydraulic equilibrium conditions at a contaminated site. They developed a relation as

$$r_w^2 \frac{dh_w(t)}{dt} = \frac{2K_w}{\ln\left(\frac{r_e}{r_w}\right)} E(t)\,[z(t)+h(t)-H-(1-\rho_r)\,h_w(t)] \qquad (2.4)$$

Where $h_w(t)$, $z(t)$ and $h(t)$ represent the LNAPL thickness in the monitoring well, water table elevation and LNAPL thickness in the formation, respectively. Finally they concluded that the physical equilibrium models ignoring the effect of ground water table fluctuations are not a reliable tool to estimate LNAPL volume at a spill site.

2.3.2 Lenhard Hysteresis /Entrapment Algorithms

Lenhard (1992) presented a comprehensive set of algorithms for computing fluid saturation in a porous media considering saturation hysteresis and entrapment of nonwetting phases. The hysteretic saturation-pressure (S-P) model accounts for different contact angles associated with drainage and imbibition processes, irregular pore geometry, and entrapment of nonwetting fluid.

The model provides an algorithm for computing fluid saturation in two-phase (air-water) and three-phase (air-oil-water) systems based on soil and fluid properties. The effective saturation of water, oil and total liquid in than phase system may be given as

$$\bar{S}_w = \frac{S_w - S_r}{1 - S_r} \tag{2.5}$$

$$\bar{S}_o = \frac{S_o}{1 - S_r} \tag{2.6}$$

$$\bar{S}_a = \frac{S_a}{1 - S_r} \tag{2.7}$$

$$\bar{S}_t = \frac{S_w + S_o - S_w}{1 - S_r} \tag{2.8}$$

Where

$\overline{S_a}, \overline{S_w}, \overline{S_o}$ and $\overline{S_t}$ are three-phase effective saturation of air, water and NAPL and actual total liquid saturation. It is assumed that wetability decreases in the order water to oil to air.

As shown on figure 2.1, Lenhard defines *apparent water saturation* as equal to actual water saturation plus the saturation of air entrapped by water plus the saturation of oil entrapped by water. In addition, *apparent total liquid saturation* is equal to apparent water saturation plus continuous oil phase saturation plus the saturation of air entrapped by oil. Apparent saturation depends on current capillary pressure and previous saturation history. Prior to the introduction of oil, the porous media is a two-phase system and the apparent water saturation is controlled by the air-water capillary pressure. After the introduction of oil, the porous media becomes a three-phase system. Apparent water saturation is then assumed to be controlled by the oil-water capillary pressure and apparent total liquid saturation is controlled by the air-oil capillary pressure. Once oil has been introduced into a volume element of the medium, that element continues to behave as a three-phase system even if the oil subsequently drains to negligible saturation.

Apparent saturation is defined as the sum of the effective saturation of a continuous fluid phase and the effective saturation of any entrapped dissimilar fluids that may be occluded by the continuous fluid phase.

$$\overline{\overline{S}}_w = \overline{S}_w + \overline{S_{ot}} + \overline{S_{atw}} \tag{2.9}$$

$$\overline{\overline{S}}_t = \overline{S}_w + \overline{S_o} + \overline{S_{at}} \tag{2.10}$$

where $\bar{S}_{ot}$ is the effective entrapped NAPL saturation, $\bar{S}_{atw}$ is the effective entrapped air saturation that is occluded by water, and $\bar{S}_{at}$ is the effective total entrapped air saturation (either by water or NAPL).

The 'effective total entrapped' air saturation (i.e. occluded by NAPL and water) and the 'effective entrapped' air saturation occluded by water only for a given saturation path history could be predicted from following system of equations,

For $\bar{\bar{S}}_t^{min} > {}^{\Delta}\bar{S}_w^{aw}$

$$\bar{S}_{at} = \bar{S}_{arw}\left[\frac{\left(\bar{\bar{S}}_t^{min} - {}^{\Delta}\bar{S}_w^{aw}\right)}{\left(1 - {}^{\Delta}\bar{S}_w^{aw}\right)}\right] + \bar{S}_{aro}\left[\frac{\left(\bar{\bar{S}}_t - \bar{\bar{S}}_t^{min}\right)}{\left(1 - \bar{\bar{S}}_t^{min}\right)}\right] \tag{2.11}$$

and for $\bar{S}_t \geq \bar{\bar{S}}_t^{min}$

$$\bar{S}_{atw} = \bar{S}_{arw}\left[\frac{\left(\bar{\bar{S}}_t^{min} - {}^{\Delta}\bar{S}_w^{aw}\right)}{\left(1 - {}^{\Delta}\bar{S}_w^{aw}\right)}\right] + \bar{S}_{aro}\left[\frac{\left(\bar{\bar{S}}_w - \bar{\bar{S}}_t^{min}\right)}{\left(1 - \bar{\bar{S}}_t^{min}\right)}\right] \tag{2.12}$$

and for $\bar{\bar{S}}_t^{min} > \bar{\bar{S}}_w > {}^{\Delta}\bar{S}_w^{aw}$

$$\bar{S}_{atw} = \bar{S}_{arw}\left[\frac{\left(\bar{\bar{S}}_w - {}^{\Delta}\bar{S}_w^{aw}\right)}{\left(1 - {}^{\Delta}\bar{S}_w^{aw}\right)}\right] \tag{2.13}$$

and for $\bar{\bar{S}}_w \leq {}^{\Delta}\bar{S}_w^{aw}$

$$\bar{S}_{atw} = 0 \tag{2.14}$$

For $\bar{\bar{S}}_t^{min} \leq {}^{\Delta}\bar{S}_w^{aw}$

$$\bar{S}_{at} = \bar{S}_{aro}\left[\frac{\left(\bar{\bar{S}}_t^{min} - {}^{\Delta}\bar{S}_w^{aw}\right)}{(1-\bar{\bar{S}}_t^{min})}\right] \tag{2.15}$$

and for $\bar{\bar{S}}_w > \bar{\bar{S}}_t^{min}$

$$\bar{S}_{atw} = \bar{S}_{aro}\left[\frac{\left(\bar{\bar{S}}_w - \bar{\bar{S}}_t^{min}\right)}{\left(1-\bar{\bar{S}}_t^{min}\right)}\right] \tag{2.16}$$

and for $\bar{\bar{S}}_w \leq \bar{\bar{S}}_t^{min}$

$$\bar{S}_{atw} = 0 \tag{2.17}$$

Where

${}^{\Delta}\bar{S}_w^{aw}$ = effective water saturation in an air-water system at reversal point.

$\bar{S}_{atw}$ = effective entrapped air saturation in water phase.

$\bar{S}_{aro}$ = effective entrapped residual air saturation in LNAPL phase.

$\bar{\bar{S}}_t$ and $\bar{\bar{S}}_w$ = current apparent total liquid and water saturation, respectively.

The effective entrapped air saturation in NAPL '$\bar{S}_{ato}$' for any saturation path could be obtained from,

$$\bar{S}_{ato} = \bar{S}_{at} - \bar{S}_{atw} \tag{2.18}$$

There may be some entrapped air present within the trapped NAPL phase, resulting from air-water or air-NAPL interfaces. In order to account for concomitant entrapment of air and NAPL by NAPL-water interfaces, an 'effective total entrapped NAPL saturation $\bar{S}_{ott}$ ' may be defined by,

$$\bar{S}_{ott} = \bar{S}_{ot} + \bar{S}_{otw} + \bar{S}_{oto} \tag{2.19}$$

Where

$\bar{S}_{ot}$ = effective entrapped NAPL saturation.

$\bar{S}_{otw}$ = effective entrapped air saturation contained 'within the trapped NAPL' that resulted from air water interfaces.

$\bar{S}_{oto}$ = effective entrapped air saturation contained 'within the trapped NAPL' that resulted from air-NAPL interfaces.

The main retaining and drainage curves for apparent water saturation and apparent total liquid saturation are described by the van Genuchten (1980) saturation model in conjunction with the Parker *et al.* (1987) scaling theory. The main imbibition and drainage apparent saturation-capillary pressure branches were described respectively, by:

$$ {}^{I}S^{*}(h^{*}) = \left[1 + \left(\alpha^{I} h^{*}\right)^{h}\right]^{-m} \tag{2.20} $$

$$ {}^{D}S^{*}(h^{*}) = \left[1 + \left(\alpha^{D} h^{*}\right)^{h}\right]^{-m} \tag{2.21} $$

Where ${}^{I}\alpha\left[L^{-1}\right], {}^{D}\alpha\left[L^{-1}\right]$ and n are curve shape parameters with m = 1 – 1/n, S^{*} is either $\overline{\overline{S}}_{w}^{aw}$ in a two-phase system and $\overline{\overline{S}}_{w}$, or $\overline{\overline{S}}_{t}$ in a three-phase system. h^{*} is a scaled capillary pressure head represented as:

$$ \overline{\overline{S}}_{w}^{aw}\left(h_{aw}\right) = \overline{\overline{S}}_{w}^{aw}\left(\beta_{aw} h_{aw}\right) = S^{*}(h^{*}) \tag{2.22} $$

$$ \overline{\overline{S}}_{w}^{ow}\left(h_{ow}\right) = \overline{\overline{S}}_{w}^{ow}\left(\beta_{ow} h_{ow}\right) = S^{*}(h^{*}) \tag{2.23} $$

$$ \overline{\overline{S}}_{o}^{aw}\left(h_{ao}\right) = \overline{\overline{S}}_{o}^{aw}\left(\beta_{ao} h_{ao}\right) = S^{*}(h^{*}) \tag{2.24} $$

Prefatory superscripts ^{I} and ^{D} in equations (2.20) and (2.21) are used to denote main imbibition and drainage S-P branches, respectively.

Lenhard (1992) presented some algorithms for computing apparent saturations on scanning paths between the main retaining/drainage curves. For imbibition $S^{*}(h^{*})$ scanning paths, the main imbibition branch is scaled to pass through the appropriate reversal points to give:

$$ S^{*}(h^{*}) = \left[{}^{I}S^{*}(h^{*}) - {}^{I}S^{*}({}^{ID}h^{*})\right)\left({}^{DI}S^{*} - {}^{ID}S^{*}\right)\Big] $$

$$ \times\left[{}^{I}S^{*}({}^{DI}h^{*}) - {}^{I}S^{*}({}^{ID}h^{*})\right]^{-1} + {}^{ID}D^{*} \tag{2.25} $$

If, within a volume element, the Van Genuchten (VG) equation predicts the apparent total liquid saturation to be less than the water saturation, the algorithm will force the apparent total liquid saturation to be equal to the apparent water saturation. In

this case, the mobile oil saturation is zero and only immobile (entrapped) oil can exist within the volume element.

Apparent water saturation and apparent total liquid saturation are both assumed to approach the same irreducible saturation value at high capillary pressures. Irreducible saturation is therefore considered as a property of the porous media and is independent of fluid properties.

2.3.3 Hysteretic / Entrapment Model

Using the Lenhard (1992) algorithms, Marinelli and Durnford (1996) developed an analytical model to describe the distribution of fluid saturation considering the effects of hysteresis and non-wetting phase entrapment. The model was used to evaluate systems with fluctuating water tables and/or changes in specific oil volume.

Computations were performed by discretizing the soil profile into volume elements and using the Lenhard algorithms to compute air, oil, and water saturation within each element. In addition to the concepts discussed by the Lenhard (1992) in his algorithms, the hysteretic/entrapment model incorporates the following assumptions:

1. For a moving water table or variations in specific oil volume, fluid saturation distributions were modelled assuming a *succession* of hydrostatic pressure distributions (quasi-equilibrium approach).
2. Both the VG and BC capillary pressure vs. saturation relations were incorporated as model options. The latter represents an extension of the Lenhard algorithms.

3. Air-water, air-oil, and oil-water interfacial tensions were used to estimate the capillary pressure scaling factors.
4. During the first entry of oil into a volume element, it was assumed that apparent total liquid saturation is on its main imbibition curve and apparent water saturation is on its main drainage curve.
5. If it was predicted that all available oil in the soil profile is entrapped, the saturation distribution of (entrapped) oil remains fixed until conditions are reached where some of the oil is remobilised.

The uniform irreducible saturation assumed in the Lenhard algorithms implies that for the hydrostatic case, neither mobile nor entrapped oil can exist at relatively large distances above the water table. Any LNAPL originally present at these elevations is predicted to drain downward to elevations closer to the water table.

Uncertainty in the LNAPL thickness in monitoring wells was also studied by other researchers and the following observations were reported:

1. Monitoring wells may not contain observable LNAPL, even though soil sampling indicates significant LNAPL in the adjacent formation above and/or below the water table (Ballestero *et al.* 1994; Marinelli and Durnford in 1996).
2. LNAPL thickness in wells tends to decrease when the water table rises. However the thickness increases when the water table falls (Kemblowski and Chiang, 1988; Hunt *et al.*, 1989; Kemblowski and Chiang, 1990).
3. There can be sudden appearances or disappearances of LNAPL in monitoring wells across a site (Marinelli and Durnford in 1996).

4. If the water-table level drops below its previous range of fluctuation, LNAPL may disappear from monitoring wells (Marinelli and Durnford in 1996).

These uncertainties in the measurement of hydrocarbon thickness in monitoring wells forced interested researchers to probe more into the relation of hydrocarbon thickness with the dynamic behavior of the groundwater table. Recently, a numerical based model was developed by Aral and Liao (2002). The model simulates groundwater table dynamic conditions and its effects on LNAPL thickness in the monitoring well, and is based on volumetric equilibrium and multi-phase Darcian flow principles. They started from pressure head expressions for LNAPL/air and water/LNAPL as,

$$\mathrm{h_{oa}} = \frac{\mathrm{P_{oa}}}{\rho_{\mathrm{o}}\mathrm{g}}$$
$$\mathrm{h_{wo}} = \frac{\mathrm{P_{wo}}}{\rho_{\mathrm{w}}\mathrm{g}} \qquad (2.26)$$

Where $\mathrm{P_{oa}}$ and $\mathrm{P_{wo}}$ are capillary pressures at the LNAPL/air interface and water/LNAPL interface, respectively, ρ_o and ρ_w are the density of LNAPL and water phases, respectively, and g is the gravitational accelaration. They are defined from the Darcy law and the conservation of mass principle for the water phase,

$$-K_w k_{rw} \frac{\Phi_w - H}{\Phi_w} = f_w \frac{dZ_w}{dt} \qquad (2.27)$$

where K_w and k_{rw} are the saturated hydraulic conductivity and the dimensionless relative permeability of the water phase and f_w is the replaceable porosity of water, Φ_w and H are the initial and final water table elevations. Z_w is the water/LNAPL interface elevation.

The conservation of mass principle for the LNAPL phase yields the following relationship,

$$f_o \frac{dZ_o}{dt} + \frac{Q_o}{A_p} = f_w \frac{dZ_w}{dt} \tag{2.28}$$

where Q_o is the volumetric inflow rate of LNAPL to the monitoring well, A_p is the effective aerial distribution of the continuous LNAPL phase in the aquifer, and f_o is the replaceable porosity at the LNAPL/air interface. Then the rate of change of the water table elevation is given as,

$$\frac{dZ_w}{dt} = -\frac{K_w k_{rw}\left[\rho_r \Phi_o + (1-\rho_r)Z_w - h_{wo} - H\right]}{f_w\left[\rho_r \Phi_o + (1-\rho_r)Z_w - h_{wo}\right]} \tag{2.29}$$

The final equation they presented as,

$$\frac{d}{dt}\begin{bmatrix} Z_w \\ \Phi_o \\ D_o \end{bmatrix} = \begin{bmatrix} F_w(Z_w, \Phi_o)/\, f_w \\ [F_w(Z_w, \Phi_o) - \alpha F_o(Z_w, \Phi_o, D_o)]/\, f_o \\ \dfrac{dH(t)}{dt} + (1-\rho_r)\beta F_o(Z_w, \Phi_o, D_o) \end{bmatrix} \tag{2.30}$$

where, D_o is the LNAPL surface elevation in the monitoring well.

$$\alpha = \frac{\pi K f_o k_{ro}}{A_p \ln(1 + \Delta L / r_w)} \tag{2.31}$$

$$\text{and} \quad \beta = \frac{K f_o k_{ro}}{r^2{}_w \ln(1 + \Delta L / r_w)} \tag{2.32}$$

They concluded that the effect of capillary pressures, both at the water/LNAPL interface and LNAPL/air interface, has significant effects on the predictions. However, they did not come up with a quantitative model which can predict spilled LNAPL volume at a

given LNAPL thickness in a monitoring well. Van Geel and Roy (2002) proposed a model modified from Parker and Lenhard (1987) and Lenhard (1992). They incorporated a residual NAPL term into the previous model. A new parameter was introduced as, apparent total liquid saturation at the reversal point from primary wetting curve to a drainage curve (${}^{\Delta\Delta}\underline{\underline{S}}_t$). They assumed four types of formulations: linear, constrained and unconstrained exponential and one similar to the Land (1968) equation.

Linear: $$\underline{S}_{res}^{\max} = {}^{\Delta\Delta}\underline{S}_t^{D}\,\underline{S}_{res}^{\max} \tag{2.33}$$

Exponential (constrained): $$\underline{S}_{res}^{\max} = [1 - e^{-z^{\Delta\Delta S_t}}]\underline{S}_{res}^{\max} \tag{2.34}$$

Exponential (unconstrained): $$\underline{S}_{res}^{\max} = [1 - e^{-z^{\Delta\Delta S_t}}]\underline{S}_{res}^{fit} \tag{2.35}$$

Land : $$\underline{S}_{res}^{\max} = {}^{\Delta\Delta}\underline{\underline{S}}_t / [1 + {}^{D}R\,{}^{\Delta\Delta}\underline{\underline{S}}_t] \tag{2.36}$$

Where:

$\underline{S}_{res}^{\max}$ = effective maximum residual NAPL saturation based on total saturation reversal point

${}^{\Delta\Delta}\underline{S}_t^{Dt}$ = apparent total liquid saturation reversal point

z = fitting parameter for the constrained and unconstrained exponential equations

${}^{D}\underline{S}_{res}^{fit}$ = additional fitting parameter of the unconstrained expontial model

${}^{D}R = (1/{}^{D}\underline{S}_{res}^{\max}) - 1$

${}^{D}\underline{S}_{res}^{\max}$ = absolute maximum effective residual NAPL saturation

They concluded that the formation similar to that of Land (1968) for fluid entrapment was deemed to give a reasonable approximation of this relationship. The inclusion of a residual NAPL term in a predictive model will improve the prediction of NAPL distribution within the subsurface.

The literature review revealed that with the increase in environmental awareness, the increase in the study of soil and groundwater contamination has become the focus of numerous researchers. The literature reviewed here includes articles roughly from 1940 onwards. A qualitative presentation of reported work is shown in figure 2.3. The statistics of the articles examined are summarised in table 2.1.

It seems that a revolution in the investigation scheme has appeared in related literature. Investigators tackle the problem from different angles, and different analytical and quantitative methods have been developed for free product estimation in spills under constant water table conditions. However, there has been a marked paucity of research under dynamic water table conditions. There is a need for studying the relationship between hydrocarbon thickness in observation wells and hydrocarbon in the adjacent formation, taking into account the history of water table fluctuation along with entrapment, and hysteresis.

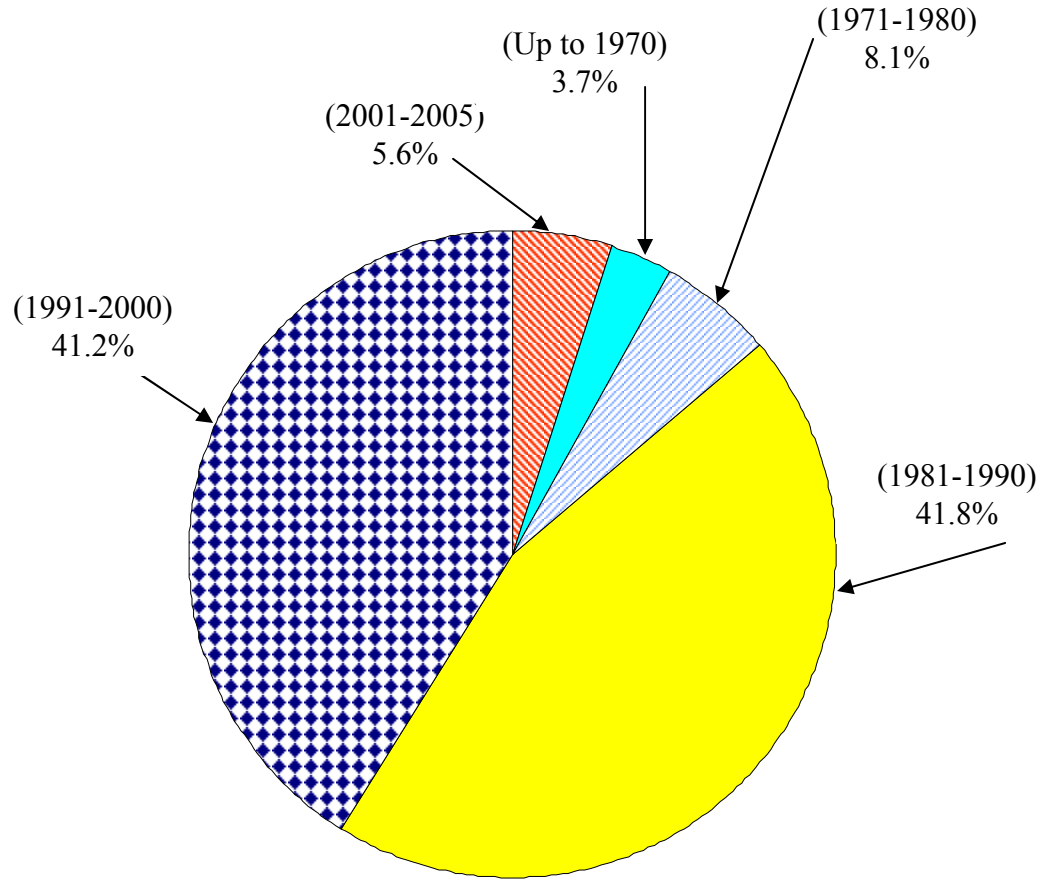

Figure 2.3. Summary of literature survey on spilled LNAPL volume estimation.

TABLE 2.1. Summary of the Literature Survey on Hydrocarbon Volume Estimation Studies by Category.

Research Area	**Up to 1970**	**1971-1980**	**1981-1990**	**1991-2000**	**2001-2005**
LNAPL transport through porous media: General overview	6	11	36	48	6
Quantification of spilled LNAPL volume: General overview	--	1	31	18	3
Direct methods	--	1	11	2	--
Indirect methods	--	--	20	16	3
A. Based on measurement of other parameters in the field.	--	--	14	5	1
B. Based on predictive models	--	--	6	11	2
a) Empirical	--	--	3	5	--
b) Analytical	--	--	1	4	1
c) Semi-analytical	--	--	2	2	1
Total = 160	**6**	**13**	**67**	**66**	**9**

2.4 Mathematical Modeling of the Process

In order to model the situation more accurately, it is essential to first understand the mechanisms and mode of movement of NAPL in the porous media where three phases (air, water and NAPL) exist. Saturation 'S' and pressure 'P' relationship in the porous media have also been widely used to model transient variably saturated fluid flow in soils. Due to the lack of simple experimental techniques to directly measure fluid saturation-pressure (S-P) relations of three-phase systems, functional relationships measured in two-phase NAPL-water and air-NAPL systems are commonly used to estimate fluid behaviour in air-NAPL-water systems. Experimental methods pertinent to the measurement of S-P relations in porous media with two fluid phases have been well-documented and are fairly simple to perform (Brooks and Corey, 1964; Corey, 1986; Scheidegger, 1974; Su and Brooks, 1980).

Leverett and Lewis (1941) suggested the extension of two-phase S-P relations to predict three-phase behaviour. In three-phase air-NAPL-water systems, in which water is the dominant wetting fluid, the total liquid saturation would thus be the function of air-NAPL capillary pressure, where capillary pressure is defined as the difference in pressures between contiguous nonwetting and wetting fluids. Whenever the fluid wettabilities follow the order water to NAPL to air, (i.e. wetting to non-wetting fluid) effective water saturation in an air-NAPL-water system is commonly assumed a function of the NAPL-water capillary pressure (Aziz and Settari, 1979). This assumption was indirectly corroborated from experimental work on three-phase air-oil-water relative

permeability-saturation relations conducted by Leverett and Lewis (1941) and Corey *et al.* (1956).

In a system where water and a NAPL coexist, capillary pressure, Pc, can be written as

$$Pc = Pn - Pw = \frac{2T}{r} \tag{2.1}$$

where *Pc* is the capillary pressure, *Pn* is the NAPL pressure, *Pw* is the water pressure and *T* is the interfacial surface tension.

In the two phase Brooks-Corey (1966) model, saturation-pressure relations are represented by

$$S'w = \left[\frac{Pd}{Pc}\right]^{\lambda}; \qquad Pc > Pd \tag{2.2}$$

$$S'w = 1 \; ; \qquad Pc \le Pd \tag{2.3}$$

where $S'w$ is effective water saturation,

$$S'w = \frac{(S_w - S_r)}{(1 - S_r)}$$

where S_r is the irreducible wetting fluid saturation, *Pd* is displacement pressure and λ is a pore size distribution index. While van Genuchten (1980), gave a relation independent of displacement pressure by

$$S'w = [1 + (\alpha Pc)^n]^{-m}; \qquad Pc > 0 \tag{2.4}$$

$$S'w = 1; \qquad Pc \le 0 \tag{2.5}$$

where α and n are model parameters and m = 1-1/n.

If fluid pressure distributions can be inferred from well fluid levels, and three phase saturation-pressure relations for the soil (considering the hysteresis and entrapment) are known, fluid saturation distributions can be predicted and integrated to determine the corresponding hydrocarbon specific volumes.

2.5 Limitations of the Existing Models and Need for the Study

A variety of models are available to get quantitative determination of spilled hydrocarbon volume. However, use of certain models is limited by the site-specific properties or data acquisition technology. Many of the models are sensitive to parameters such as permeability, porosity, and hydrocarbon spill history that is often unknown or poorly defined. Thus, significant uncertainty in the accuracy of the results may exist, even at relatively well-characterized sites (Newell *et al*., 1995). Uncertainty in the relationships between hydrocarbon thickness in the monitoring wells, specific oil volume, and water table elevation render applicability of these models limited. It seems that the relationships between these parameters are strongly affected by entrapment of oil and water, pore water blockage, and saturation history of the soil profile due to water table fluctuation.

Therefore, it is believed that there is a need to make the assessment of the relationship between the spilled hydrocarbon volume and its thickness in monitoring wells considering the water table fluctuation history. It is also expected that this study will yield valuable information and provide more knowledge about the estimation of

spilled LNAPL volume. The outcome of this study will contribute to the understanding of uncertainties and variations in the correct estimation of spilled LNAPL volume.

CHAPTER 3

THEORETICAL MODEL DEVELOPMENT

A one dimensional semi analytical model was developed to evaluate the effect of water table fluctuations in the porous media on the hydrocarbon thickness measurements in the monitoring well. The model was used to predict the extent of LNAPL contamination from the volumetric point of view.

3.1 General

It is well established that the water table in an unconfined aquifer is always in a transient state. Under a transient state, the asymptotic physical equilibrium conditions may never be reached to justify the use of the theory based on static equilibrium conditions. In the following model based on the work of Liao and Aral (1999) and Van Gell and Roy (2002), an attempt has been made to represent LNAPL thickness fluctuation with the rising and falling water table conditions in an unconfined aquifer. The modified model developed consists of three parts. The first part describes the governing equations for the LNAPL movement in an unconfined aquifer caused by piezometric head fluctuations. The second part of the model depicts the governing equations for LNAPL movement in the monitoring well. In the third part, governing equations for LNAPL movement in the monitoring well are related to the governing equations for the LNAPL

movement in an unconfined aquifer caused by piezometric head fluctuations. Simplified assumptions were introduced to incorporate the effect of entrapment, hysteresis and residual saturations. The model derived in this study may be utilized in estimating LNAPL thickness and volume in aquifers under fluctuating water table conditions. Detail description of the model is discussed in the following sections.

3.2 Vertical Flow Model for LNAPL Movement in Unconfined Aquifer

Consider an unconfined aquifer having a spilled LNAPL thickness $h(t)$ in the porous media. This LNAPL thickness represents the equivalent volume of vertically distributed LNAPL per unit planimetric area of the aquifer. However, in reality distributed LNAPL coexist with some entrapped water and air. Assume that initially the water table in the aquifer at $t = t_o$ is at an elevation of H_o. After some time t, the water table is suddenly changed to H causing an upward and downward movement in the aquifer and monitoring well. Another assumption used in the subsequent derivation is the concept of a sharp interface between any two of the fluids discussed (LNAPL, water, and air). One may define the groundwater velocity in the aquifer based on the continuity relationship as

$$V_w = f_w \frac{dz}{dt} \tag{3.1}$$

where, z is the LNAPL groundwater interface elevation datum as shown in figure 3.1 and f_w is the replaceable porosity for the water phase. Nonwetting fluid hysteresis/entrapment considerations will also be taken care of in the following sections. In the case of a rising water table i.e. ($H > H_0$), f_w may be defined as follows,

$$f_w = \phi_e (1\text{-}S_{tR}) \tag{3.2}$$

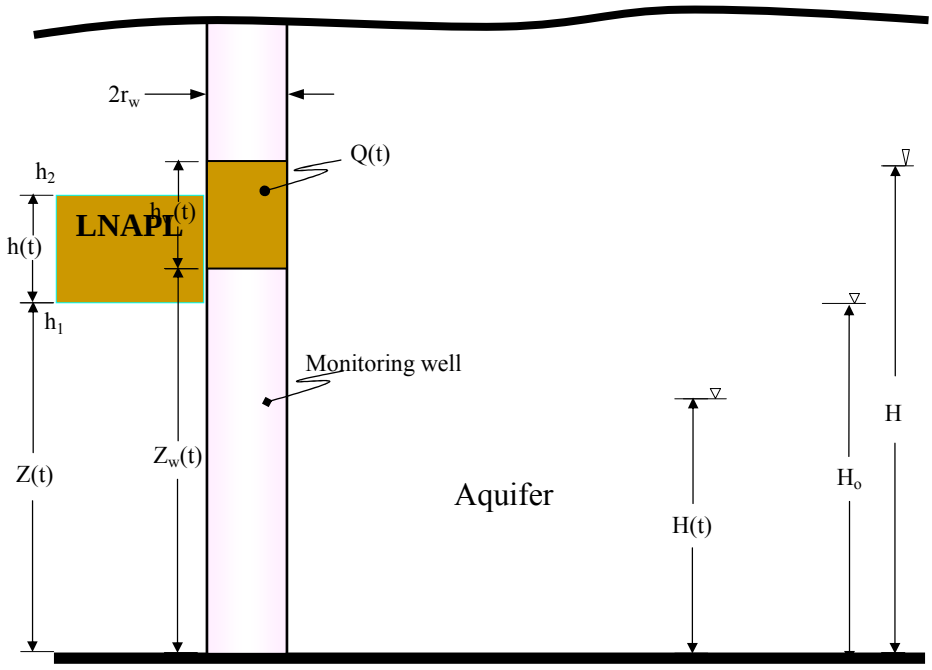

Figure 3.1. Definitions of LNAPL thickness in an unconfined homogenous aquifer with a fully penetrated monitoring well.

where ϕ_e is the effective porosity of the aquifer, and S_{tR} is the total entrapped fluid saturation due to flooding of groundwater. In the case of a falling groundwater table i.e. ($H < H_0$), f_w may take the form,

$$f_w = \phi_e (1\text{-}S_{htF}) \tag{3.3}$$

where S_{htF} is the historically entrapped total residual non-wetting fluid saturation in the case of a falling groundwater table.

Now define the vertical oil phase Darcy velocity 'V_o' as

$$V_o = f_o \frac{d(h+z)}{dt} \tag{3.4}$$

where, h is the thickness of LNAPL in the porous media, and f_o is the replaceable porosity of oil phase. In the case of a rising groundwater table, i.e. ($H > H_o$), f_o may take the form,

$$f_o = \phi_e (1\text{-}S_{hoR}) \tag{3.5}$$

where S_{hoR} is the historical entrapped residual oil saturation in the vadose zone due to the movement of the LNAPL/air interface. In the case of a falling groundwater table, i.e. ($H < H_o$), f_o may take the form,

$$f_o = \phi_e (1\text{-}S_{oF}) \tag{3.6}$$

where S_{oF} is the entrapped residual oil saturation due to the movement of the LNAPL/air interface. Utilizing the Darcy velocities V_w, V_o, and the conservation of mass principle produces the following

$$f_o\, d(h+z) = f_w\, dz \tag{3.7}$$

$$f_o\, dh + f_o\, dz = f_w\, dz \tag{3.8}$$

$$f_o\, dh = -(f_o - f_w)\, dz \tag{3.9}$$

$$dh = -\left(1 - \frac{f_w}{f_o}\right) dz \tag{3.10}$$

or

$$dh = -k\, dz \tag{3.11}$$

where,

$$k = 1 - \frac{f_w}{f_o} \tag{3.12}$$

The above relation shows that if the replaceable porosity for groundwater f_w is larger than the replaceable porosity of the oil phase f_o, then k < 0, which implies that as the groundwater/LNAPL interface z rises the thickness of free product h increases. Otherwise, if the replaceable porosity for groundwater f_w is less than the replaceable porosity for oil phase f_o, then k > 0, which implies that as the groundwater/LNAPL interface z rises the thickness of free product h decreases. If $f_w = f_o$, then the thickness of the oil phase will not change relative to the movement of the groundwater phase.

In a given system, the amount of nonwetting fluid j entrapped by wetting fluid k during imbibition will depend on the current fluid saturation and the saturation path history. Possible sources of entrapped fluid in a three-phase system are air trapped by water, air trapped by oil, and oil trapped by water. A typical entrapment of nonwetting fluids in a sand matrix is shown in figure 3.2. The procedure proposed here for the prediction of fluid entrapment assumes that these processes in a three-phase system may be evaluated from observations made in two-phase air-water, oil-water, and air-oil

systems. Historic minimum saturations are the smallest fluid contents for a given saturation path history.

Primary drainage and imbibition pathways within a given system define specific saturation paths. There are many instances during water table fluctuations however, where the saturation path does not follow the primary drainage or imbibition pathways. A system may switch from drainage to imbibition before the irreducible value is reached or, conversely, from imbibition to drainage before the maximum saturation is reached. Intermediate pathways may be represented by hysteretic scanning curves interpolated from primary drainage and imbibition functions.

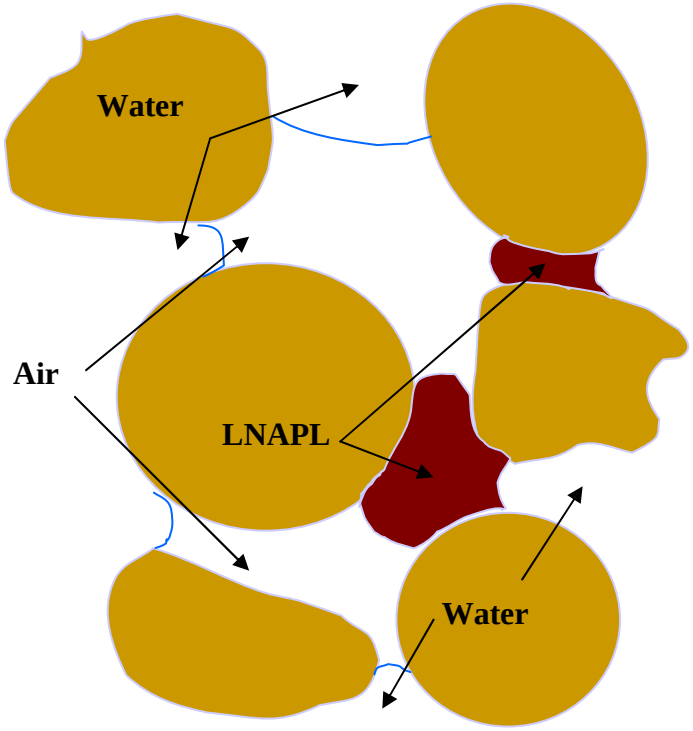

Figure 3.2 Typical entrapment of nonwetting fluids in a sand matrix.

In order to incorporate the effect of hysteresis/entrapment functions in the calculation of entrapped volume one has to define the relation between entrapped and total saturation. White and Lenhard (1993) scaled the entrapped volume between zero and the maximum entrapment value, based on the location of the saturation reversal point from the primary drainage curve. Assuming an empirical relationship based on the work of Land (1968), Parker and Lenhard (1987) defined the maximum effective entrapped saturation level based on the initial drainage-imbibition reversal point as

$$\overline{S}_{jr}^{jk} = \frac{1 - {}^{\Delta}\overline{S}_{k}^{jk}}{1 + R_{jk}\left(1 - {}^{\Delta}\overline{S}_{k}^{jk}\right)} \tag{3.13}$$

where, i, j and k are corresponding fluid phases and

$$R_{jk} = \frac{1}{{}^{i}\overline{S}_{jr}^{jk}} - 1 \tag{3.14}$$

${}^{\Delta}\overline{S}_{k}^{jk}$ is the effective saturation (of the wetting fluid) at the reversal from the main drainage curve to a primary imbibition scanning curve. $\overline{S}_{jr}^{jk}$ is the maximum effective entrapped saturation corresponding to ${}^{\Delta}\overline{S}_{k}^{jk}$. Similarly ${}^{i}\overline{S}_{jr}^{jk}$ is the maximum effective entrapped saturation corresponding to the main imbibition branch of $\overline{S}_{k}^{jk}$ (h_{jk}) as shown in figure 3.3.

The algorithm estimates bound on the amount of nonwetting fluid that can be trapped in a porous media with two immiscible fluids. To interpolate between these two end-points, it is assumed that all pores will entrap nonwetting fluid in proportion to their

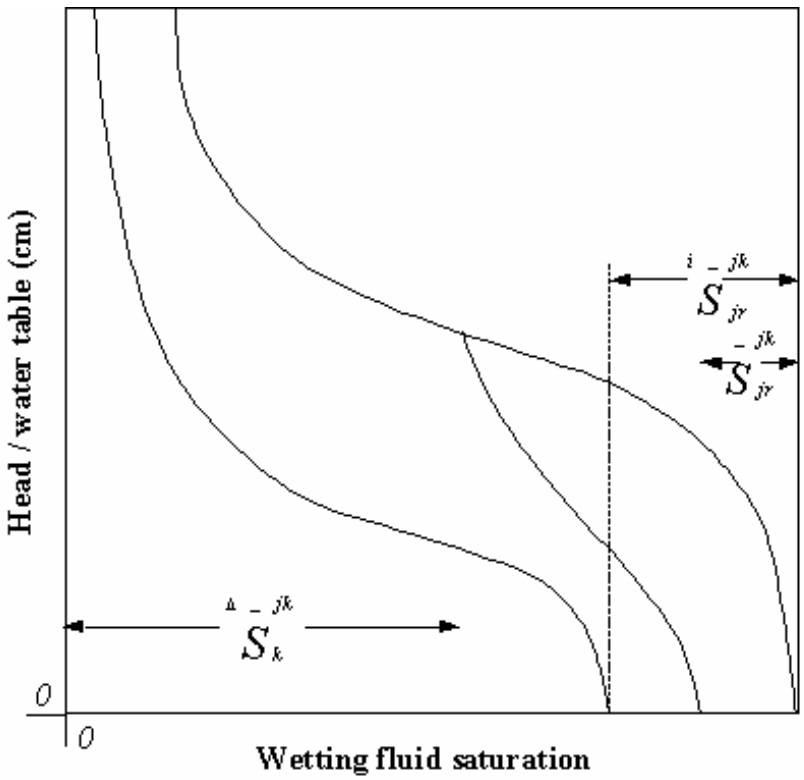

Figure 3.2. Fluid hysteresis / entrapment model showing main drainage and imbibition curves, primary scanning imbibition curve, and relevant terminology. (Modified from Parker and Leahard, 1987).

volumes. Accordingly, the amount of entrapped nonwetting fluid is predicted to vary linearly (Lenhard, 1992).

$$\overline{S}_{jt}^{jk} = \overline{S}_{jr}^{jk} \left(\frac{\overline{S}_k^{jk} - {}^{\Delta}\overline{S}_k^{jk}}{1 - {}^{\Delta}\overline{S}_k^{jk}} \right) \tag{3.15}$$

where $\overline{S}_{jr}^{jk}$ is given by (3.13). Considering the rising water table scenario, the total entrapped nonwetting fluid saturation S_{tR} and S_{hoR} may be represented as:

$$S_{tR} = S_{otw} + S_{atw+} S_{ato} \tag{3.16a}$$

and $$S_{hoR} = S_{how} + S_{haw} \tag{3.16b}$$

where, $S_{otw,}$ S_{atw} and S_{ato} are the total oil entrapped by water, total air entrapped by water and total air saturation entrapped by oil due to the movement of the water/LNAPL interface respectively. Similarly, S_{how} and S_{haw} are historically entrapped residual oil and air saturation levels. One may conduct two-phase (air – LNAPL, and air – water) saturation pressure experiments and utilize from (3.13) to (3.15) to obtain corresponding entrapped saturations. The above saturations afterwards may be used to predict replaceable porosity of water f_w from (3.2). Similarly, replaceable porosity for the oil f_o may be predicted from (3.5) by incorporating historical entrapped residual saturation S_{hoR} in a similar manner.

In the case of a falling ground water table, total entrapped nonwetting fluid saturation S_{htF} and S_{oF} may be represented as:

$$S_{htF} = S_{hotw} + S_{hatw+} S_{hato} \tag{3.17a}$$

and $$S_{oF} = S_{ow} + S_{aw} \tag{3.17b}$$

where, S_{hotw}, S_{hatw} and S_{hato} are the historic entrapped oil and air saturation due to the movement of the water/LNAPL interface respectively. Similarly S_{ow} and S_{aw} are entrapped oil and air saturations. One has to determine these values by conducting a two phase (air – LNAPL, and air – water) saturation-pressure laboratory experiment. Utilizing equations 3.13 to 3.15 the corresponding entrapped saturations can be obtained. The replaceable porosity for water f_w then can be predicted from (3.3).

In order to determine the replaceable porosity of oil f_o in a falling water table scenario, one has to get entrapped air saturation in the oil 'S_{oF} 'due to the movement of the LNAPL/air interface. After getting entrapped saturations using a similar procedure to that above, replaceable porosity may be predicted as

$$f_o = \phi_e (1 - S_{oF}) \tag{3.18}$$

We may rewrite equation (4.11) as

$$h = h_o - k (z - z_o) \tag{3.19}$$

where h_o and z_o are initial LNAPL thickness and groundwater/oil phase interface elevation in the unconfined aquifer.

From Darcy's law, for the water phase

$$V_w = K_w \frac{dh}{dz} \tag{3.20}$$

or $$V_w = K_w \frac{(H - h_1)}{Z} \tag{3.21}$$

$$V_w Z = K_w(H\text{-}h_1) \tag{3.22}$$

and for the LNAPL phase

$$V_o = K_o \frac{(h_1 - h_2)}{h} \tag{3.23}$$

substituting h_2 in the above equation

$$hV_o = K_o (h_1 - h_2) = K_o[h_1 - (z + \rho_r h)] \tag{3.24}$$

where h_1 and h_2 are the piezometric heads at the groundwater /oil phase interface and the free product/air interface respectively, K_w is the permeability of the aquifer for water, K_o is the permeability of the aquifer for oil, ρ_r is the density ratio (ρ_o/ρ_w) where ρ_o is the density of oil phase and ρ_w is the density of water.

Substituting h_1 from equation (3.22) into equation (3.24) and rearranging terms, the following equation is obtained:

$$\frac{V_w}{K_w} z + \frac{V_o}{K_o} h = H - (z + \rho_r h) \tag{3.25}$$

Substituting Darcy velocities V_w and V_o into equation (3.25) gives:

$$\frac{f_w}{K_w} z \frac{dz}{dt} + \frac{f_o}{K_o} h \frac{d(z+h)}{dt} = H - (z + \rho_r h) \tag{3.26}$$

Now substituting value of 'h' into (3.26) to get:

$$\frac{f_w}{K_w} z \frac{dz}{dt} + \frac{f_o}{K_o} \{h_0 - k(z - z_0)\} \frac{d(z + h_0 - zk + z_0 k)}{dt} \backslash = H - (z + \rho_r h_o - \rho_r kz + \rho_r kz_0) \tag{3.27}$$

Rearranging

$$\frac{f_w}{K_w} z \frac{dz}{dt} + \frac{f_o}{K_o} [h_0 - k(z - z_0)](1 - k) \frac{dz}{dt} = H - (z + \rho_r [h_0 - k(z - z_0)]) \tag{3.28}$$

which can be written as:

$$\left[\left(\frac{f_w}{K_w}-k\left(1-k\right)\frac{f_o}{K_o}\right)z+\left(1-k\right)\left(h_0+k\,z_0\right)\frac{f_o}{K_o}\right]\frac{dz}{dt} = \left(1-k\rho_r\right)z+\left[H-\left(\rho_r\left(h_0+k\,z_0\right)\right)\right] \tag{3.29}$$

one may write equation (3.29) in a general form as,

$$\left(a_1\,z+a_0\right)\frac{dz}{dt}=z+b_0 \tag{3.30}$$

Where,

and

$$a_1=-\frac{f_w/K_w-k\left(1-k\right)f_o/K_o}{1-k\rho_r},\qquad a_0=-\frac{\left(1-k\right)\left(h_0+k\,z_0\right)f_o/K_o}{1-k\rho_r}$$
$$b_0=-\frac{H-\rho_r\left(h_0+k\,z_0\right)}{1-k\rho_r} \tag{3.31}$$

The analytical solution of equation (3.30) can be given as,

$$a_1\,z+\left(a_0-a_1\,b_0\right)\ln\left(z+b_0\right)=t+C \tag{3.32}$$

where C is the integration constant using initial condition at $t = 0$, $z = z_0$

Therefore,

$$C=a_1\,z_0+\left(a_0-a_1\,b_0\right)\ln\left(z_0+b_0\right) \tag{3.33}$$

Substitution of C will give the solution for z as a function of time

$$a_1\,z-a_1\,z_0+\left(a_0-a_1\,b_0\right)\left[\ln\left(z+b_0\right)-\ln\left(z_0+b_0\right)\right]=t \tag{3.34}$$

or

$$a_1\left(z-z_0\right)\left(a_0-a_1\,b_0\right)\ln\frac{z+b_0}{z_0+b_0}=t \tag{3.35}$$

In order to introduce LNAPL thickness in the unconfined aquifer, the value of z from (3.19) is substituted in the above equation. Therefore, after simplification one may get

$$\frac{a_1}{k}(h_0 - h) + (a_0 - a_1)\ln\frac{h_0 - h + z_0 k + b_0 k}{z_0 k + b_0 k} = t \tag{3.36}$$

The above equation is the solution for the free product thickness 'h' in an unconfined aquifer due to a change in the groundwater table from H_o to H at time t.

3.3 Vertical Flow Model for LNAPL Movement in the Monitoring Well

Considering the definitions in figure 3.1, an unconfined aquifer having a spilled LNAPL thickness '$h(t)$' in the porous media and the aquifer is fully penetrated with a monitoring well of radius 'r_w', where $Z_w(t)$ is defined as the LNAPL/groundwater interface elevation in the monitoring well and '$h_w(t)$' is the distinct free LNAPL thickness in the well. As the vertical permeability of wells is much larger than that in porous media, we may write

$$Z_w(t) + \rho_r h_w(t) = H \tag{3.37}$$

As water level rises faster in the well as compared to in the aquifer, therefore, in the case of rising water table, the LNAPL thickness elevation in the well is higher than that in the porous media. Thus, at least initially, LNAPL is expected to flow from the well into the aquifer. Considering the flow entering the monitoring well as positive discharge, then one can define the flow rate of LNAPL into the aquifer as

$$Q_w(t) = A\frac{dh_w(t)}{dt} \tag{4.38}$$

also $$= 2\pi r_w\, l(t)\, K_{fp}\left[\frac{\Delta H_w(t)}{\Delta L}\right] \tag{4.39}$$

where, ΔL is the filter pack thickness, and K_{fp} is the permeability of filter packing. $\Delta H_w(t)$ is the difference of the LNAPL surface elevation between the porous media and the monitoring well which can be written as:

$$\Delta H_w(t) = Z(t) + h(t) - Z_w(t) - h_w(t) \tag{3.40}$$

where, $l(t)$ is the depth of LNAPL in the direction of flow. For convenience assuming $l(t)$ as the thickness of LNAPL at the well, if the LNAPL discharge from the well to the aquifer, otherwise $l(t)$ is the thickness of LNAPL in the aquifer. Thus $l(t)$ may be written as

$$l(t) = \begin{cases} h_w(t)\Lambda\ \Lambda\ z(t) + h(t) - z_w(t) - h_w(t) \le 0 \\ h(t)\Lambda\ \Lambda\ z(t) + h(t) - z_w(t) - h_w(t) > 0 \end{cases} \tag{3.41}$$

Using the conservation of mass principle for oil in the monitoring well, we have,

$$\pi\ \ r^2\ \frac{dh_w(t)}{dt} = Q_w = 2\pi\ \ r\ \ K_{fp}\,\lambda(t)\,\frac{\Delta H_w(t)}{\Delta L} \tag{3.42}$$

Substituting the value of ΔH_w from equation (3.40) in the above equation and rearranging

$$r\frac{dh_w(t)}{dt} = \frac{2K_{fp}}{\Delta L}\lambda(t)\,[z(t) + h(t) - z_w(t) - h_w(t)] \tag{3.43}$$

Substituting $z_w(t)$ from (3.37) and collecting terms yields,

$$r\frac{dh_w(t)}{dt} = \frac{2K_{fp}}{\Delta L}\lambda(t)\,[z(t) + h(t) - H - (1-\rho_r)\,h_w(t)] \tag{3.44}$$

The above equation is the vertical flow model for LNAPL movement in the monitoring well. In this equation, $h_w(t)$ is the unknown LNAPL thickness in the monitoring well, $z(t)$, $h(t)$ are known functions of time which can be calculated from (3.35) and (3.36) under the transient conditions, $\lambda(t)$ is defined by (3.41), and all other parameters are defined previously. The equation (3.44) will be solved in the next section.

3.4 Relating Monitoring Well and Unconfined Aquifer Flow Models

In order to relate both models one has to define the initial oil surface in the monitoring well. The initial condition may be written as

$$\text{at } t = 0 \qquad h_w(t) = h_{w0} \tag{3.45}$$

Substituting the above condition in (3.37) yields

$$Z_w(0) + \rho_r h_{w0} = H_0 \tag{3.46}$$

Therefore, we may write

$$Z_w(t) - Z_w(0) + \rho_r[h_w(t) - h_{w0}] = H - H_0 \tag{3.47}$$

Now considering the equation (3.44), where $z(t)$, and $h(t)$ are known as functions of time which can be calculated from (3.35) and (3.36).

Considering some critical time t_c the oil surface in the well may be equal to that in the porous media. This implies

$$\Delta H_w(t_c) = z(t_c) + h(t_c) - z_w(t_c) - h_w(t_c) = 0 \tag{3.48}$$

3.4.1 Rising Water Table Scenario

After this critical time, the oil surface in the monitoring well will be lower than the oil surface in the porous media for $t > t_c$. In order to solve (3.44) we may define $\lambda(t)$ as

$$l(t) = \begin{cases} h_w(t) & t \le t_c \\ h(t) & t > t_c \end{cases} \tag{3.49}$$

Substituting (3.49) into (3.44) and collecting terms yields,

$$\begin{aligned} &\frac{dh_w}{dt} + \frac{2K_{fp}}{r\Delta L}\left[H - z(t) - h(t)\right]h_w = -\frac{2K_{fp}}{r\Delta L}(1-\rho_r)h_w^2 && t \le t_c \\ &\frac{dh_w}{dt} + \frac{2K_{fp}}{r\Delta L}(1-\rho_r)h(t)h_w = -\frac{2K_{fp}}{r\Delta L}\left[H - z(t) - h(t)\right]h(t) && t > t_c \end{aligned} \tag{3.50}$$

Equation (3.50) can be rewritten as,

$$\begin{aligned} &\frac{dh_w}{dt} + p(t)h_w + q\,h_w^2 = 0 && t \le t_c \\ &\frac{dh_w}{dt} + qh(t)h_w + p(t)h(t) = 0 && t > t_c \end{aligned} \tag{3.51}$$

where q is a constant defined as,

$$q = \frac{2K_{fp}}{r\Delta L}(1-\rho_r) \tag{3.52}$$

and $p(t)$ is a known function defined as,

$$p(t) = \frac{2K_{fp}}{r\Delta L}\left[H - z(t) - h(t)\right] \tag{3.53}$$

The first part in equation (3.51) is a Bernoulli equation. Letting $u = 1/h_w$ yields,

$$\frac{du}{dt} - p(t)u = q \tag{3.54}$$

which is a linear equation. The general solution of (3.54) can be given as,

$$u(t) = e^{\int_0^t p(\tau)d\tau}\left[\int_0^t qe^{-\int_0^\xi p(\tau)d\tau} d\xi + c\right] \tag{3.55}$$

where c is a constant. Substituting $u = 1/h_w$ back into (3.55) yields the general solution as

$$h_w(t) = e^{-\int_0^t p(\tau)d\tau}\left[\int_0^t qe^{-\int_0^\xi p(\tau)d\tau} d\xi + c\right]^{-1} \tag{3.56}$$

Substituting the initial condition $h_w(0) = h_0$ yields $c = 1/h_0$. Thus, equation (3.51) can be written as

$$h_w(t) = e^{-\int_0^t p(\tau)d\tau}\left[\frac{1}{h_0} + \int_0^t qe^{-\int_0^\xi p(\tau)d\tau} d\xi\right]^{-1} \qquad t \le t_c \tag{3.57}$$

The second part in equation (3.51) is a linear equation. The general solution of this equation is,

$$h_w(t) = -e^{-\int_0^t qh(\tau)d\tau}\left[\int_{t_c}^t p(\xi)h(\xi)e^{\int_{t_c}^\xi qh(\tau)d\tau} d\xi + c\right] \tag{3.58}$$

The initial condition for this equation is,

$$h_w(t) = h_{wc} = e^{-\int_0^{t_c} p(\tau)d\tau}\left[\frac{1}{h_0} + \int_0^{t_c} qe^{-\int_0^{\xi} p(\tau)d\tau} d\xi\right]^{-1} \qquad \text{for } t = t_c \qquad (3.59)$$

Substituting the initial condition (3.59) into (3.58) yields,

$$h_w(t) = e^{-\int_{t_c}^{t} qh(\tau)d\tau}\left[h_{wc} - \int_{t_c}^{t} p(\xi)h(\xi)e^{\int_{tc}^{\xi} qh(\tau)d\tau} d\xi\right] \qquad t > t_c \quad (3.60)$$

Combining equations (3.57) and (3.60) one may obtain the solution of LNAPL thickness in a monitoring well for the rising piezometric head case,

$$h_w(t) = \begin{cases} e^{-\int_0^{t} p(\tau)d\tau}\left[\frac{1}{h_0} + q\int_0^{t} e^{-\int_0^{\xi} p(\tau)d\tau} d\xi\right]^{-1} & t \le t_c \end{cases} \qquad (3.61a)$$

$$h_w(t) = \begin{cases} e^{-q\int_{t_c}^{t} h(\tau)d\tau}\left[h_{wc} - \int_{t_c}^{t} p(\xi)h(\xi)e^{q\int_{tc}^{\xi} h(\tau)d\tau} d\xi\right] & t > t_c \end{cases} \qquad (3.61b)$$

where h_{wc} is defined by (3.59).

3.4.2 Declining Water Table Scenario

As the water table in the unconfined aquifer decreases, the oil surface in the monitoring well is expected to be lower than that in the aquifer at least for a certain period

of time. Similar to the previous case, defining t_c as the critical time point when ΔH_w (t) changes from positive to negative or it may be infinite. Thus, $l(t)$ can be defined as,

$$l(t) = \begin{cases} h(t) & t \le t_c \\ h_w(t) & t > t_c \end{cases} \tag{3.62}$$

Substituting (3.62) into (3.44) and collecting terms yields,

$$\begin{aligned} &\frac{dh_w}{dt} + \frac{2K_{fp}}{r\Delta L}(1-\rho_r)h(t)h_w = -\frac{2K_{fp}}{r\Delta L}\left[H - z(t) - h(t)\right]h(t) && t \le t_c \\ &\frac{dh_w}{dt} + \frac{2K_{fp}}{r\Delta L}\left[H - z(t) - h(t)\right]h_w = -\frac{2K_{fp}}{r\Delta L}(1-\rho_r)h_w^2 && t > t_c \end{aligned} \tag{3.63}$$

Equation (3.63) can be rewritten as,

$$\begin{aligned} &\frac{dh_w}{dt} + qh(t)h_w + p(t)h(t) = 0 && t \le t_c \\ &\frac{dh_w}{dt} + p(t)h_w + q\,h_w^2 = 0 && t > t_c \end{aligned} \tag{3.64}$$

Similar to the solutions given in the previous section, the solution of (3.64) can be written as,

$$h_w(t) = \left\{ e^{-\int_0^t qh(\tau)d\tau} \left[h_0 - \int_0^t p(\xi)h(\xi)e^{\int_0^\xi qh(\tau)d\tau} d\xi \right] \right. \qquad t \le t_c \tag{3.65a}$$

$$h_w(t) = \left\{ e^{-\int_{t_c}^{t} p(\tau)d\tau} \left[\frac{1}{h_{wc}} + q\int_{t_c}^{t} e^{-\int_{t_c}^{\xi} p(\tau)d\tau} d\xi \right]^{-1} \right. \qquad t > t_c \qquad (3.65b)$$

where h_{wc} is defined by the following equation.

$$h_{wc} = e^{-\int_{0}^{t_c} qh(\tau)d\tau} \left[h_0 - \int_{0}^{t_c} p(\xi)h(\xi)e^{\int_{0}^{\xi} qh(\tau)d\tau} d\xi \right] \qquad (3.66)$$

This completes the solution of both cases of water table fluctuations. Using the above theoretical model a computer program was developed in *MATLAB-6.5*. The flow chart and program listing are presented in Appendices-A and B. The computer program was later utilized for simulation purposes. Results obtained from the simulation runs are discussed in chapter 5 with results and discussion.

3.5 Assumptions and Limitations of the Developed Model

It is important to note that the developed model is for an unconfined homogenous aquifer and it is valid for a clean (e.g. without any organic matter) and non-reactive porous media. Further more, the basic assumptions are

1) model considers a sharp interface between fluids

2) model assumes a uniform spilled LNAPL thickness in the porous medium

3) spilled LNAPL is highly immiscible and its solubility in water is negligible

4) possible sources of entrapped fluid are air trapped by water, air trapped by oil, and oil trapped by water

5) model assumes an isothermal system and neglects the effect of temperature on the porous medium as well as on the spilled LNAPL.

CHAPTER 4

PHYSICAL MODELING

An experimental study plan was designed to verify the developed mathematical model described in chapter 3. The objectives of this study were achieved by designing and fabricating a physical model followed by experimental runs, data collection and processing. Data obtained from the experimental work were utilized to verify the analytical model.

After careful and detailed analysis of the problem, the work plan was divided into two main tasks. In the first task, a detailed literature survey about the physical modelling was completed. The object of this task was to reach an optimum design of the experimental setup. Relevant past and present studies were reviewed and compiled. This study acted as a foundation for this part of the work. In the second task, detailed experimental work was performed. The preliminary run was performed to check the feasibility and workability of the physical model to be used in the actual experimental runs.

4.1 Materials and Methods for Experimental Work

The laboratory work consisted of three main tasks. In the first task selection and acquisition of experimental materials such as sand and LNAPL were completed. In the

second stage procurement of plexiglas and fabrication of the experimental setup were accomplished. The third task consisted of performing and conducting the experimental runs. The following sections discuss the experimental work in detail.

4.1.1 Materials

The materials used in the study are porous media, LNAPL, Plexiglas, a pressure cell, a pump, and pressure and vacuum gauges and their accessories. Initially, porous media, LNAPL, the pressure cell and experimental set up materials were procured. Fabrication of the experimental setup and the pressure cell were carried out in parallel with the acquisition of porous media and LNAPL properties. Basic porous media and LNAPLs properties were determined by literature review and prevalent laboratory techniques.

4.1.1.1 Porous media

Two types of sand (porous material) were used for the experimental study: namely uniform sand and well graded sand. The uniform sand was collected from the outskirts of Aziziyah, in the Dhahran area. Sand was selected as the porous medium because, 1) it has high permeability as compared to silt and clay; 2) the capillary fringe of sand is not high as compared to silt and clay, and 3) it is considered inert material i.e., has no chemical interaction with water or LNAPL. The well-graded sand was prepared using a blend of different grain sizes available from three sands. Grain sizes in the range of ASTM sieve #10, #20, #30 and #40 were sieved from the sand obtained from the Ras Tanura area; those in the range of #40, #60 and #80 were sieved from the sand obtained from the Bagga area. Both Bagga and Ras Tanura are within 50 km of Dhahran. The

grains in the range of # 100, #140 and #200 were sieved using sand available from the KFUPM beach on the outskirts of Aziziyah, Dhahran. The sieving was done in the Geotechnical Engineering laboratory at KFUPM using mechanical shakers. The blended sand can be classified as well-graded sand according to Unified Soil Classification System (USCS). The grain size distribution was determined using ASTM-D2487. The grain size distribution for both sands is shown in figure 4.1

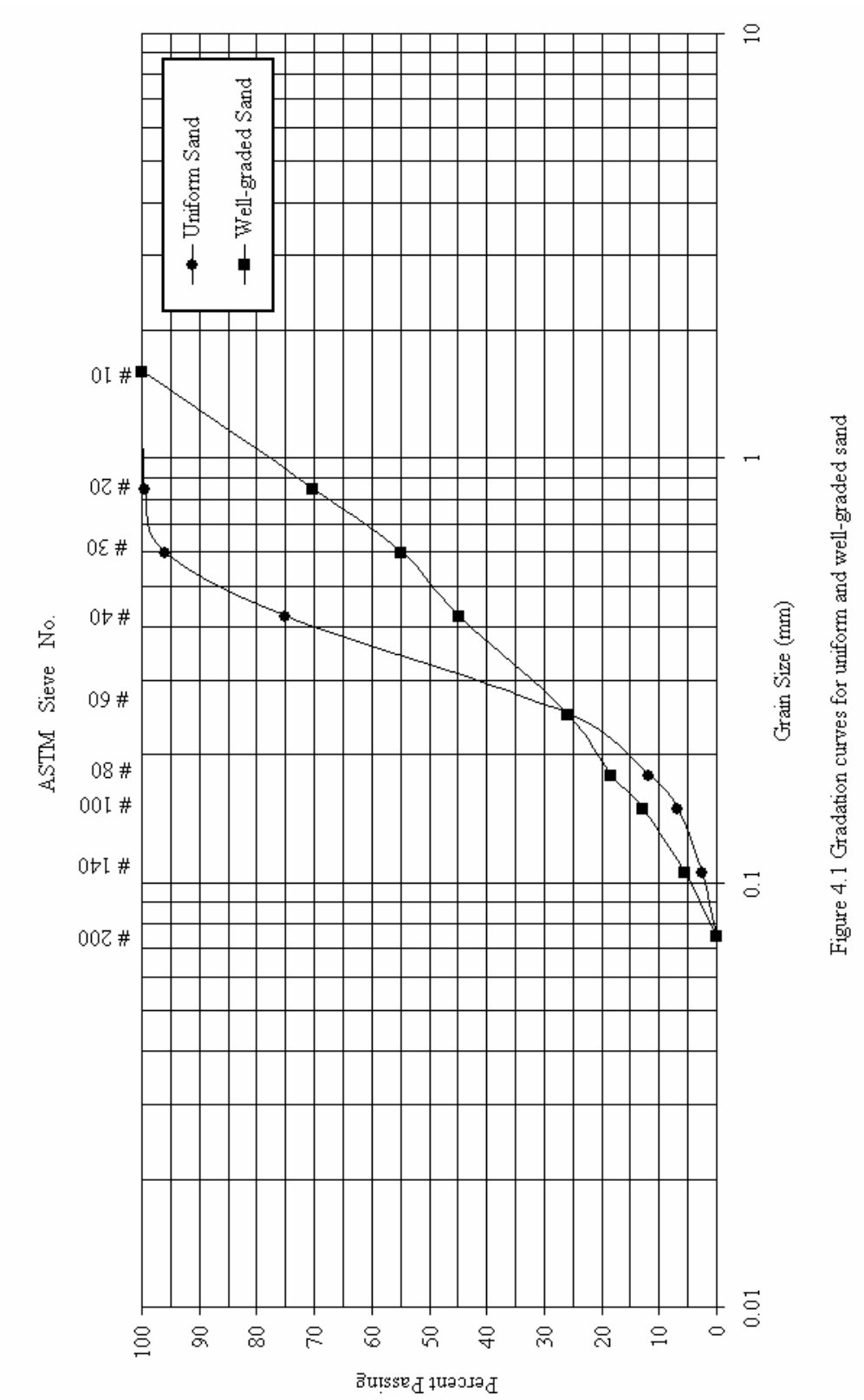

Figure 4.1 Gradation curves for uniform and well-graded sand

The grain size distribution, porosity (ϕ), uniformity coefficient (C_u), effective grain size (D_{10}) and curvature coefficient (C_c) are presented in table 4.1.

4.1.1.2 LNAPL

Two types of LNAPL were used in this study: kerosene and diesel. Usually contamination potential of such distillates is assumed to be the highest among petroleum hydrocarbon fractions (Rubin *et al*, 1998). Benzene was not used in this study because of safety reasons in the laboratory. The interfacial tension and specific gravity of the LNAPLs were measured in the Petroleum Engineering Laboratory at KFUPM. Measured and published properties of LNAPLs are presented in table 4.2. The Sudan IV (C.I. 26105, DC Pnreac Quimica), which is a color dye insoluble in water but soluble in hydrocarbon, was used to color the LNAPL in order to distinguish the LNAPL from water during experimental study. Red colored kerosene, dyed with Sudan IV is shown in plate 4.1.

4.1.2 Physical Model Description

A plexiglas sandbox was fabricated in the central workshop at KFUPM. The setup was utilized to simulate the contamination of unconfined sandy aquifer by a leaking LNAPL source. Dimensions of the set-up were selected on the basis of cost and feasibility of fabrication. In addition, the selected size was expected to be adequate for the porous media and the fluids to be used in the experiments.

TABLE 4.1. Properties of uniform and well graded sand

Properties	Uniform sand	Well graded sand
Color	Peach to wheat	Peach to sandy brown
Dry density (g/cm^3)	1.68	1.92
Specific gravity	2.67	2.67
Porosity ϕ_e.	0.37	0.28
Effective grain size (D_{10}) mm	0.18	0.12
Uniformity coefficient (C_u)	1.94	5.1
Curvature coefficient (C_c)	1.15	1.14
*USCS classification	SP	SW
Hydraulic conductivity (cm/sec)	0.02	0.016
Organic matter	~ 0.0	~ 0.0

*Unified Soil Classification System.

Plate 4.1 Red colored kerosene dyed with Sudan IV.

TABLE 4.2. Properties of kerosene oil and diesel fuel

Properties	Kerosene	Diesel fuel
Color	Colorless	Colorless to light straw
API number	43	32
* (MSDS)	U1080	U7770
Specific gravity	0.80	0.875
Viscosity (cP) at 68°C	2.1	4.1
Flash Point (°C)	65	37.8
Auto-ignition Temperature (°C)	220	256.7
Interfacial tension (dynes/cm), at 22.5 °C		
LNAPL-water	40.9	26.6
LNAPL-air	29.92	26.3
Air-water	70.9	70.9
Solubility in water	Very low	Very low

* Material Safety Data Sheet

The height and width of the sandbox were 1220 mm and 2000 mm, respectively. In order to simulate a two-dimensional section of an unconfined sandy aquifer, effective thickness of the sandbox was kept as 250 mm. Two water sumps were provided at both ends of sandbox having a cross-sectional area of 200 mm x 250 mm (as shown in figure 4.2) to provide water in order to simulate the water table fluctuations in the aquifer. Pumps and other accessories were also provided to control the water table movement.

Seven semi-circular monitoring wells, having a diameter of 25 mm, were installed inside the sand box. These monitoring wells were fully screened by a # 100 opening steel mesh. Similarly sixteen piezometers were also installed to monitor the water table position at an elevation of 30 mm to 80 mm from the base of the sand box. A schematic illustration of the setup is presented in figure 4.2 and the complete setup is shown in plate 4.2.

Three oil spill tanks of 500 mm x 250 mm having a depth of 100 mm were fabricated for the sandbox and placed at the top of the sandbox as shown in plate 4.2. Uniformly spaced perforation was provided at the base of each spill tank to ensure aerial distribution of the LNAPL inside the sandbox.

4.1.3 Fabrication of Pressure Cell

A pressure cell setup was required to generate saturation pressure data for the determination of non-wetting fluid entrapped saturations. This data was required as input for developed computer model to perform computer simulations. The pressure cell setup

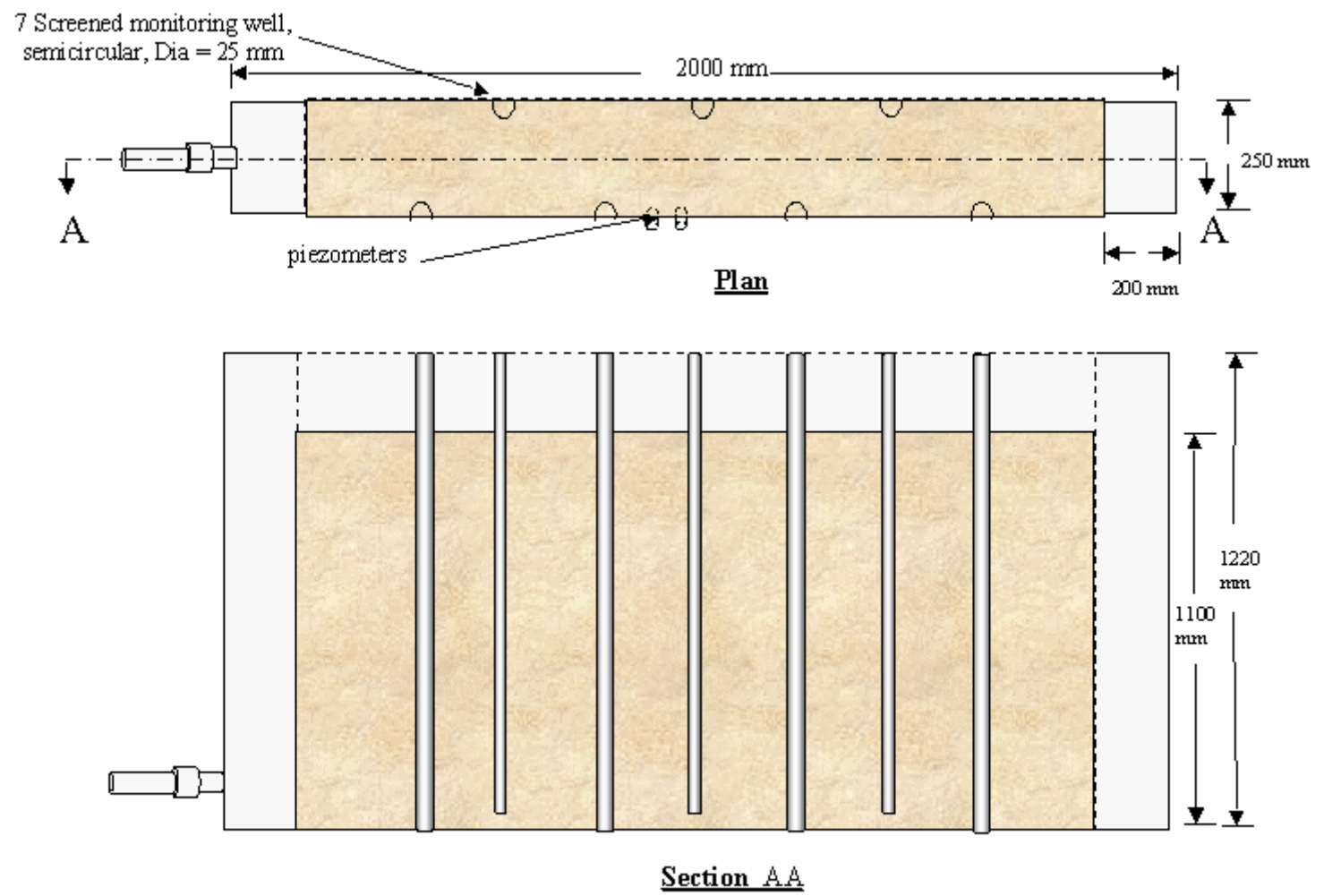

Fig. 4.2 . Section and plan of the sand box setup

Plate 4.2 Complete experimental set-up used in physical modeling.

Plate 4.3 Pressure cell set-up with accessories.

shown in plate 4.3 was fabricated in the Geotechnical and Environmental Engineering laboratories of the Civil Engineering Department at KFUPM. A simplified schematic of the pressure cell is illustrated in figure 4.3 and the complete setup of the pressure cell with accessories is illustrated in figure 4.4.

4.1.4 Experimental Procedure

In order to validate the theoretical model, detailed experimental studies were conducted. The experimental procedure consisted of a preliminary run and the main experimental study. The details of the experimental program are described below.

4.1.4.1 Preliminary experimental run

In the preliminary run, four main points were considered: First, the extent, if any, of leakage from the sandbox; second, volume of spillage of LNAPL required for a run; third whether modifications in the setup were required; and, finally, to identify operational problems that might be encountered during the main study.

The preliminary run began by filling the sandbox with the uniform sand using a pulviation technique. A total mass of 924 kg of sand was pulviated into the sand box to approximate the natural conditions in the aquifer. The dry sand was then saturated by raising the water table and flooding the sand with water. This was done to remove the entrapped air from the sand, and subsequently to maintain a water table at an elevation of 30 cm above the base of the sandbox. Leaks were discovered and sealed using epoxy until the setup was found to be leak free.

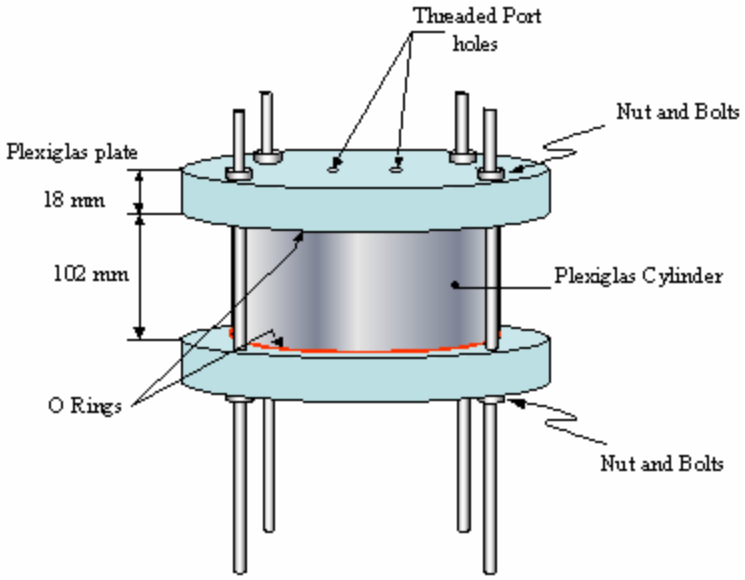

Schematic of pressure cell

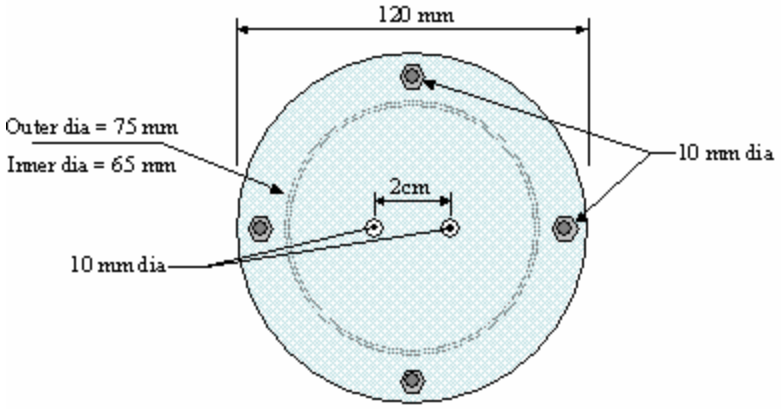

Plan View of pressure cell

Figure 4.3. Simplified schematic and plan view of the pressure cell.

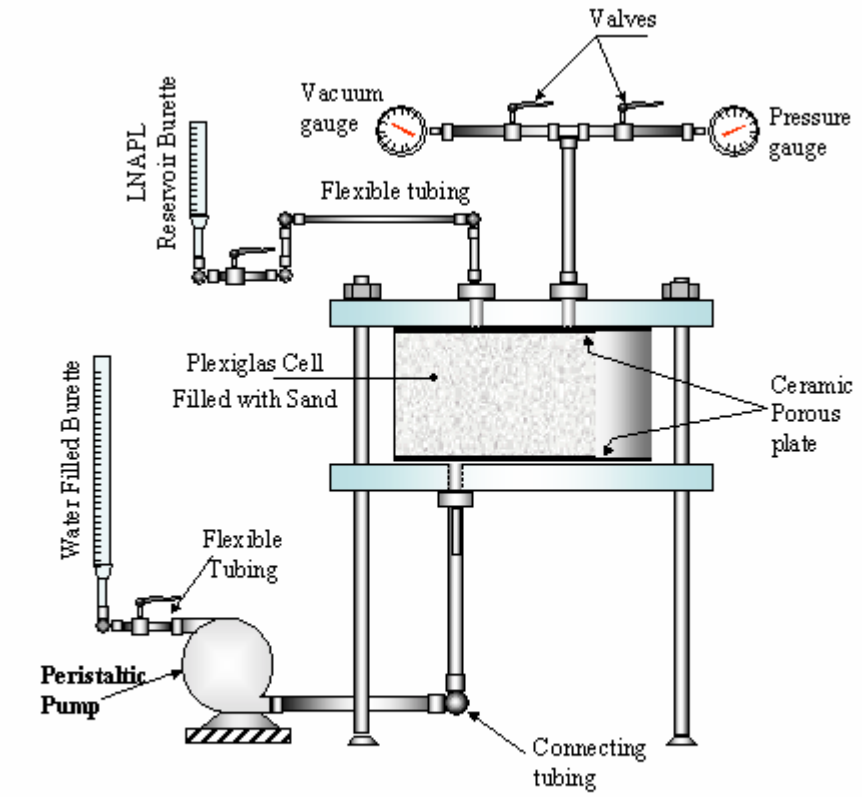

Figure 4.4. Schematic of pressure cell with accessories.

Once the quasi-static moisture distribution in the soil was achieved (which took about 10 days) diesel dyed with Sudan IV was released into the sand box. In the first day 10000 ml of diesel was released into the sandbox and at the end of 24 hours 4000 ml/day of diesel was released every day for three more days. A total of 22000 ml of diesel was released through the spill tanks were which provided at the top of the sandbox. The movement of the clearly visible red colored plume of LNAPL was monitored. The plume continued to move downwards and after a period of about two weeks from the beginning of the spill, the diesel appeared in one of the monitoring wells (plate 4.4) and within one hour it appeared in all other monitoring wells. The volume of the diesel held in the sandbox before appearing in the monitoring wells gave a conservative estimate of the critical volume below which the diesel existed at only a negative pressure in the porous media and would not be observed in the monitoring wells. The diesel level in the monitoring wells equilibrated within 10 days. The main experimental program started as soon as the preliminary run was over. Plate 4.5 and 4.6 show the preparation stages for the main runs.

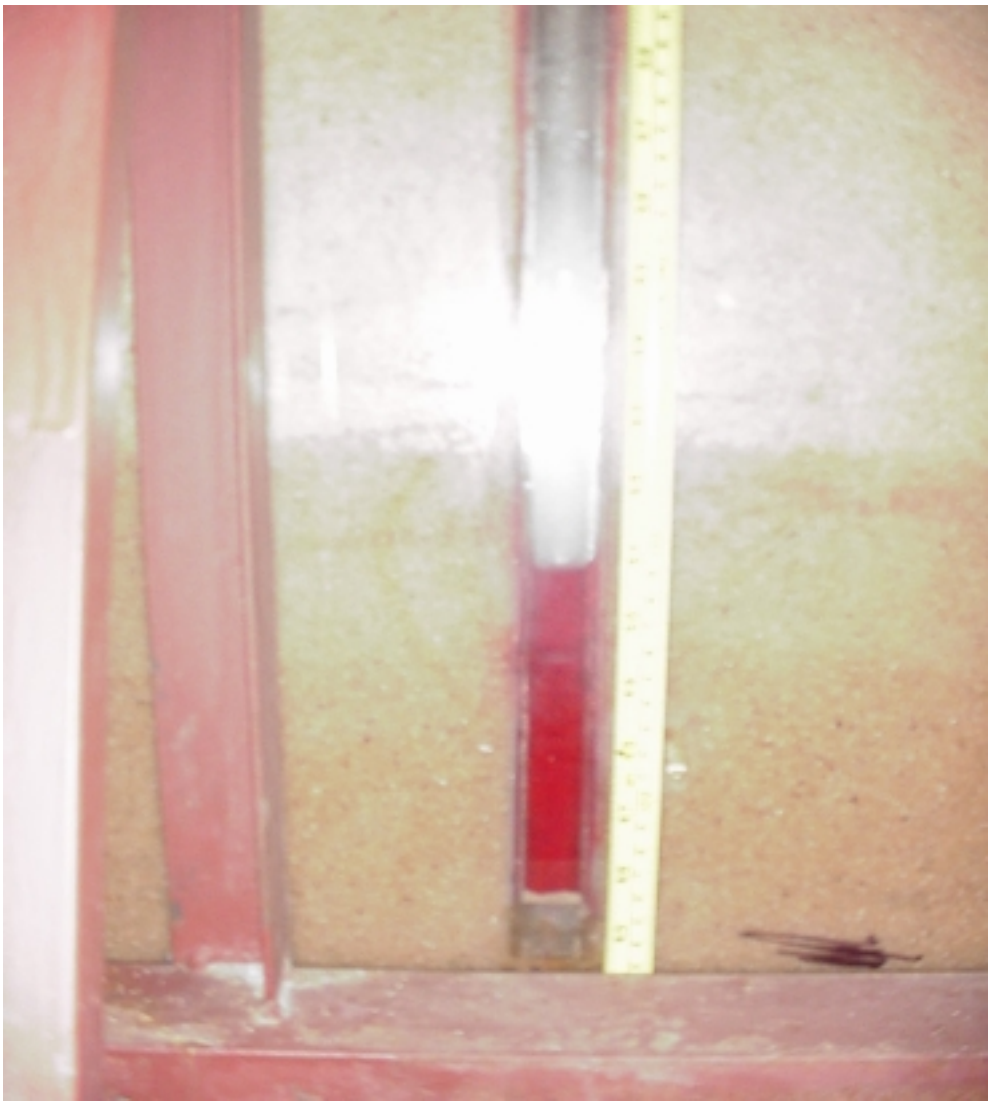

Plate 4.4 Diesel thickness in the monitoring well, appearing after spill of critical volume in porous media.

Plate 4.5 Preparation stage for main runs.

Plate 4.6 Experimental set-up with spill containers.

4.1.4.2 Main experimental runs

As two types of sand and two types of LNAPLs were used in the experimental study, four main experimental runs were performed. In the first run, uniform sand was used as the porous medium and diesel as the LNAPL and in the second run kerosene was used as the LNAPL with the same porous medium. Similarly, in third and fourth runs well-graded sand was used with diesel and kerosene, respectively.

The preliminary run helped a lot in the conduct of the main experimental runs. For the main experimental run, the setup was first cleaned and washed. The sandbox was then filled with uniform sand, up to the effective height of 1100 mm, using a pulviation technique. Once the sandbox was filled with uniform sand, it was gradually saturated by providing water from water sumps. Flow was controlled with the help of a pump with water flowing in an upward manner through the bottom openings as shown in figure 4.2. Subsequently, the water was drained from the sand and the water level was kept at 30 cm above the base of the sandbox.

After 10 days when quasi-static equilibrium had been reached, a diesel spill was initiated into the sandbox. On the basis of preliminary run experience an initial volume of diesel was released at the top of sand into the sandbox. The system was then allowed to equilibrate for 10 to 15 days. During this period the diesel plume (dyed with Sudan IV) moved laterally as well as vertically. If at any time during the initial spill the diesel appeared in any of the monitoring wells, the system was allowed to reach equilibrium for at least 10 days. However, if diesel did not appeared in any well at the end of this period, an additional volume of 3000 ml of diesel was spilled until the diesel appeared in one of

the monitoring wells. This volume of the diesel was noted as the critical volume below which the diesel existed at only a negative pressure in the porous medium and was not expected to appear in the monitoring wells. Once the quasi-static equilibrium had been reached, the quantity of diesel in to the porous medium and in the monitoring wells was noted. Subsequently, a known volume of LNAPL was spilled and again the same data was collected. In the case of the fluctuating water table study, the water table varied with the help of a pump while observing a controlled flow rate, and changes in the LNAPL thickness in the monitoring well corresponding to the water table fluctuation were noted. Five to six observation points were generated for the LNAPL thickness in the monitoring well and the corresponding water table position. At the end, a further 3000 ml of diesel was spilled out and the same procedure was repeated to get above specified observation points.

The same procedure was used for the other three main experimental runs. Each run took approximately 70 to 85 days which is the time from the initial LNAPL spill to the last observation made in the sandbox. The results of the four main runs, obtained with the help of the physical model and simulation results obtained from the theoretical model, are discussed in the next chapter.

4.1.5 Two Phase Retention Data Measurements

Two phase (air-water; air-oil; and oil-water) saturation-capillary pressure data points were required for the theoretical model simulation. Definitions of these required parameters are depicted in figure 4.5. These saturation-capillary pressure data points were generated in the laboratory with the help of the pressure cell. The cell was initially filled

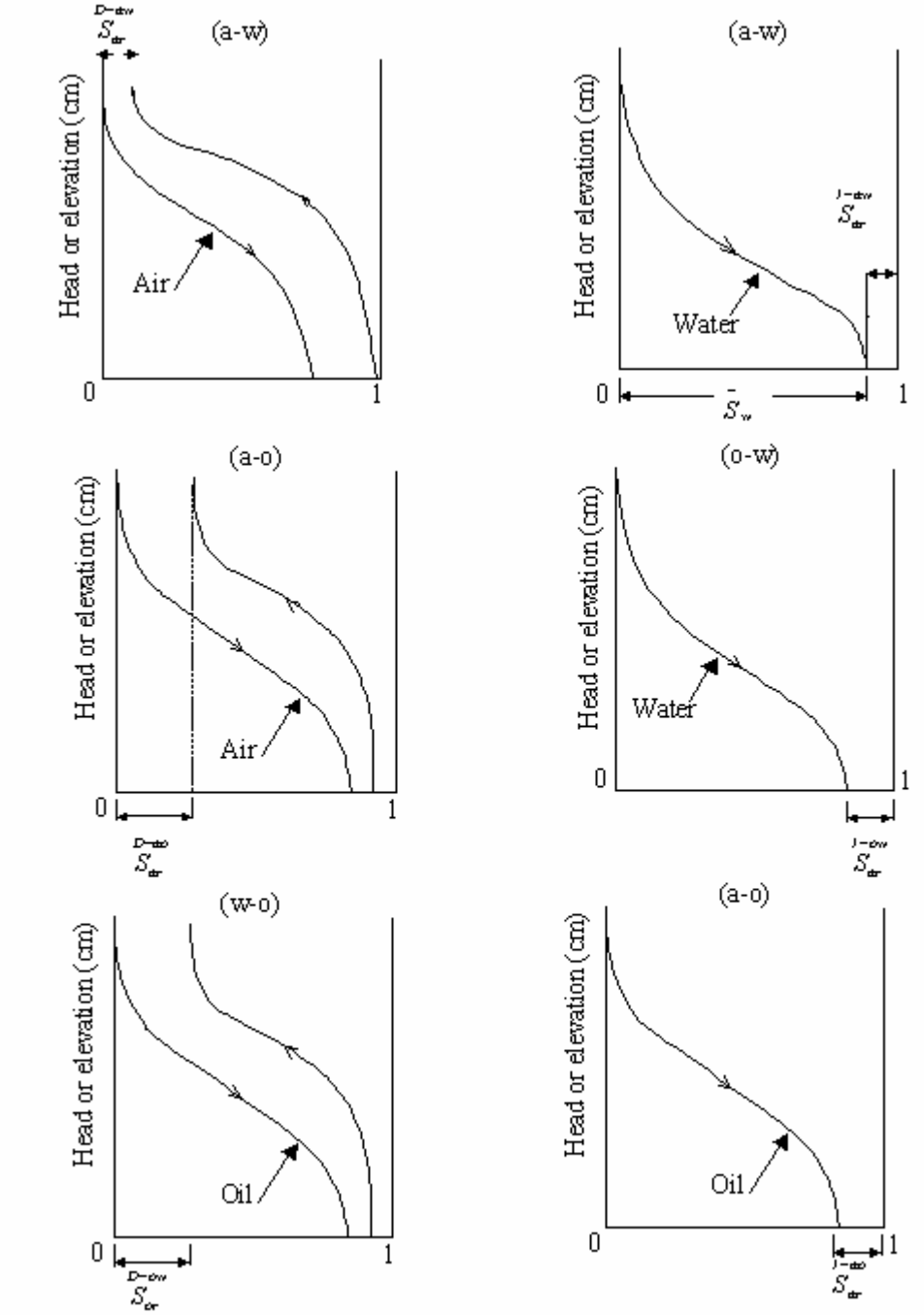

Figure 4.5: Definition of parameters defined in theoretical modeling (where a, o, and w stand for air, oil and water system).

with sand, as homogenous as possible, before the system was sealed using o-rings and pressure generated by the bolt connectors. The porosity values were determined using the weight of the cell with and without sand.

A vacuum/pressure gauge was attached to the top of the cell to measure the water pressure within the cell. A port at the bottom of the cell fitted with a fine porous ceramic disc was attached to a length of flexible tubing and a burette. During the experiment a pinhole was open to the atmosphere to allow the air to freely move into or out of the cell in response to a change in water pressure. The top of the burette was covered with a cap having only a pinhole in it to allow for the movement of air and reduce potential evaporation.

To generate saturation-water pressure data points, the flexible tubing joining the cell and burette was fed through a peristaltic pump. The tubing was used to pump water into and out of the cell. At each stage of the experiment, the volumes and pressure were recorded to generate the imbibition and drainage curves. During the entire experiment, a control was established to monitor evaporation losses.

In the case of the oil-water system, the cell was initially flushed with CO_2 for 5 minutes prior to cell saturation. This was done to eliminate air being entrapped in the water phase during filling, as CO_2 is more readily dissolved in water. A minimum of three pore volumes of water was passed through the cell prior to initiating the experiment.

4.2 Problems Encountered During Physical Modeling

During the course of the experimental work several problems were encountered. It is worthwhile mentioning them here as follow:

- At the end of the last runs several minor leaks appeared in the sandbox. Waterproof epoxy was utilized to stop the leaks. However, careful monitoring was done to avoid any loss of fluid from the system.
- Some hydrocarbon entered the water sump during the preliminary run (plate 4.7). It happened when the water table decreased below 30 cm (datum) accidentally.
- Kerosene and diesel are acting solvents and gradually degrade silicone sealant (plate 4.8). Therefore, after each run the setup was cleaned and sealed again with glue in order to avoid any leak during the experimental stage.
- It was difficult to handle a huge setup especially during cleaning and replacement of porous media.
- After each run a significant amount of waste material needed to be dumped. This part of experimental study was exhaustive and required great effort and a lot of time.

Plate 4.7 Accidental entrance of LNAPL into the water sump during preliminary run.

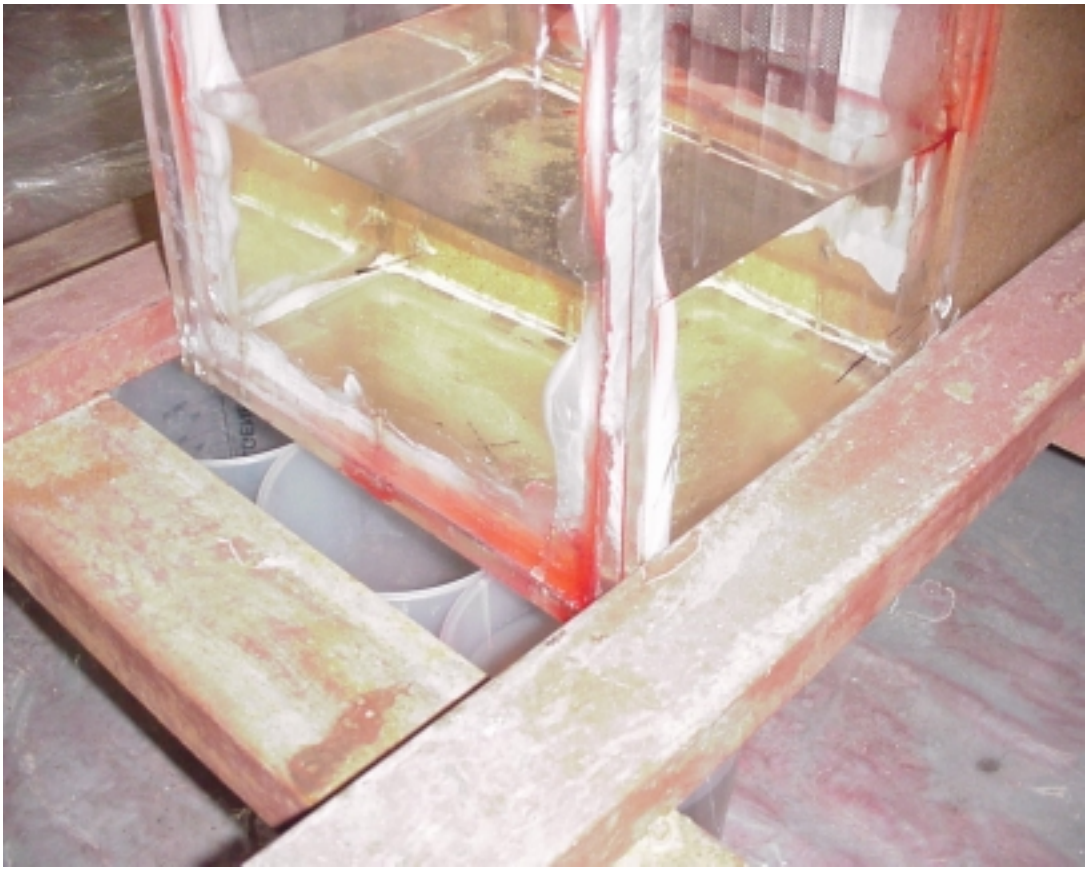

Plate 4.8 Degradation of Silicone Sealant with the Contact of LNAPL.

CHAPTER 5

RESULTS AND DISCUSSION

This chapter discusses the results obtained from the experimental program as well as the results obtained from simulations utilizing the mathematical model presented in chapter 3. Validation and verification of the model were performed by comparing the simulated results with the experimental results. Comparison was also made with the results obtained from a wide variety of models available in the literature. The mathematical model was tested and verified for static as well as for fluctuating water table conditions. As the preliminary run was performed to test the setup for the main run, only the results obtained during the main runs are discussed here.

The main experimental program consists of the following four runs:

1. Uniform porous medium with diesel contamination.
2. Uniform porous medium with kerosene contamination.
3. Well-graded porous medium with diesel contamination.
4. Well-graded porous medium with kerosene contamination.

Oil, kerosene, diesel, and hydrocarbon will be used synonymously in further discussion. Detailed discussion on the results from each study is presented in the following sections.

5.1 Uniform Porous Medium with Diesel Contamination

The sandbox filled with the uniform sand was gradually saturated by supplying water from the water sump. Water was supplied through the bottom openings to minimize the entrapment of air within the porous medium. Subsequently, the water was drained from the sand until the water level reached a point 300 mm above the base of the sandbox. Later, this height represented the initial groundwater elevation. The sand box was left idle until the quasi-static equilibrium had been reached. The system approached the quasi-static equilibrium after 10 days.

On the basis of the preliminary run, an initial volume of 20000 ml of dyed diesel was released into the sandbox. Plate 5.1 presents the intial spill of hydrocarbon into the uniform sand. Red colored hydrocarbon is clearly visible in the plate. The system was then allowed to reach quasi-static equilibrium for 12 days. After two weeks, an additional volume of 1000 ml was released. During the development of a saturated hydrocarbon fringe, no hydrocarbon was observed to flow into the well. The process continued until diesel appeared in one of the monitoring wells. After the development of a saturated hydrocarbon fringe the excess hydrocarbon started to drain into the well. Within one hour, the red coloured diesel appeared in all seven monitoring wells. The critical volume noted for the system was 24000 ml. Clearly visible red colored hydrocarbon thickness in monitoring wells is shown in plate 5.2.

Plate 5.1 Initial hydrocarbon spill in the porous media.

Plate 5.2 Hydrocarbon thickness in monitoring wells.

5.1.1 Data Based on Static Water Table Conditions

Once the diesel appeared in the monitoring wells, the change in the water table elevation, and the quantity of diesel in the porous medium and in the monitoring well were noted.

An additional volume of diesel was spilled incrementally and the system was allowed to reach quasi-static equilibrium. Subsequently, the above stated data were collected every time.

A graph plotting specific spilled volume versus thickness of diesel in all seven monitoring wells is presented in figure 5.1. It can be seen in the graph that the critical spilled volume of diesel for the uniform sand is 4.8 cm. Figure 5.1 also shows that with the increase in the volume of spilled diesel in the porous medium diesel thickness in the monitoring wells increased. However, the thickness of diesel in the monitoring wells varied. Although the difference is small, with levels in most of the wells stabilizing within two weeks, it seems that more time is required to attain representative equilibrium conditions and to stabilize the levels in the wells. In addition, some inherent spatial heterogeneity within the sand may cause this effect. Figure 5.1 also shows the graph of specific spilled volume versus average thickness of diesel in monitoring wells. It can be seen from the graph that the average thickness of diesel in monitoring wells does not differ significantly (with maximum standard deviation of 1.29). Therefore, the average thickness of hydrocarbon in the monitoring wells may be used as a representative estimate of hydrocarbon thickness for further analysis and comparative studies. Figure 5.1 shows that the graph can be divided in two segments. The first segment, at lower

spilled volumes, when the rate of increase of diesel thickness in the monitoring wells is higher and the second segment, at higher spilled volumes, when the rate of increase is low. Some researchers (Ballestero *et al.* 1993; Bashir 1997; and Charbeneau *et al.* 2000) reported similar results. This behavior of the curve may be attributed to some sort of steady state condition achieved within the system at higher spilled volumes.

In order to verify the mathematical model developed in this study, simulations were performed and results were obtained for comparison purposes. Data were generated for both static and fluctuating water table conditions. In the following sections both scenarios are discussed in detail.

5.1.1.1 Verification of mathematical model for hydrostatic conditions

Simulations, based on static water table conditions, were performed to check the capability of the model to predict the relation between spilled diesel in a porous media and its thickness in monitoring wells.

Uniform porous medium and diesel properties presented in table 4.1 and 4.2 were used as model input. Similarly, to strengthen the verification, different available empirical and analytical models reported in the literature were used in the comparison. The models which were used for comparison with the experimental results and the developed mathematical model are those of: DePastrovich *et al.* (1979), Black and Hall (1984), Hall *et al.* (1984), Schiegg (1985), Farr *et al.* (1990), and Ballestero *et al.* (1994).

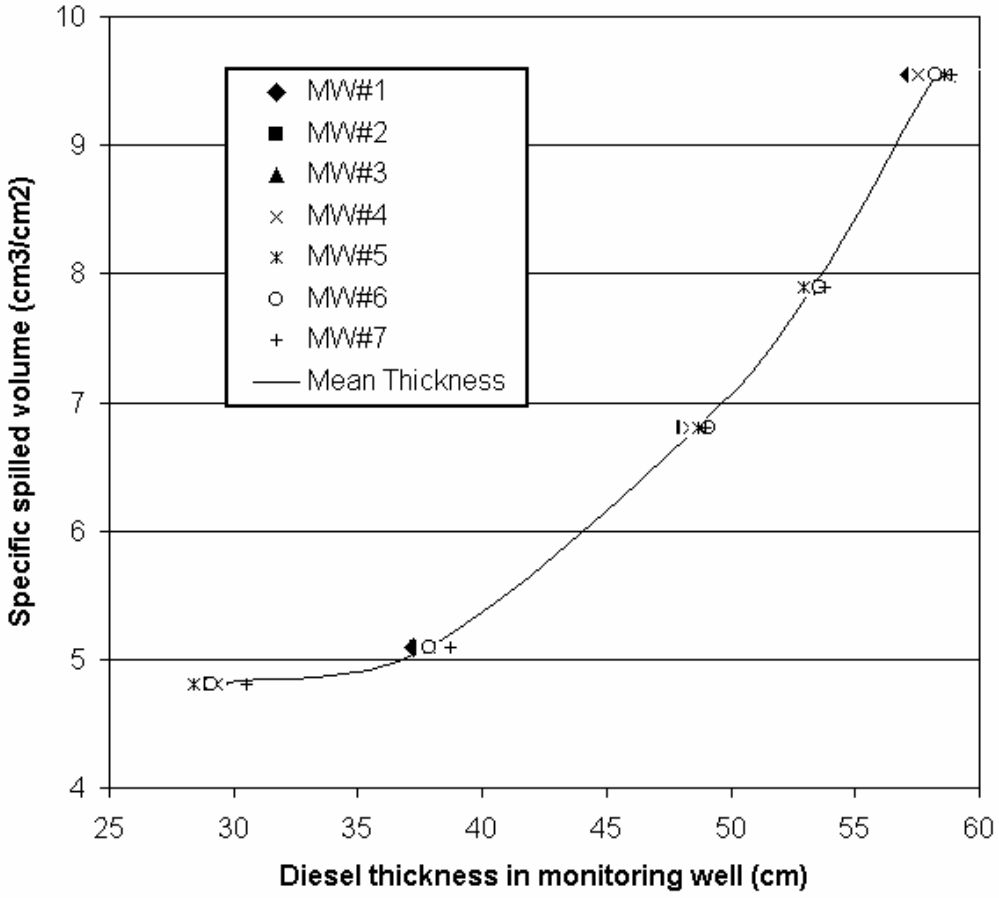

Figure 5.1: Specific spilled volume as a function of average and measured diesel thickness in seven monitoring wells (uniform sand).

The actual measurements of x and h_a were used to indicate the validity of the equations having the parameters of the Black and Hall (1984) model, where x is the interface distance below groundwater table within well and h_a is the free product distance to the groundwater table within the porous media. All relevant parameters required in the models were obtained for the present case, namely uniform sand as a porous medium and diesel as hydrocarbon contamination for comparison purposes. The same properties of sand and diesel were used to calculate the predicted diesel thickness in the monitoring well as a function of spilled diesel in the porous medium. The comparison of the experimental results with the results predicted by different empirical, analytical and mathematical models is presented in table 5.1. Pictorial comparison of results is presented in figure 5.2.

It can be seen from table 5.1 and figure 5.2 that the predictions made by the methods of dePastrovich *et al.* (1979), Black and Hall (1984), and the mathematical model developed in the present study are close to the experimental results. However, errors in these studies are in the range of 3.4 to 17.6%, 7.1 to 51.5% and 5.8 to 10.7% respectively. The comparative study shows that the predictions obtained from the developed mathematical model, which is based on well-established theoretical relations and laws, are very close and the standard deviation ranges between 0.1 and 11.5. A comparison was also made by calculating the average percentage error in the predictions and is presented in table 5.1. The developed theoretical model was found to be the best predictor of diesel thickness in the monitoring wells with a percentage error of 5.8 to 10.7% (average 7.18%).

Table 5.1: Comparison of experimental results with the results from predictive models (uniform sand with diesel).

Specific Spilled Volume in PM.	Measured Diesel Thickness in MW.	Predicted Diesel Thickness in MW						
		DePastrovich *et al.* (1979)	Hall *et al.* (1984)	Black and Hall (1984)	Schiegg (1985)	Farr *et al.* (1990)	Ballestero *et al.* (1994)	Present Study
4.80	29.10	33.60	12.30	29.10	16.80	61.28	60.00	30.00
5.92	43.70	41.44	13.42	35.19	17.92	65.05	67.92	42.80
6.80	49.60	47.60	14.30	37.16	18.80	68.01	74.08	50.80
7.90	53.10	55.30	15.40	38.97	19.90	71.72	82.16	53.20
9.55	58.20	66.85	17.05	41.64	21.55	77.27	94.72	74.60
Average % Error		8.73	67.98	19.92	57.77	52.88	65.69	7.18

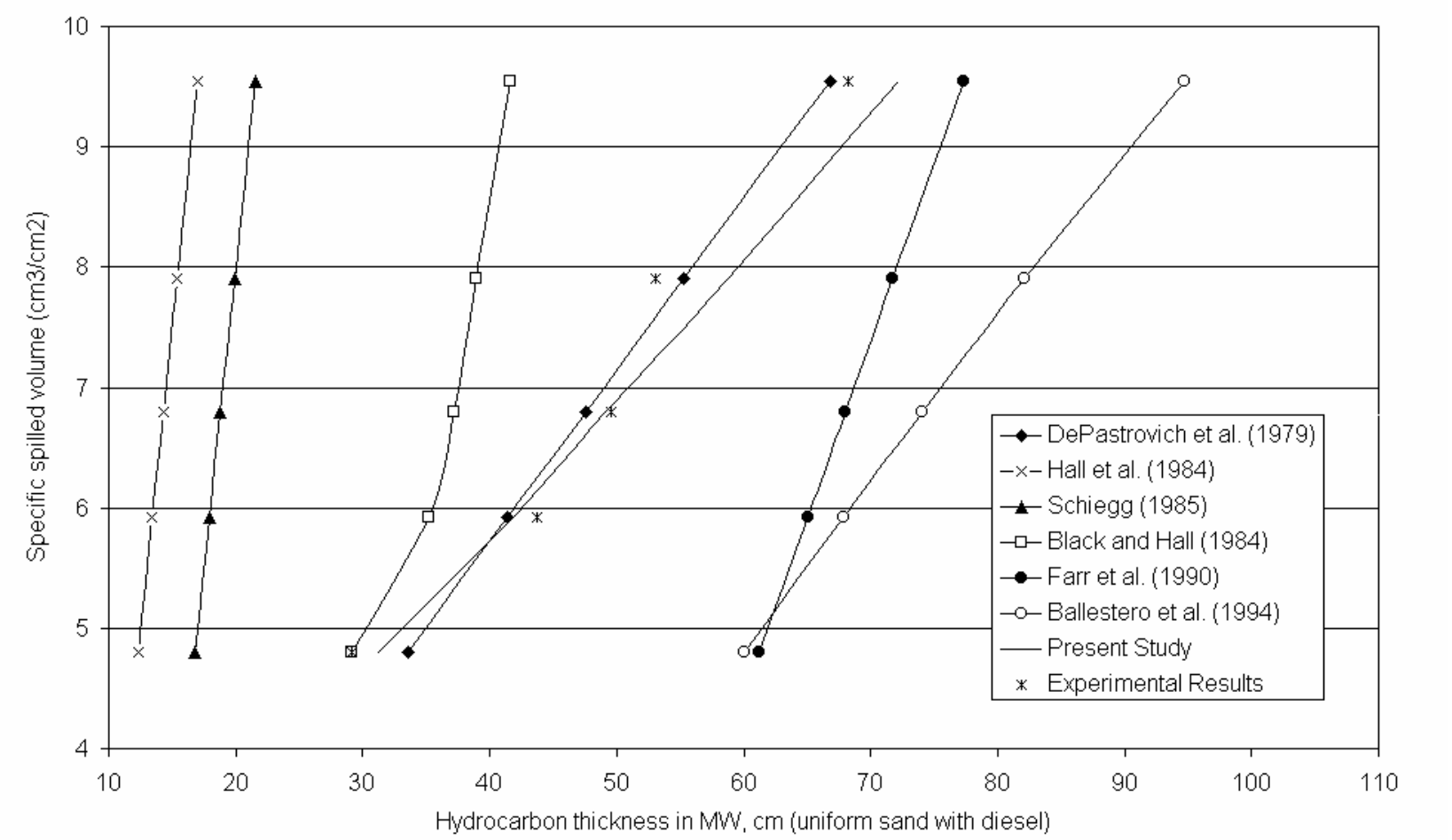

Figure 5.2: Comparison of experimental results with the results from predictive models.

5.1.2 Data Based on Fluctuating Water Table Conditions

In order to assess the relationship between spilled hydrocarbon volume and its thickness in the monitoring well with water table fluctuations, data was collected with water table fluctuating conditions. In the experimental study the water table elevation was changed (increased and decreased) in gradual increments from the initial level of 30 cm. With each water table elevation, data of spilled diesel in the porous medium and in the monitoring well were collected along with the depth of diesel/water and diesel/air interfaces.

In the rising water table scenario, the water table varied from 30 cm to 70 cm with an increment of 10 cm. Similarly, for the falling water table scenario, the water table was decreased from 70 cm to 30 cm with a decrease of 10 cm.

5.1.2.1 Verification of mathematical model for fluctuating water table conditions

Computer simulations were performed to obtain the model predictions based on dynamic water table conditions. A step of 5 cm (change in the water table elevation) was used to perform water table rising and falling simulations. It is to be noted that at the highest and lowest water table elevation regions a step of 1 cm was used to get a clearer picture at the reversal points. Experimental results obtained during the first run under fluctuating water table conditions were utilised for comparison with the simulation results. Figure 5.3 presents the comparison of the experimental and predicted results obtained under fluctuating water table conditions. It can be seen from the figure that the model over-predicted the diesel thickness in the monitoring wells at the low water table

region (maximum deviation is 85.1%). It is also obvious that the falling water table scenario predictions are much closer as compared to the rising water table scenario. However, at the higher water table region model predictions (based on rising and falling water table scenarios) are in close agreement with the experimental results (maximum deviation is 16.2%). Some of the differences may be accounted for by measurement error, non-equilibrium or experimental technique problems and heterogeneity effects.

Considering the shape of the curves at the higher water table region it can be seen that at the reversal point (i.e. historically maximum water table value) a slight decrease in the water table causes a sudden increase in diesel thickness in the monitoring well. This prediction is consistent with the field observations reported by several researchers in the past (Kemblowski and Chiang, 1990; Ballestero *et al.* 1994; Marinelli and Durnford (1996). Marinelli and Durnford reported that for a relatively large rise in water table elevation, complete entrapment is expected to cause a dramatic disappearance of LNAPL in a well. When the water table falls, substantial thicknesses of LNAPL can suddenly appear in the well.

Results show that as the water table rises, an increasingly large proportion of the entrapped hydrocarbon and the hydrocarbon which can flow (the mobile phase) decreases. These simulation results also suggest that the amount of hydrocarbon which can be removed from the soil is at its maximum when the water table elevation is at its historically low value (water table elevation < 30 cm). Similarly one can see from figure 5.3 that as the water table rises, a point can be reached where all the mobile phase hydrocarbons may become entrapped (water table elevation > 70 cm).

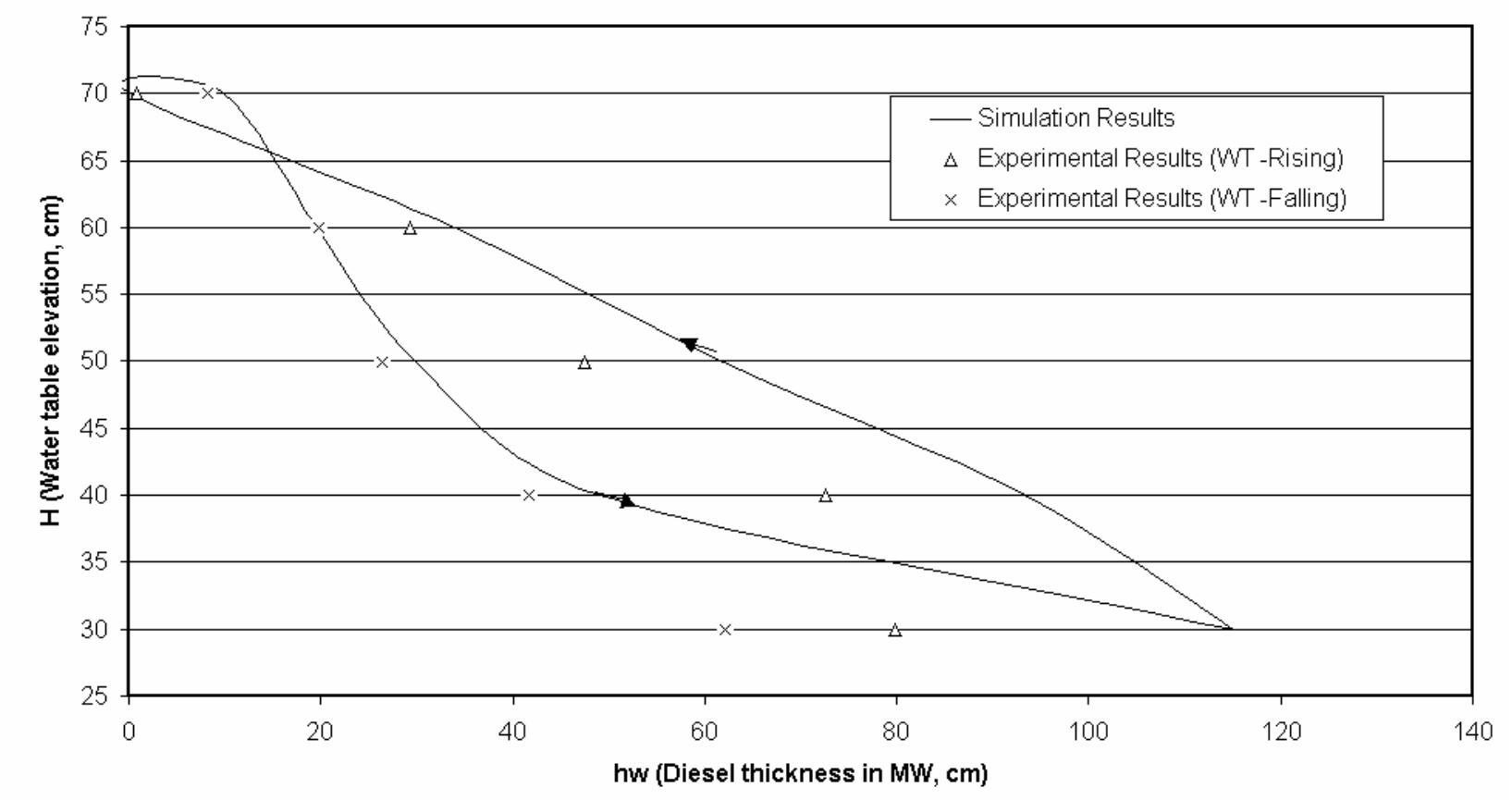

Figure 5.3: Comparison of simulation results with the experimental results (Uniform sand with diesel).

5.2 Uniform Porous Medium with Kerosene Contamination

In the second run, similar to the first run, the sandbox was filled with uniform sand, saturated with water and subsequently drained up to the water level at 30 cm above the base of the sandbox. Afterwards the sand box was allowed to reach the quasi-static equilibrium for 10 days.

An initial volume of 20000 ml of dyed kerosene was released into the sandbox. The system was then allowed to reach quasi-static equilibrium for 12 days. After 12 days an additional volume of 500 ml was released. The process continued until kerosene appeared in one of the monitoring wells. Once the coloured kerosene appeared in all seven monitoring wells the critical volume was then noted. The critical volume for this run was found to be equal to 21500 ml.

5.2.1 Data Based on Static Water Table Conditions

A graph of specific spilled volume versus average thickness of kerosene in the monitoring wells is presented in figure 5.4. It can be seen in the graph that the critical spilled volume of kerosene for uniform sand is 4.3 cm. It can be seen that with the increase in spilled volume of kerosene in the porous medium, kerosene thickness in the monitoring wells also increases. However, the rate of increase slowed when the kerosene thickness in the monitoring well reached 40 cm. Similar to the results of previous run, Figure 5.4 clearly shows two distinct segments. The first segment, at lower spilled volumes, when the rate of increase of kerosene thickness in monitoring wells is higher (up to the kerosene thickness of 40 cm) and the second segment, at higher spilled volumes, when the rate of increase is low and the slope is steep. By comparing the graphs

of figure 5.1 and figure 5.4, it can be seen that the point of inflection (at which slope changes from temperate to steeper) is reached earlier in the case of diesel which has a higher specific gravity than kerosene (0.875 versus 0.8).

5.2.1.1 Verification of mathematical model for hydrostatic conditions

In order to perform the simulations, uniform porous medium and kerosene properties, presented in table 5.1 and 5.2, were used as model input. Verification of the mathematical model was also done by comparing the simulation results with different empirical and analytical models mentioned in section 5.1.1.1. The comparison of the experimental results with the results predicted by different empirical, analytical and mathematical models is presented in table 5.2. and in figure 5.5.

Table 5.2 and figure 5. show that the predictions made by the methods of Black and Hall (1984), dePastrovich *et al.* (1979), and the mathematical model developed in the present study are close to the experimental results. However, errors in these studies are in the range of 0.2 to 44.9%, 7.6 to 24.9% and 3.7 to 19.7% respectively. Comparison shows that the predictions obtained from the developed mathematical model are very close and the standard deviation ranges from 0.4 to 5.5. Comparison based on calculated average percentage error shows that the developed theoretical model was found to be the best predictor of kerosene thickness in the monitoring wells with a percentage error of 3.7 to 19.7% (average 7.77%).

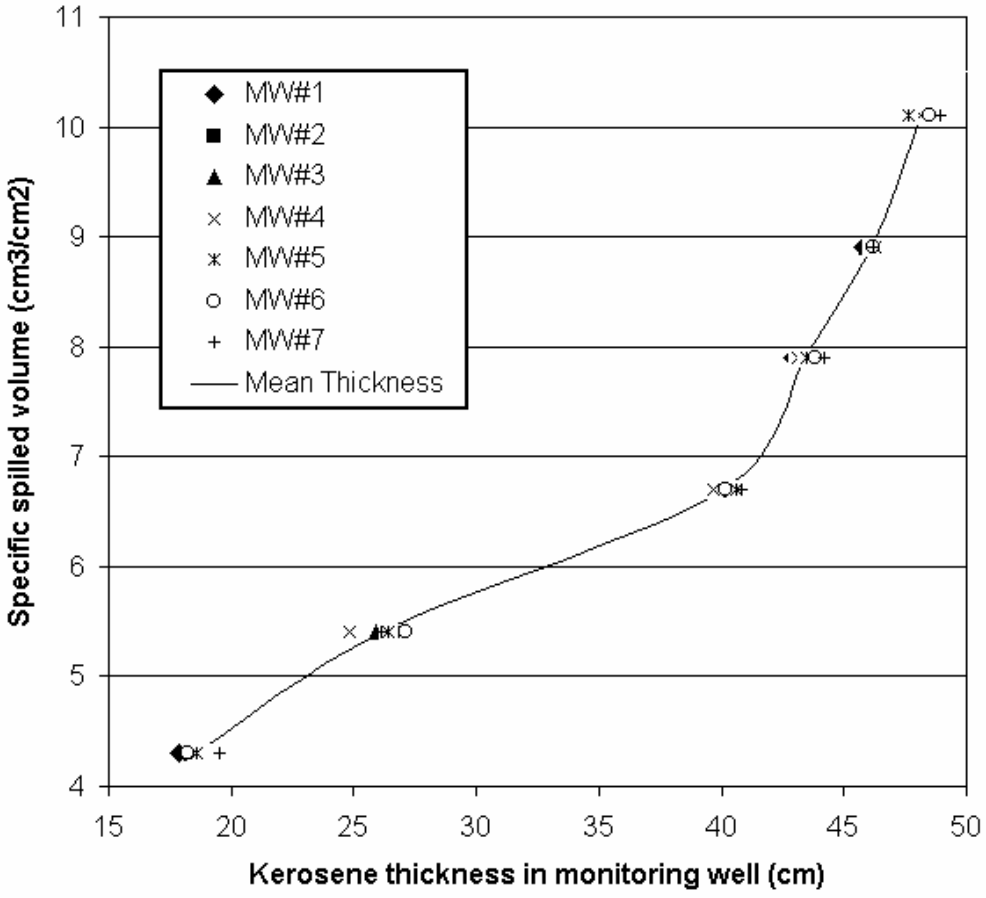

Figure 5.4: Specific spilled volume as a function of average and measured kerosene thickness in seven monitoring wells (uniform sand).

Table 5.2: Comparison of experimental results with the results from predictive models (uniform sand with kerosene).

Specific Spilled Volume in PM.	Measured Kerosene Thickness in MW.	Predicted Kerosene Thickness in MW						
		DePastrovich *et al.* (1979)	Hall et al. (1984)	Black and Hall (1984)	Schiegg (1985)	Farr et al. (1990)	Ballestero *et al.* (1994)	Present Study
4.3	18.6	17.2	11.8	25.3	16.3	40.24	35	17.9
5.4	26.2	21.6	12.9	29.57	17.4	43.94	39.85	24.9
6.7	40.1	26.8	14.2	35.01	18.7	48.32	46.05	32.2
7.9	43.4	31.6	15.4	38.4	19.9	52.36	51.5	39
8.9	46.1	35.6	16.4	40.13	20.9	55.72	56.15	44.2
10.1	48.1	40.4	17.6	41.99	22.1	59.76	61.95	50
Average % Error		20.71	57.38	16.46	43.70	45.05	37.40	7.77

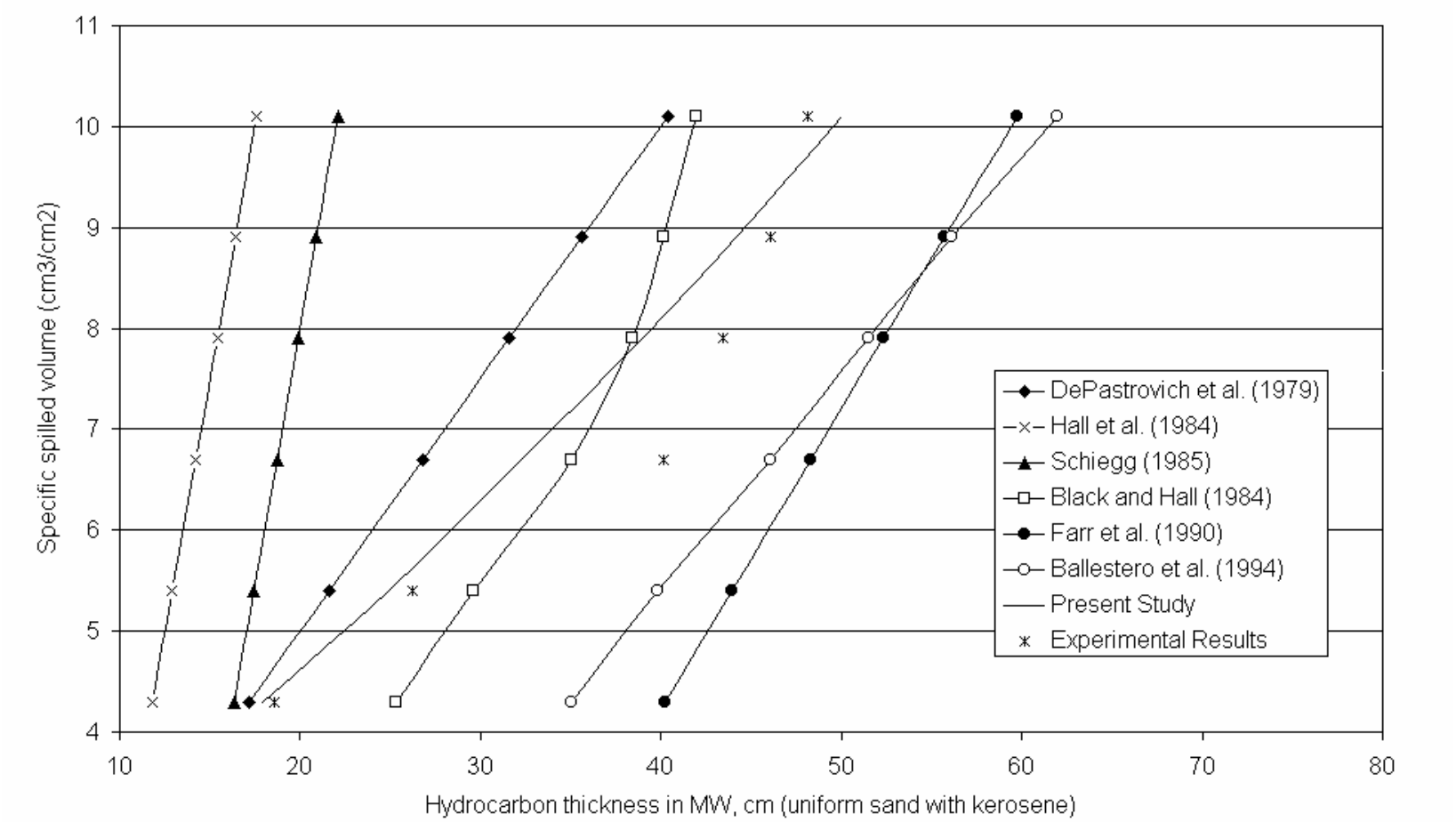

Figure 5.5: Comparison of experimental results with the results from predictive models.

5.2.2 Data Based on Fluctuating Water Table Conditions

In the second run, data of kerosene thickness in the monitoring wells and in the porous medium were collected with the water table fluctuating conditions. As with the first run, the water table elevation was changed (increased and decreased) in gradual increments of 10 cm from the initial level of 30 cm. With each water table elevation, data of spilled kerosene in the porous medium in the monitoring well along with the depth of kerosene/water and kerosene/air interfaces were collected. The same procedure was adopted to get the falling water table data.

5.2.2.1 Verification of mathematical model for fluctuating water table conditions

Computer simulations were performed to obtain the predicted results of kerosene thickness in the monitoring well based on fluctuating water table conditions. The water table elevation varied in steps of 1 to 5 cm for both falling and rising water table scenarios. Simulation results obtained were compared with the experimental results obtained during the second experimental run. A comparison of the experimental results and model predictions are presented in figure 5.6. It is seen from figure 5.6 that the model overpredicted the results at high water table region (maximum deviation 47.2%). However, at low water table region model predictions (based on rising and falling water table scenarios) are in close agreement with the experimental results (maximum deviation 7.9%). Reasons for differences in the results could be measurement error or and heterogeneity. It may also be possible that the system may not have reached quasi-static

equilibrium when the reading was taken. However, the preliminary run showed that 10 to 12 days were enough for the system to reach quasi-static equilibrium.

5.3 Well-Graded Porous Medium with Diesel Contamination

In the third run, the sandbox was filled with well-graded sand, saturated with water and subsequently drained up to the water level at 30 cm above the base of the sandbox. The sand box was then allowed to reach the quasi-static equilibrium for 10 days.

In this run, an initial volume of 20000 ml of dyed diesel was released into the sandbox following quasi-static equilibrium achievement. The system was then allowed to reach quasi-static equilibrium for 12 days. Subsequently an additional volume of 500 ml was released. The process continued until diesel appeared in one of the monitoring wells. Once the coloured diesel appeared in all seven monitoring wells, the critical volume was noted. The critical volume for this run was found to be equal to 20750 ml.

5.3.1 Data Based on Static Water Table Conditions

Data of specific spilled volume and corresponding hydrocarbon thickness in all monitoring wells for the third run are presented in figure 5.7. It is seen that the critical spilled volume of diesel for well-graded sand is 4.15 cm. Figure 5.7 also shows that with

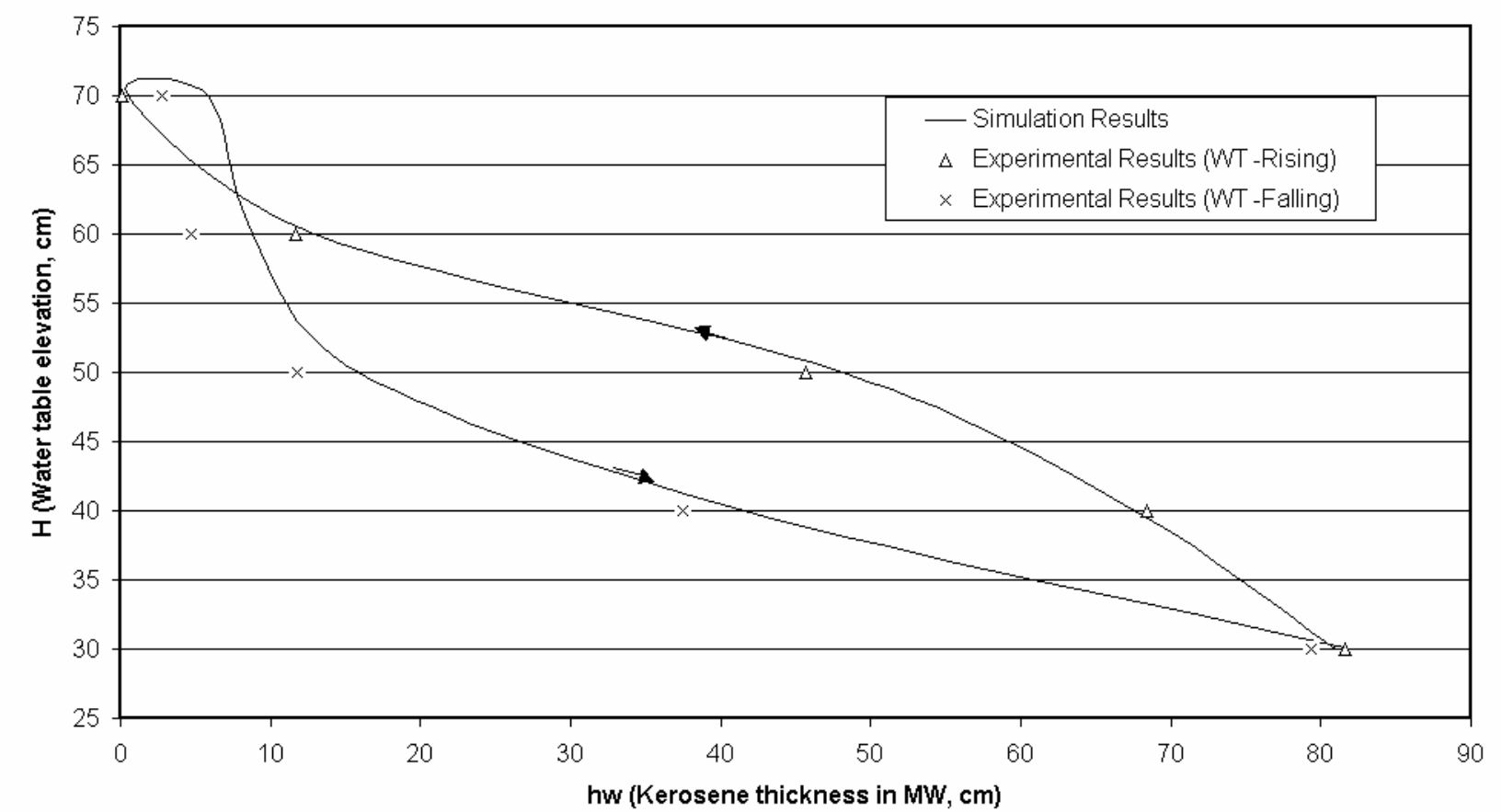

Figure 5.6: Comparison of simulation results with the experimental results (Uniform sand with kerosene).

the increase in volume of spilled diesel in the porous medium, the thickness of diesel in the monitoring wells also increased. It is important to note that unlike the first and second runs, which had uniform soil as porous medium, well-graded sand does not show two distinct segments in the plot. This could be attributed to the high capillary fringe available for well-graded sand as compared to uniform sand.

5.3.1.1 Verification of mathematical model for hydrostatic conditions

Once again, simulations based on static water table conditions were performed to get the predicted results for comparison. Predicted results were compared with the measured as well as with different empirical and analytical models mentioned in section 5.1.1.1.

Comparison of the experimental results with the results predicted by different empirical, analytical and mathematical models is presented in table 5.3. A graphical comparison of results is also presented in figure 5.8.

It is clear from table 5.3 and figure 5.8 that the predictions made by the methods of dePastrovich *et al.* (1979), and the mathematical model developed in the present study are close to the experimental results. However, errors in both studies are in the range of 1.9 to 15.5% and 0.6 to 6.1% respectively. Comparison shows that the predictions obtained from the developed mathematical model are very close with a standard deviation of 0.1 to 1.4. On the basis of average percentage error, the developed theoretical model was found to be the best predictor of diesel thickness in the monitoring wells with a percentage error of 0.6 to 6.1% (average 2.44%).

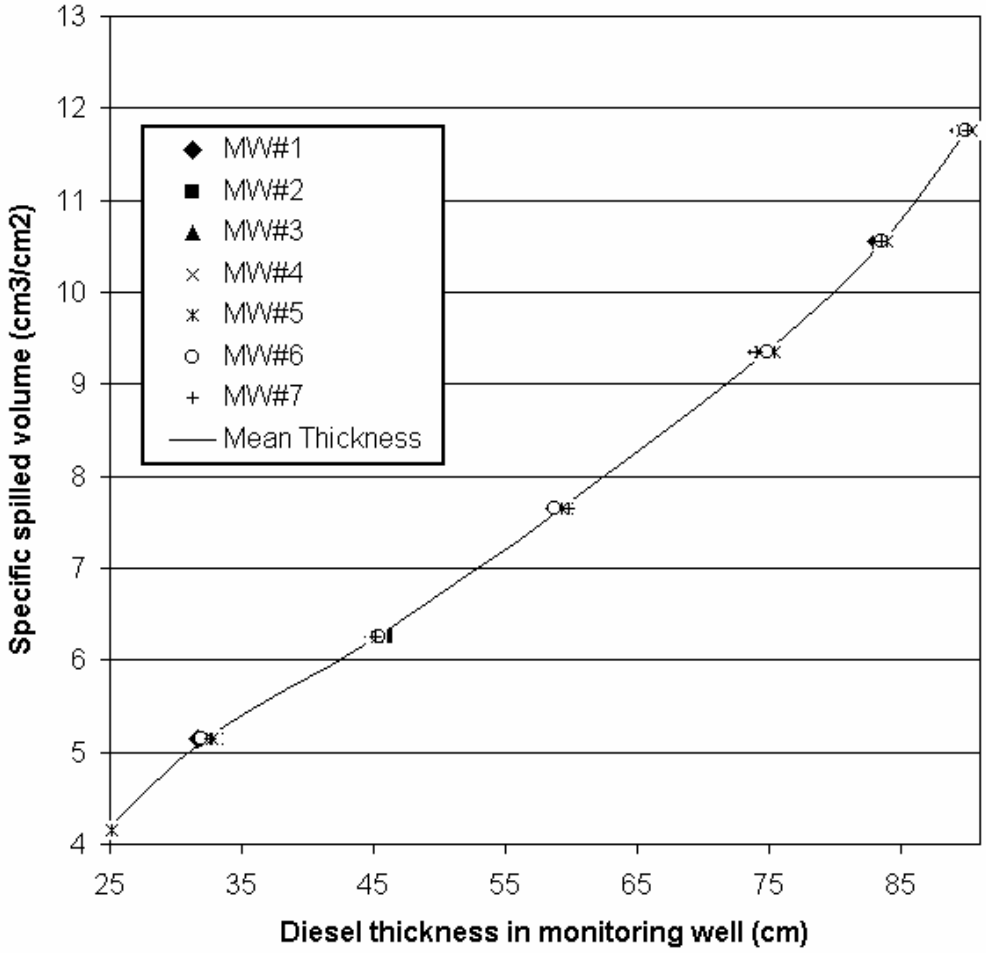

Figure 5.7: Specific spilled volume as a function of average and measured diesel thickness in seven monitoring wells (well-graded sand).

Table 5.3: Comparison of experimental results with the results from predictive models (well-graded sand with diesel).

Specific Spilled Volume in PM.	Measured Diesel Thickness in MW.	Predicted Diesel Thickness in MW						
		DePastrovich *et al.* (1979)	Hall *et al.* (1984)	Black and Hall (1984)	Schiegg (1985)	Farr et al. (1990)	Ballestero *et al.* (1994)	Present Study
4.15	24.7	29.05	16.65	26.45	16.15	62.22	54.8	23.8
5.15	32.4	36.05	17.65	31.77	17.15	66.34	62.16	34.4
6.25	45.3	43.75	18.75	35.26	18.25	70.86	70.08	45
7.65	59.3	53.55	20.15	38.25	19.65	76.63	80.4	59.1
9.35	74.7	65.45	21.85	40.68	21.35	83.62	93.44	73.4
10.55	83.6	73.85	23.05	42.1	22.55	88.56	102.4	82.8
11.75	89.9	82.25	24.25	43.63	23.75	93.50	111.44	93.1
Average % Error		10.65	59.85	30.48	60.90	52.03	53.65	2.44

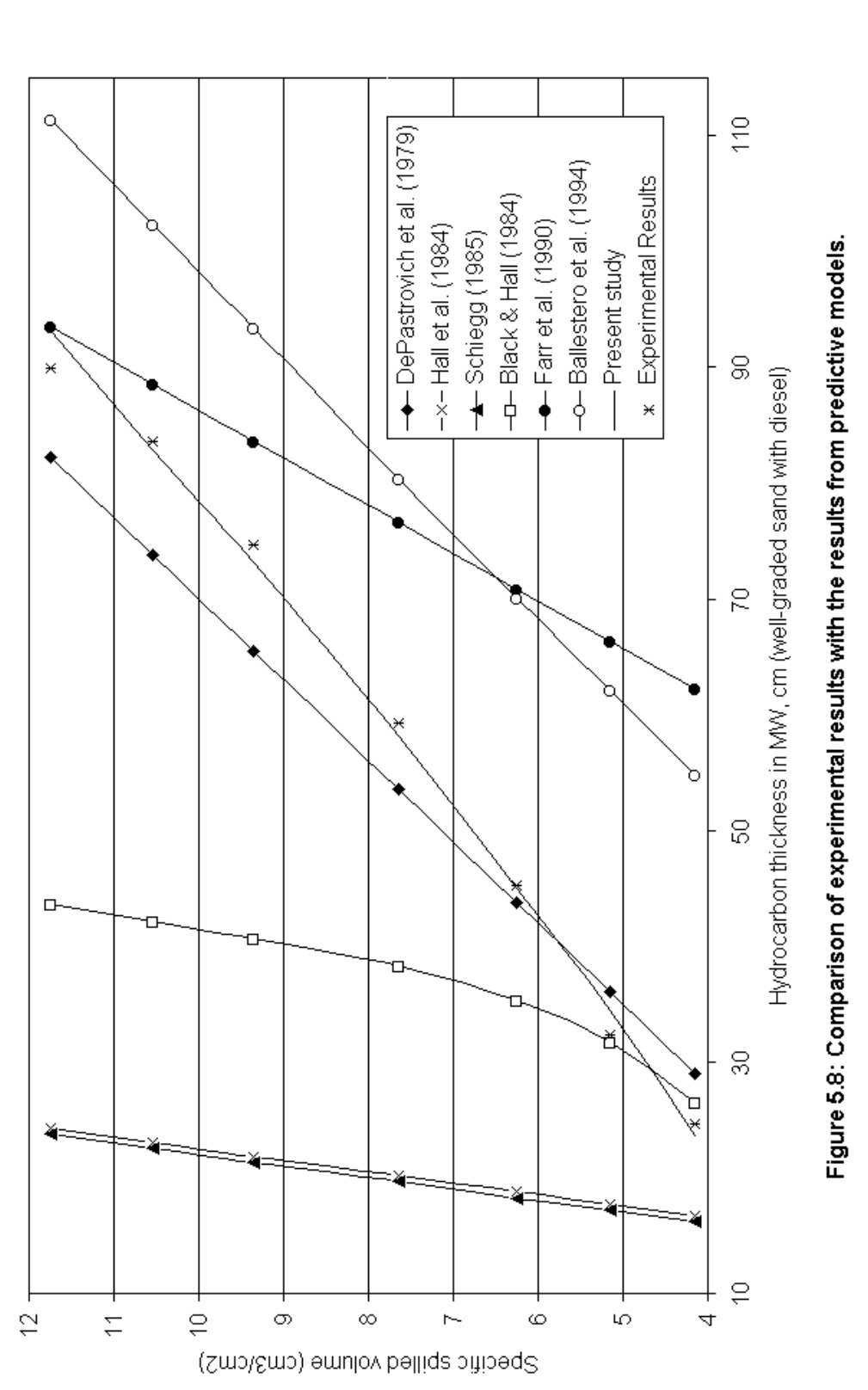

Figure 5.8: Comparison of experimental results with the results from predictive models.

5.3.2 Data Based on Fluctuating Water Table Conditions

In order to verify the model for fluctuating water table conditions data of water table elevation and the corresponding diesel thickness in the monitoring well were collected. As with the previous runs, water table elevation was changed (increased and decreased) in 5 cm increments and all relevant data were collected.

5.3.2.1 Verification of mathematical model for fluctuating water table conditions

A comparison of the simulation results with the experimental results for the third run is presented in figure 5.9. It can be seen from figure 5.9 that the model predictions are higher than the experimental results at low water table region (maximum deviation 70.3%). However, at higher water table regions the model predictions (based on rising and falling water table scenarios) are comparable with the experimental results. The maximum deviation observed is 6.4 It is clear from figure 5.3, 5.6, and 5.9 that the model predictions are much better in lower water table region for less denser hydrocarbons (e.g. kerosene) while model predictions are in close agreement at a higher water table region for denser hydrocarbons (e.g. diesel).

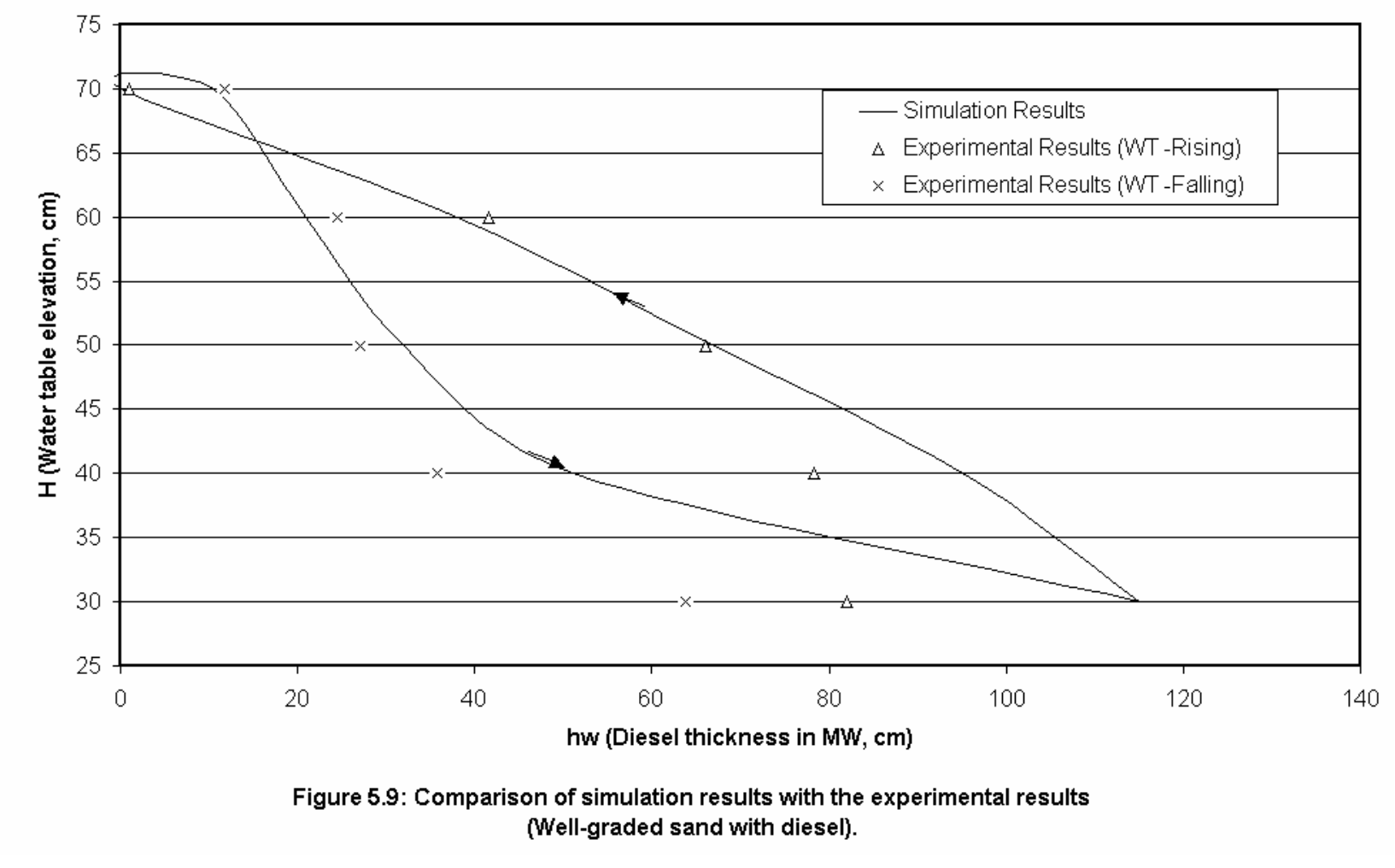

Figure 5.9: Comparison of simulation results with the experimental results (Well-graded sand with diesel).

5.4 Well-Graded Porous Medium with Kerosene Contamination.

In the fourth and last run, the sandbox was again filled with fresh well-graded sand, saturated with water and subsequently drained up to the water level of 30 cm above the datum. After draining, the sandbox was allowed to reach the quasi-static equilibrium for 10 days. Following (the quasi-static equilibrium) achievement of this state, an initial volume of 18500 ml of dyed kerosene was released into the sandbox. The system was agin left for 12 days to allow it to reach quasi-static equilibrium (for 12 days). After two weeks an additional volume of 500 ml was released. This process continued until the coloured kerosene appeared in all monitoring wells and then the critical volume was noted. The critical volume for this run was found to be 19500 ml.

5.4.1 Data Based on Static Water Table Conditions

A graph plotting of specific spilled volume versus average thickness of kerosene in the monitoring wells is presented in figure 5.10. It may be seen that the critical spilled volume of kerosene for well-graded sand is 3.9 cm. Figure 5.10 shows that with the increase in spilled volume of kerosene in the porous medium, kerosene thickness in the monitoring wells also increased. However, as with the third run (well-graded sand as the porous medium) but unlike the first and second runs (uniform soil as the porous medium) well-graded sand does not show two distinct segments in the graph. By comparing figures 5.1, 5.4, 5.7, and 5.10 it can be concluded that the general shape of the first two curves is similar, showing two distinct segments, while the last two curves show similar single

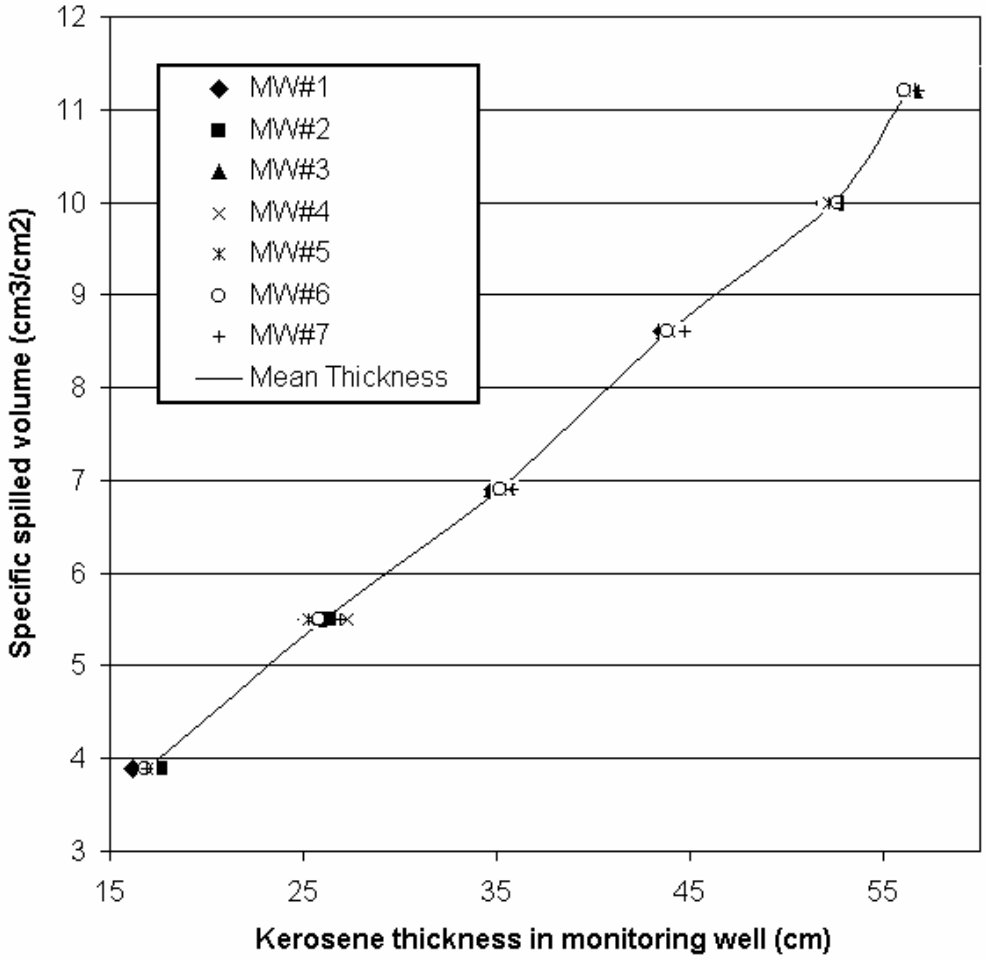

Figure 5.10: Specific spilled volume as a function of average and measured kerosene thickness in seven monitoring wells (well-graded sand).

curves. Furthermore, in the case of well-graded sand, hydrocarbon thickness in the monitoring wells increases at nearly a constant rate. However, the dependency of the rate of hydrocarbon thickness increase in the monitoring wells needs further investigation.

5.4.1.1 Verification of mathematical model for hydrostatic conditions

The comparison of experimental results based on hydrostatic conditions with the results predicted by different empirical, analytical and mathematical models is presented in table 5.4. and figure 5.11. As with the last three runs, figure 5.11 enables us to compare the pattern of the predictions visually. Predictions made by the methods of Black and Hall (1984), dePastrovich *et al.* (1979), Schiegg (1985), and the mathematical model developed in the present study are close to the experimental results. However, errors in these studies are in the range of 11.5 to 36.2%, 7.5 to 33.1%, 15.1 to 59.2% and 1.6 to 10.0% respectively Comparison shows that the predictions obtained from the developed mathematical model are very close to the standard deviation of 0.8 to 3.0. Comparison based on average percentage error (table 5.4) shows that the developed theoretical model was found to be the best predictor of kerosene thickness in the monitoring wells with a percentage error of 1.6 to 10.0 (average 5.64%). However, the predictions of Black and Hall (1984) are also in close agreement with an average percentage error of 17.36%.

5.4.2 Data Based on Fluctuating Water Table Conditions

In the last and fourth run, data of kerosene thickness in the monitoring wells and in the porous medium was collected with the water table fluctuating conditions again.

Table 5.4: Comparison of experimental results with the results from predictive models (well-graded sand with kerosene).

Specific Spilled Volume in PM.	Measured Kerosene Thickness in MW.	Predicted Kerosene Thickness in MW						
		DePastrovich *et al.* (1979)	Hall *et al.* (1984)	Black and Hall (1984)	Schiegg (1985)	Farr *et al.* (1990)	Ballestero *et al.* (1994)	Present Study
3.9	16.9	15.6	16.4	24.5	26.9	41.81	33	15.2
5.5	26.1	22	18	27.27	28.5	48.40	40.35	24.9
6.9	35.2	27.6	19.4	35.26	29.9	54.16	46.8	33
8.6	43.9	34.4	21.1	39.87	31.6	61.15	54.85	42.7
10	53.3	40	22.5	41.59	33	66.91	61.45	49
11.2	56.2	44.8	23.7	43.05	34.2	71.85	67.25	55
Average % Error		18.65	41.07	17.36	31.45	63.23	40.45	5.64

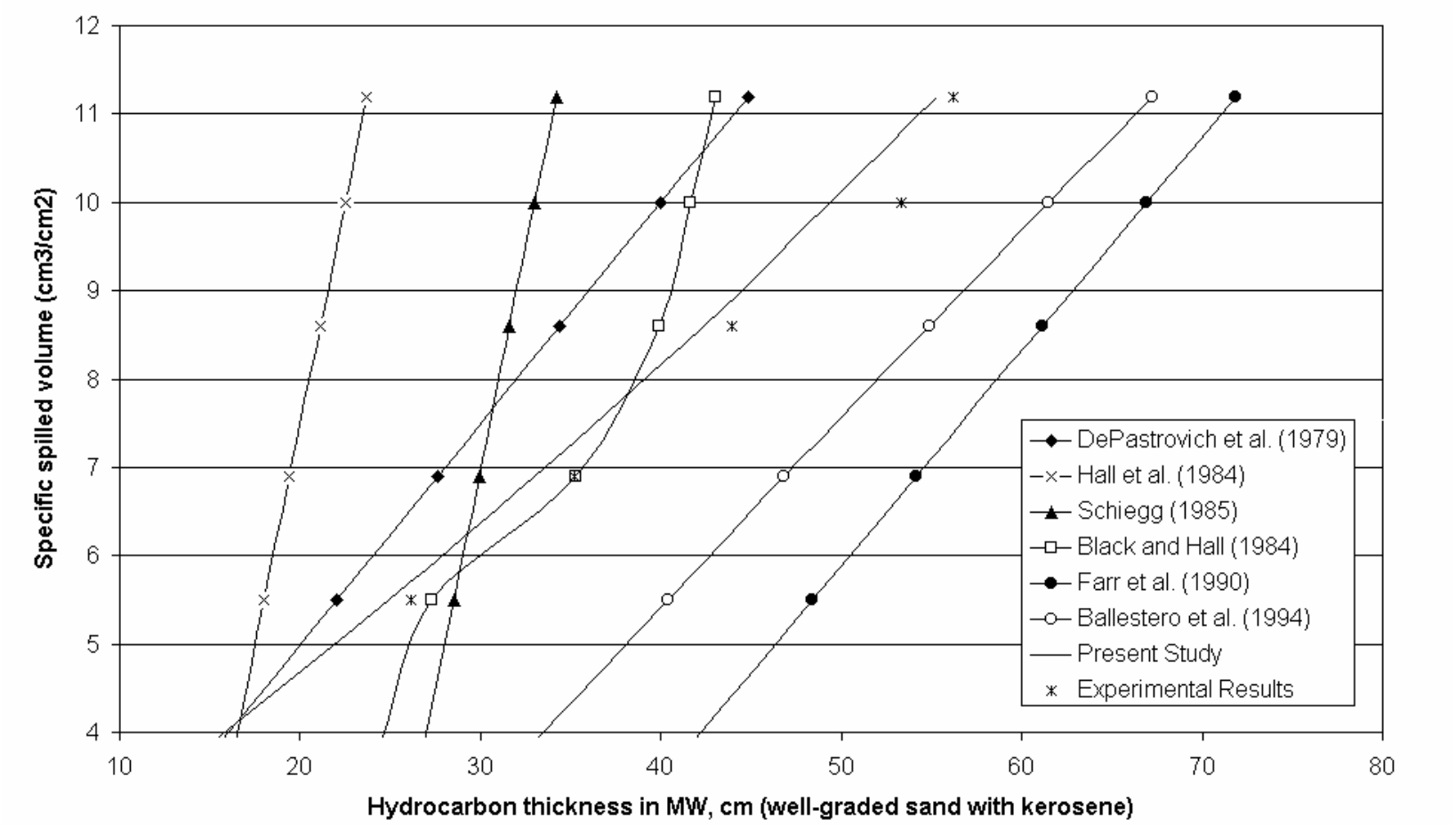

Figure 5.11: Comparison of experimental results with the results from predictive models.

As with the first run, water table elevation was changed (increased and decreased) in gradual increments of 10 cm from the initial level of 30 cm. With each water table elevation, data of spilled kerosene in the porous medium, in the monitoring well along with the depth of kerosene/water and kerosene/air interfaces, were collected. The same procedure was adopted to get the falling water table data.

5.4.2.1 Verification of mathematical model for fluctuating water table conditions

It may be seen from figure 5.12 that the model predictions deviate from experimental results at the high water table region and over-predicts the results by up to 43.4%. However, at low water table region model predictions (based on rising and falling water table scenarios) are in close agreement with the experimental results (maximum deviation 6.7%). Reasons for differences in the results are similar to those discussed in section 5.2.2.1.

5.5 Sensitivity Analysis

In order to examine the sensitivity of the developed model with the porous media and LNAPL properties a simple sensitivity analysis was performed. One parameter from each porous medium and LNAPL properties was selected and tested for model sensitivity. Sand porosity was selected to see how sensitive the model predictions are to this porous medium property. Similarly, to see the sensitivity of model predictions with the LNAPL properties, the density of LNAPL was used.

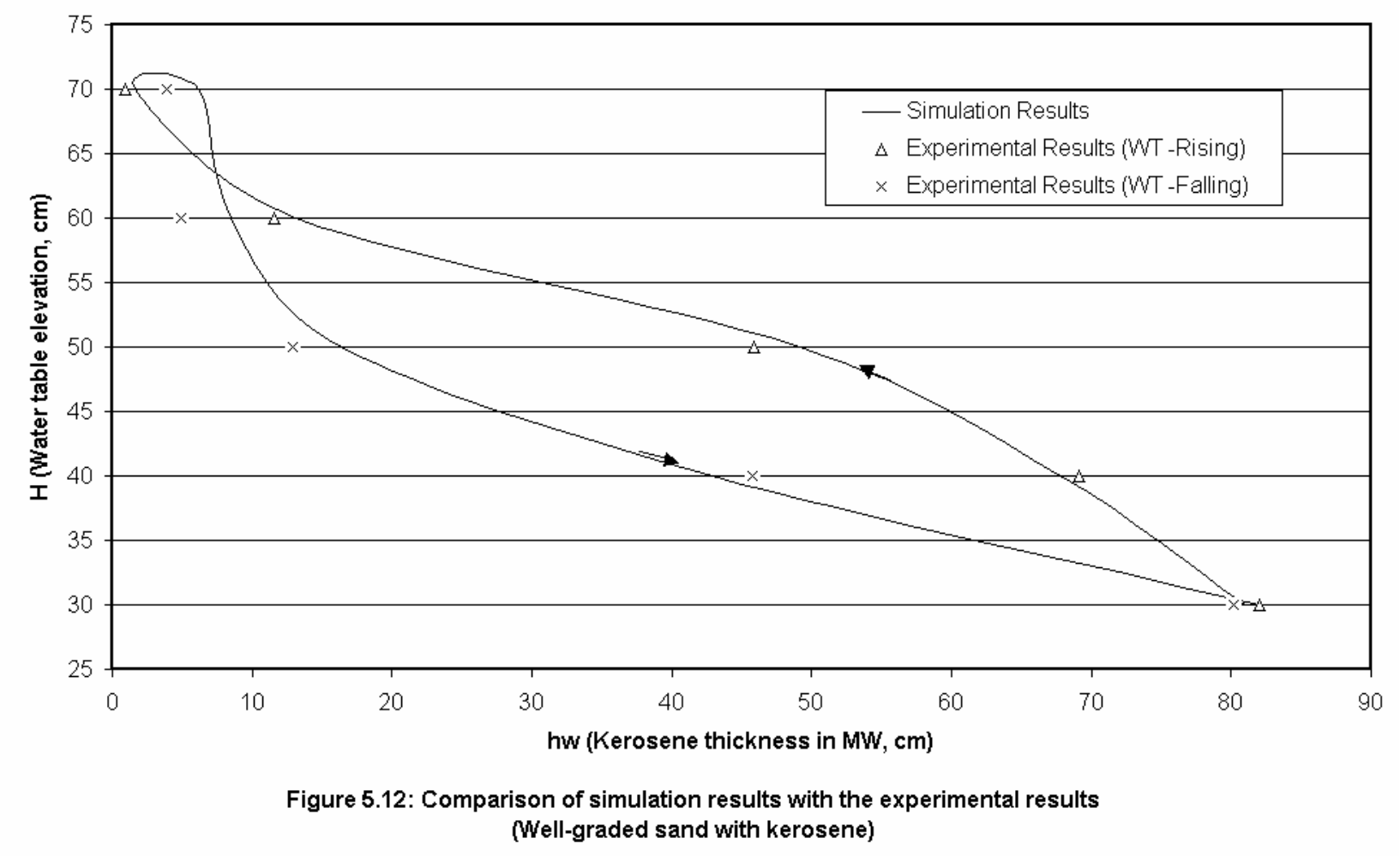

Figure 5.12: Comparison of simulation results with the experimental results (Well-graded sand with kerosene)

5.5.1 Simulation Procedure

Sensitivity analysis is used to ascertain how tested model output depends upon certain parameters. This is an important method for checking the quality of a given model, as well as a powerful tool for checking the robustness and reliability of its analysis (Saltelli *et al.,* 2000). Therefore, the sensitivity of the developed model predictions was tested by using data of the first run. The simulations carried out for the first run were considered as he base case for comparison purposes. All the input data used in the first run was kept as it is and only selected parameters were varied to see the effect of variation of selected parameter on model LNAPL thickness predictions.

5.5.1.1 Effect of sand porosity

In the base case, minimum and maximum porosity of sand was used as 0.31 and 0.41, respectively. These porosity values correspond to the maximum and minimum dry density values of uniform sand determined in the Geotechnical Engineering laboratory at KFUPM. The sensitivity of developed model predictions with the sand porosity is presented in figure 5.13. It is clear that the predicted LNAPL thickness varied slightly from each other. The effect of varying sand porosity is apparent only at intermediate values of LNAPL thickness. Curves of minimum and maximum porosity remain within the range of 9.4% of the base case which has a porosity input value of 0.37. Furthermore, the three curves tend to merge in both low and high water table regions.

5.5.1.2 Effect of LNAPL Density

Similar to previous sensitivity analysis, expected minimum and maximum density of LNAPL were used as 0.7 and 0.95, respectively. The sensitivity of developed model predictions with the LNAPL density is presented in figure 5. 14. It is seen that the predicted LNAPL thickness varied slightly from each other. The effect of varying LNAPL density is apparent only at lower and intermediate values of LNAPL thickness. Curves of the minimum and the maximum dry densities remain within the range of 7.4% of the base case which has LNAPL density input value of 0.875. In addition, all curves tend to merge at higher water table region.

If a model predictions are sensitive to one of its input elements it is usually required to further calibrate the model (DEQ, 2005). The above analysis shows that the developed model is not very sensitive to sand porosity and LNAPL density. Furthermore, this analysis shows that there is no need to put great effort into determining these parameters in the laboratory in a very accurate manner which makes the use of the model more attractive.

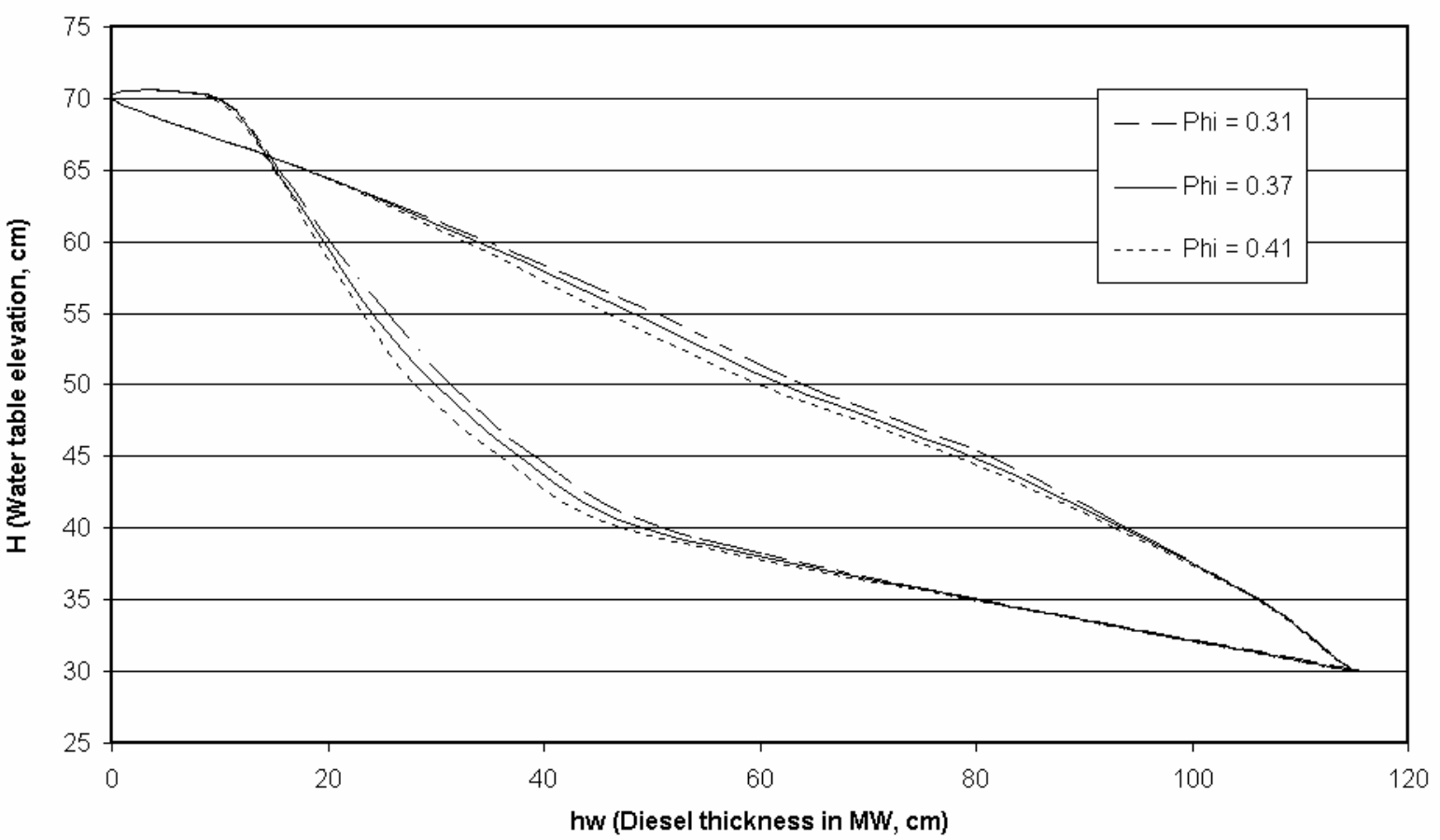

Figure 5.13: Effect of sand porosity on the model predictions (Uniform sand with diesel).

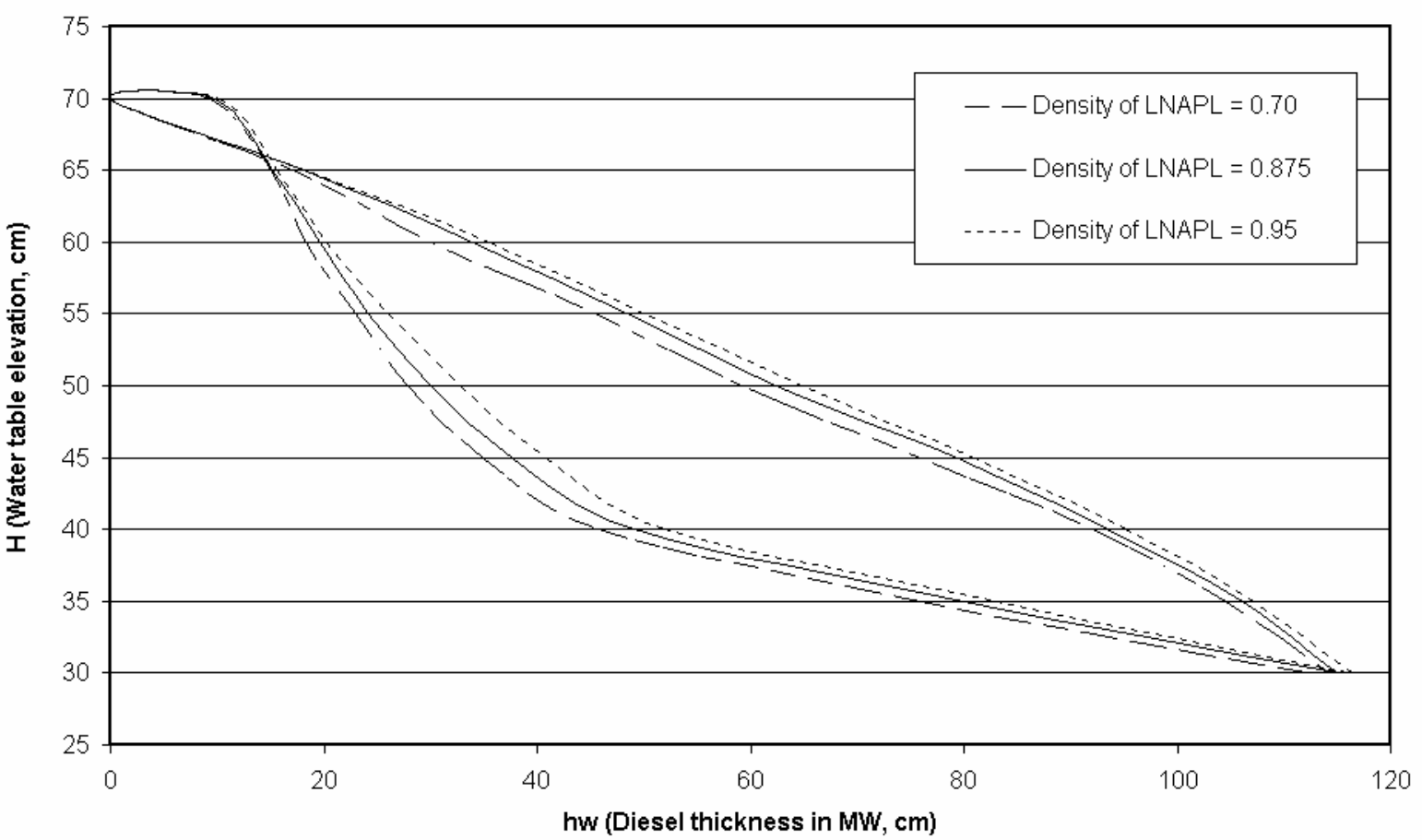

Figure 5.14: Effect of LNAPL density on the model predictions (Uniform sand with diesel).

CHAPTER 6

SUMMARY AND CONCLUSIONS

6.1 Summary

The quantification of spilled hydrocarbon has primary importance when carrying out the remediation work. In most cases, water-table elevations and hydrocarbon thickness are the primary field data, which is available in almost every field and may be used to evaluate the extent of hydrocarbon contamination. Different analytical and quantitative methods have been developed for spilled hydrocarbon estimates under constant water table conditions. However, because of uncertainty about the measurement of hydrocarbon thickness in the monitoring wells, there has been a marked paucity of research into fluctuating water table conditions.

The objective of this study was to assess the relationship between spilled hydrocarbon volume and its thickness in the monitoring well considering the history of fluctuation of the water table. In order to achieve the objectives, a mathematical model was developed which incorporates the aquifer hydrostatics and porous media properties. The developed model describes the relationship between spilled hydrocarbon in a porous media and its thickness in the monitoring wells. To obtain a better estimate of spilled hydrocarbon volume, water table fluctuation history, hysteresis and entrapment were incorporated.

An experimental setup was utilized to obtain data on hydrocarbon product thickness under the influence of water table fluctuation. The data obtained from the study were used to validate the mathematical model. Simulation results were compared with the experimental data as well as results reported in the literature.

In the laboratory study four experimental runs were performed. In the first run diesel and uniform sand were used and in the second run kerosene with the uniform sand were used. Similarly in the third and fourth runs well-graded sand was used with diesel and kerosene, respectively.

After the hydrocarbon spill was initiated, the critical spilled volumes for all four runs were noted as 4.8, 4.3, 4.15, and 3.9 cm^3/cm^2, respectively. Plots of specific spilled volume as a function of measured hydrocarbon thickness in uniform sand shows that the curve can be divided in two segments. The first segment, at lower spilled volumes, is when the rate of increase of hydrocarbon thickness in the monitoring well is higher and the second segment, at higher spilled volumes, is when the rate of increase is low. Unlike uniform sand, well-graded sand does not show two distinct segments in the curve but instead only one segment was clearly observed.

Comparison of the experimental results based on hydrostatic conditions with the results predicted by different empirical, analytical, and mathematical models was also performed. Models developed by Black and Hall (1984) and DePastrovich et al. (1979) are in good agreement with the experimental results. However, comparison on the basis of percentage error shows that the developed mathematical model is the best predictor in

all four cases (with percentage error of 5.8 to 10.7%, 3.7 to 19.7%, 0.6 to 6.1%, and 1.6 to 10.0% respectively).

In order to assess the relationship between spilled hydrocarbon and its thickness in monitoring wells with the consideration of water table fluctuations, experimental data was collected for all four cases. The model capability was validated by comparing the simulation results with the experimental results. In the first run the model overpredicted the results by up to 85.1% in the low water table elevation region. However, at higher water table elevation region, the model predictions are in close agreement with the experimental results (maximum 16.2%). Similarly, the second run model overpredicted the results with a maximum value of 47.2% and 7.9% at higher and lower water table elevation regions, respectively. In the third and fourth run, where well-graded sand was used, the model over predicted the results up to 70.3% and 43.4% in higher water table elevation region, respectively. However, model predictions are comparable with the experimental results in the low water table elevation region. The maximum over prediction of the model results are 6.4% and 6.7% in low water table elevation regions respectively.

A simple sensitivity analysis was performed in order to test the robustness and reliability of the developed model. Therefore, one parameter from each porous medium and the LNAPL properties was selected (sand porosity and LNAPL density) and tested for model sensitivity. It was found that the developed model is not very sensitive to sand porosity and LNAPL density. This analysis shows that the model is more reliable in use.

6.2 Conclusions

The following are the specific conclusions that have been drawn from the results of the model simulations and the experimental study:

1. Hydrocarbon/groundwater interface fluctuations correlate inversely with the hydrocarbon thickness in monitoring wells (i.e. as the interface in the well rises, the hydrocarbon thickness decreases, and vice versa).
2. The experimental and the simulation results show that the amount of hydrocarbon in a monitoring well is maximum when the water table elevation is at its historically low value. Similarly, as the water table rises, a point may be reached at which there will be no hydrocarbon present in the monitoring well.
3. The experimental observation shows that the hydrocarbon and water coexist in the porous media adjacent to the monitoring well from the hydrocarbon/water interface to the hydrocarbon/air interface. Furthermore, during the development of a saturated hydrocarbon fringe, no hydrocarbons flow into the monitoring well. Only the excess hydrocarbon starts to flow into the monitoring well.
4. The simulations and experimental results indicate that the relationships between hydrocarbon thickness in the monitoring well and the specific spilled volume are strongly dependent on the water table fluctuation history. Therefore, the inclusion of water table fluctuation history in a hysteretic entrapment predictive model has an impact on the predicted hydrocarbon distribution in the subsurface.
5. Comparison shows that simulated results are in close agreement with the measured experimental data. These verification studies indicated that the model presented in

this study may be used to predict the relationship between spilled hydrocarbon thickness in the porous media and in the monitoring well with reasonable accuracy.

6. It is found that the sensitivity of the developed model to the sand porosity and LNAPL density is quite low. This makes the use of the model more reliable.

CHAPTER 7

RECOMMENDATIONS

There exist a number of important areas, which need further research to predict the extent of hydrocarbon contamination. Researchers may focus their attention on refining and developing suitable models. The literature survey amply demonstrates that there exists a need to work out the relationship between field and laboratory parameters used as input for hydrocarbon transport and quantification models. This would eliminate the need for extensive field experiments.

Empirical models are mainly based on experimental evidence. Therefore, it is necessary to refine existing models or derive mathematical models from more fundamental physical laws. Most available models are derived to simulate idealized laboratory scale conditions and often do not apply to undisturbed field systems because of large-scale spatial variability effects and involved cost. An additional effort to derive field scale models is essential.

Studies on the relationship between hydrocarbon thickness in the monitoring wells and spilled hydrocarbon in the adjacent formation showed that there is potential for probing more into this area. In fact, this is a growing area of research to develop more accurate, efficient, and reliable estimates.

In order to evaluate the effect of hydrocarbons and porous media properties, a different range of hydrocarbons and porous media should be used.

A field study is needed to check the validity of developed mathematical models. The field study will also help in the calibration of the model.

Fluctuation in hydrocarbon thickness in a monitoring well depends on a number of factors, including backfill, overburden, soil heterogeneity and aquifer temperature. Therefore the influence of these factors may also improve model predictions.

APPENDIX-A

Flow Chart of Developed Mathematical Model

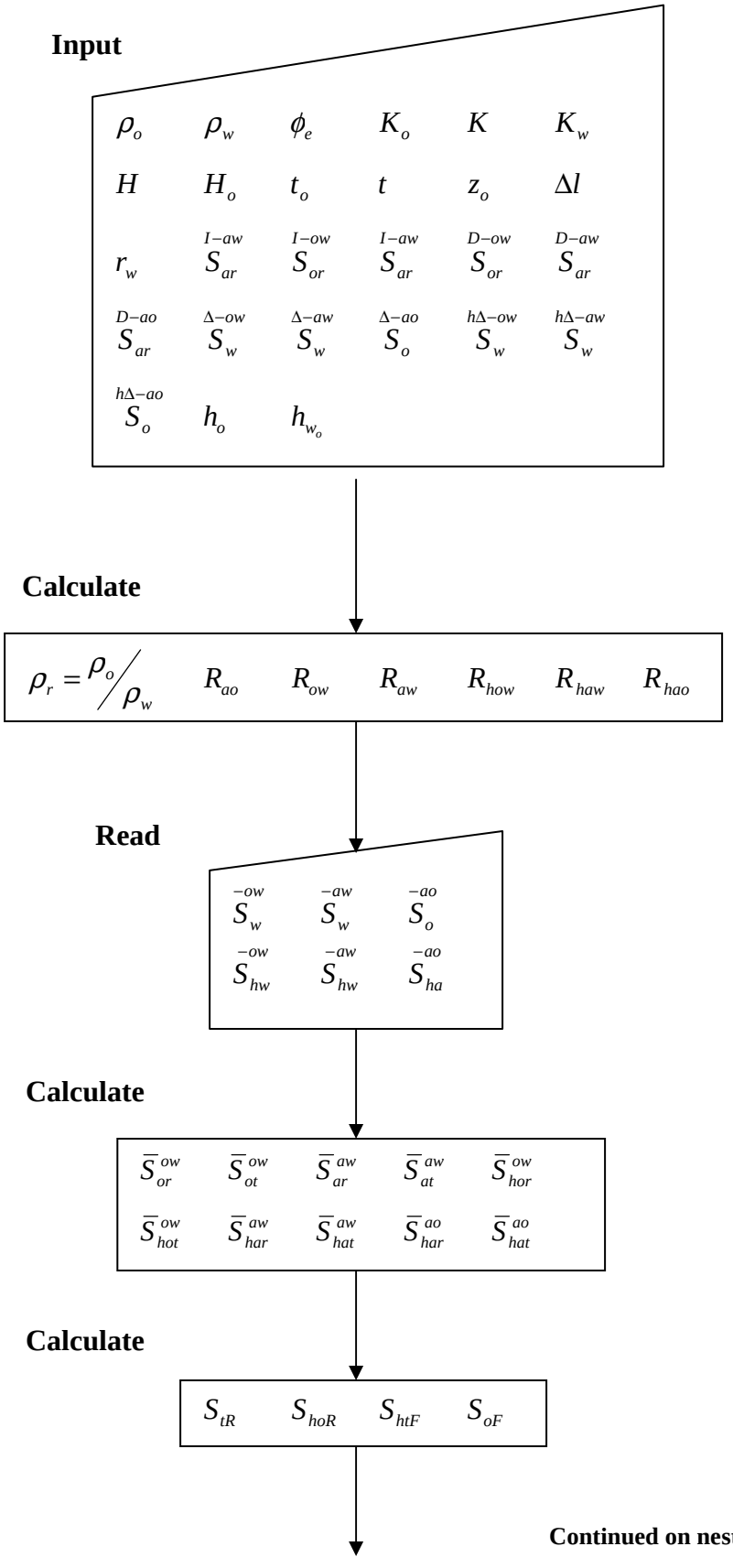

Continued on nest page

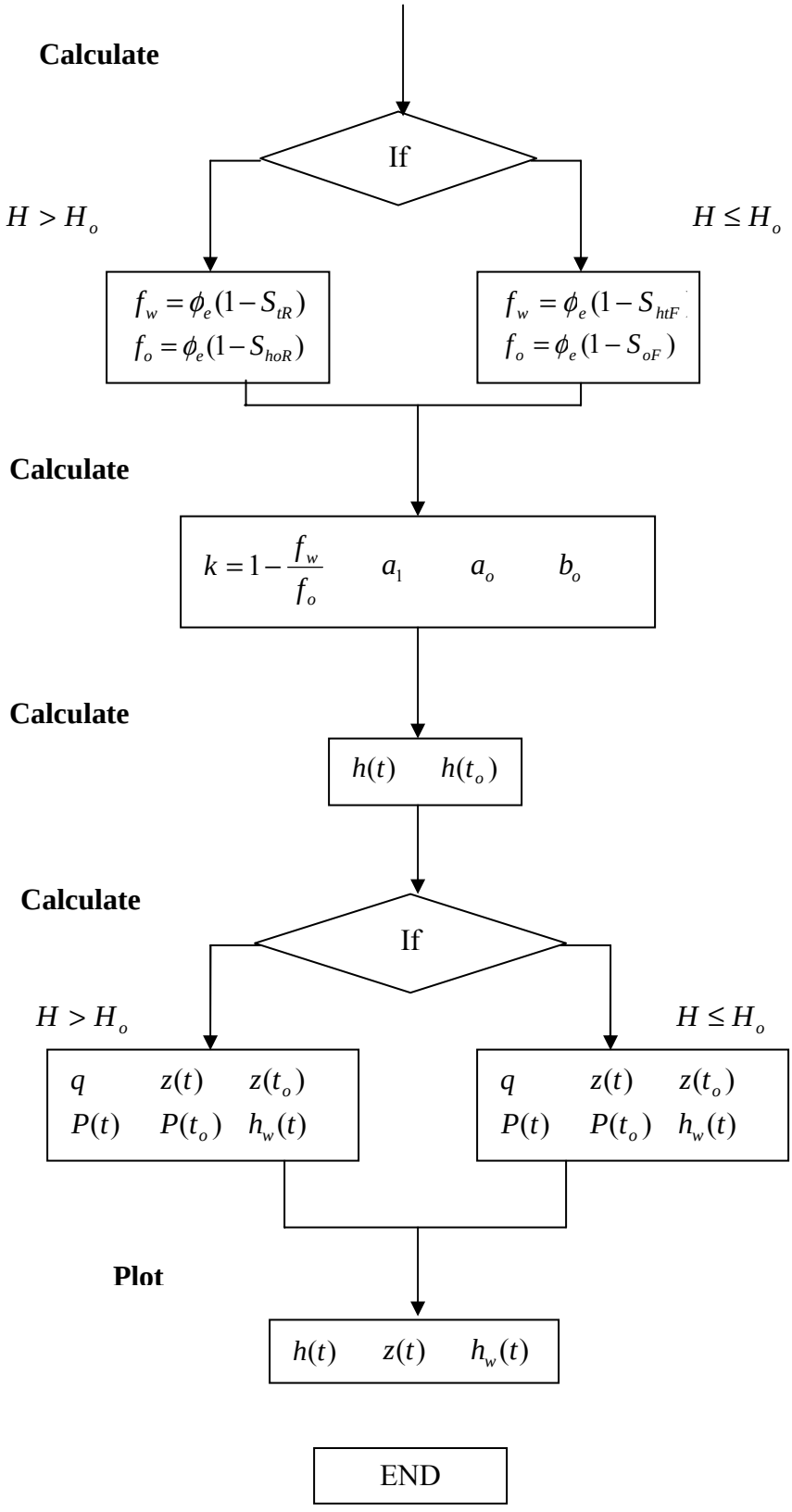
Calculate
If
$H > H_o$
$H \le H_o$
$f_w = \phi_e(1 - S_{tR})$
$f_o = \phi_e(1 - S_{hoR})$
$f_w = \phi_e(1 - S_{htF})$
$f_o = \phi_e(1 - S_{oF})$
Calculate
$k = 1 - \frac{f_w}{f_o}$ a_1 a_o b_o
Calculate
$h(t)$ $h(t_o)$
Calculate
If
$H > H_o$
$H \le H_o$
q $z(t)$ $z(t_o)$ $P(t)$ $P(t_o)$ $h_w(t)$
q $z(t)$ $z(t_o)$ $P(t)$ $P(t_o)$ $h_w(t)$
Plot
$h(t)$ $z(t)$ $h_w(t)$
END

APPENDIX-B

Program Listing of Developed Mathematical Model

```
clear all
clc

itermax = input('Enter no. of iterations: ');

temp1_min = input('Enter Minimum value for owSw: ');
temp1_max = input('Enter Maximum value for owSw: ');
temp1 = temp1_min:(temp1_max-temp1_min)/itermax:temp1_max;

temp2_min = input('Enter Minimum value for awSw: ');
temp2_max = input('Enter Maximum value for awSw: ');
temp2 = temp2_min:(temp2_max-temp2_min)/itermax:temp2_max;

temp3_min = input('Enter Minimum value for owShw: ');
temp3_max = input('Enter Maximum value for owShw: ');
temp3 = temp3_min:(temp3_max-temp3_min)/itermax:temp3_max;

temp4_min = input('Enter Minimum value for awShw: ');
temp4_max = input('Enter Maximum value for awShw: ');
temp4 = temp4_min:(temp4_max-temp4_min)/itermax:temp4_max;

temp5_min = input('Enter Minimum value for aoSha: ');
temp5_max = input('Enter Maximum value for aoSha: ');
temp5 = temp4_min:(temp4_max-temp4_min)/itermax:temp4_max;

itermax = 1;    %input('Enter no. of iterations to perform: ');

for iter3 = 1:1:itermax

    rho_o = 0.8;   %input('rho_o (g/cc): ');
    rho_w = 1;   %input('rho_w (g/cc): ');
    rho_r = rho_o/rho_w;
    Kfp = %input('Kfp (cm/s): ');
    Ko =  %input('Ko (cm/s): ');
    Kw =  %input('Kw (cm/s): ');
    dl =  %input('delta_l (cm): ');
    r =  %input('r (cm): ');
    phie =  %input('phie: ');
    H =  %input('H (cm): ');
    Ho =  %input('Ho (cm): ');
    t =  %input('t (sec): ');
    to =  %input('to (sec): ');
    ho =  %input('ho (cm): ');
    hwo =  %input('hwo (cm): ');
    zo =  %input('zo (cm): ');
    minSw =  %input('minSw: ');
    minSt =  %input('minSt: ');
    minSo =  %input('minSo: ');
    minSa =  %input('minSa: ');
    IawSar =  %input('IawSar: ');
    IaoSar =  %input('IaoSar: ');
    IowSor =  %input('IowSor: ');
    DowSor =
```

```
DawSar =
DaoSar =
owSw = temp1(itermax);  %input('owSw: ');
awSw = temp2(itermax);  %input('awSw: ');
owShw = temp3(itermax);  %input('owShw: ');
awShw = temp4(itermax);  %input('awShw: ');

dawSw =  %input('dawSw: ');

epn = 0.0000001;

Rao = (1/IaoSar)-1;
Row = (1/IowSor)-1;
Raw = (1/IawSar)-1;
Rhow = (1/DowSor)-1;
Rhaw = (1/DawSar)-1;

Rhao = (1/DaoSar)-1;
owSor = (1-dowSw)/(1+Row*(1-dowSw));
owSot = owSor*(owSw-dowSw)/(1-dowSw);
Sotw = owSot;

awSar = (1-dawSw)/(1+Raw*(1-dawSw));
awSat = awSar*(awSw-dawSw)/(1-dawSw);
Satw = awSat;

aoSar = (1-daoSo)/(1+Rao*(1-daoSo));
aoSat = aoSar*(aoSo-daoSo)/(1-daoSo);
Sato = aoSat;

StR = Sotw + Satw + Sato;
Show = Sotw
Shaw = Satw

owShor = (1-hdowSw)/(1+Rhow*(1-hdowSw));
owShot = owShor*(owShw-hdowSw)/(1-hdowSw);
Show = owShot;

awShar = (1-hdawSw)/(1+Rhaw*(1-hdawSw));
awShat = awShar*(awShw-hdawSw)/(1-hdawSw);
Shatw = awShat;

aoShar = (1-hdaoSo)/(1+Rhao*(1-hdaoSo));
aoShat = aoShar*(aoSha-hdaoSo)/(1-hdaoSo);
Shato = aoShat;

ShoR = Show + Shaw;
Sow = Shotw;
Saw = Shatw;
SoF = Sow + Saw;

ShtF = Shotw + Shatw + Shato;

if H > Ho
```

```
        fw = phie*(1-StR);
        fo = phie*(1-ShoR);

    elseif H <= Ho

        fw = phie*(1-StF);
        fo = phie*(1-SaoF);

    end

    k = 1-(fw/fo);
    a1 = -(fw/K - k*(1-k)*fo/Ko)/(1-k*rho_r);
    ao = -((1-k)*(ho+k*zo)*fo/Ko)/(1-k*rho_r);
    bo = -(H-rho_o*(ho+k*zo))/(1-k*rho_r);

    dt = (t-to)/2000;
    tt = to:dt:t;
    h = ho;

    for iter1 = 2:1:length(tt)
        for iter2 = 1:1:70
            h = h + epn;
            func2 = (a1/k)*(ho-h)+(ao-a1*bo)*log((ho-h+
zo*k+bo*k)/(zo*k+bo*k))-tt(iter1);
            h = h - 2*epn;
            func1 = (a1/k)*(ho-h)+(ao-a1*bo)*log((ho-h+
zo*k+bo*k)/(zo*k+bo*k))-tt(iter1);
            h = h + epn;
            func = (a1/k)*(ho-h)+(ao-a1*bo)*log((ho-h+
zo*k+bo*k)/(zo*k+bo*k))-tt(iter1);
            dfunc = (func2-func1)/2/epn;
            h = h - func/dfunc;
        end
        hh(iter1) = h;
    end
    hh(1) = ho;

    q = 2*Kw*(1-rho_r)/r/dl;
    z = zo;

    for iter1 = 2:1:length(tt)
        for iter2 = 1:1:70
            z = z + epn;
            func2 = a1*(z-zo) + (ao-a1*bo)*log((z+bo)/
(zo+bo)) - tt(iter1);
            z = z - 2*epn;
            func1 = a1*(z-zo) + (ao-a1*bo)*log((z+bo)/
(zo+bo)) - tt(iter1);
            z = z + epn;
            func = a1*(z-zo) + (ao-a1*bo)*log((z+bo)/
(zo+bo)) - tt(iter1);
            dfunc = (func2-func1)/2/epn;
            z = z - func/dfunc;
```

```
        end
        zz(iter1) = z;
    end
    zz(1) = zo;

    P = 2*Kw*(H-zz-hh)/r/dl;


    if H > Ho

        for xi = 2:1:201
            fint(xi) = q*((hh(1) + 4*sum(hh(2:2:10*xi-10))
 + 2*sum(hh(3:2:10*xi-11)) + hh(10*xi-9))*dt/3);
        end

        integ = P(1:10:2001).*hh(1:10:2001).*exp(fint);

        for xi = 2:1:21
            sint(xi) = (integ(1) + 4*sum(integ(2:2:10*xi-10))
 + 2*sum(integ(3:2:10*xi-11)) + integ(10*xi-9))*10*dt/3;
            tint(xi) = (hh(1) + 4*sum(hh(2:2:100*xi-100)) +
 2*sum(hh(3:2:100*xi-101)) + hh(100*xi-99))*dt/3;
        end

        hw = exp(-q*tint).*(hwo - sint);


    elseif H <= Ho

        for xi = 2:1:201
            fint(xi) = (P(1) + 4*sum(P(2:2:10*xi-10))
 + 2*sum(P(3:2:10*xi-11)) + P(10*xi-9))*dt/3;
        end

        integ = exp(-fint);

        for xi = 2:1:21
            sint(xi) = (integ(1) + 4*sum(integ(2:2:10*xi-10))
 + 2*sum(integ(3:2:10*xi-11)) + integ(10*xi-9))*10*dt/3;
            tint(xi) = (P(1) + 4*sum(P(2:2:100*xi-100)) +
 2*sum(P(3:2:100*xi-101)) + P(100*xi-99))*dt/3;
        end

        hw = exp(-tint)./(1/hwo + q*sint);

    end

end

% Plots of h(t), z(t) and hw(t)

% h(t)
figure
plot(tt,hh)
```

```
title('h(t)')
xlabel('time')
ylabel('h(t)')

% z(t)
figure
plot(tt,zz)
title('z(t)')
xlabel('time')
ylabel('z(t)')

% hw(t)
figure
plot(tt(1:100:2001),hw)
title('hw(t)')
xlabel('time')
ylabel('hw(t)')
```

CHAPTER 8

REFERENCES

Abdul A. S., Kia S. F., and. Gibson T. L., Limitations of monitoring wells for the detection and quantification of petroleum products in soils and aquifers. *Ground Water Mon. Rev*., **9**, pp. 90-99 (1989).

Abdul A.S., Gibson T.L., and Kia S.F., Contamination of soil and groundwater by automatic transmission fluid: Site description and problem assessment. *J. Hydrol*., **121**, pp. 133-153 (1991).

Abriola L.M. and Bradford S.A., Experimental investigation of entrapment and persistence of organic liquid contaminants in the subsurface environment. *Environ. Health Persp.*, **106**, pp. 1083-1095 (1998).

Abriola L.M. and Pinder G.F., A multiphase approach to the modelling of porous media contamination by organic compounds, 1: Equation development. *Water Resour. Res*., **21**, pp. 11-18 (1985a).

Abriola L.M. and Pinder G.F., A multiphase approach to the modelling of porous media contamination by organic compounds 2. Model development. *Water Resour. Res*., **21**, pp.19-26 (1985b).

Abriola L.M. Modeling multiophase migration of organic chemicals in groundwater systems: A review and assessment. *Environ. Health Perspect*., **83**, pp. 117-143 (1989).

Abriola L.M. *Multiphase migration of organic compounds in a porous media- A mathematical model. Lecture Notes in Engineering*, **8**, Springer-Varlag, New York, NY, pp. 232 (1984).

Ahmad A.M., Al-Attas O., Mohiuddin S. and Al-Suwaiyan M.S., Regulating underground fuel storage tanks (USTS), benefits and challenges. *The 6th Saudi Engineering Conference*, KFUPM, Dhahran, December 2002 (2002).

Aiban, S.A., "Construction Procedures and Specifications for Embankments around the Water Transmission Pipeline" Technical Report submitted Tekfen Construction and Installation Company, Al-Khobar, Saudi Arabia, for the Eastern Province Water Transmission System Pipeline Project, October (1998).

Ali M.A. MTBE Controversy. *5th Intern. Conf. and Exhib. On Chemistry in Indus*. Oct., 14-16, 2002. Paper no. PRO-P6, (2002).

Allain C. Joseph A., Walker C., Jennings G.D., *The regulation of Underground Storage Tanks*. Water quality & Waste Management, AG-473-23, pp 1-12 (1996);

Al-Suwaiyan M.S., Bashir K., Aiban S.A., and Ishaq A.M., Analytical model to quantify crude oil spill volume in sandy layered aquifers. *J. Environ. Eng*., **128**, pp. 320-326 (2002)

Al-Suwaiyan M.S., Ishaq A. M., Saleem M. and Essa M. H., Environmental pollution due to underground storage tanks: (a) Assessment; (b) Guidelines for prevention. *Applied Research Project* (AR-22-91), King Abdul Aziz City for Science and Technology, pp. 1-88 (2003)

API (American Petroleum Institute)., *Phase separated hydrocarbon contaminant modeling for corrective action,* Publ. 4474, API, Washington, DC, pp. 125 (1988).

API (American Petroleum Institute)., *The migration of petroleum products in the soil and groundwater, Principles and countermeasures*. API Publication no. 1628 (1980).

Aral M.M., and Liao B., Effect of groundwater table fluctuation on LNAPL thickness in monitoring wells. *Environ. Geology*, **42**, pp. 151-161 (2002).

Aral M.M., and Liao B., LNAPL thickness interpretation based on bail-down test. *Groundwater*, **38**, pp.696-701 (2000).

Arya L.M. and Dierolf T.S., Predicting soil moisture characteristics from particle-size distribution: An improved method to calculate pore radii from particle radii. In: *Proceeding of the international Workshop on indirect Methods for Estimating the Hydraulic Properties of Unsaturated Soil*, Riverside, California, October 11-13, 1989. Edited by M. Th. Van Genuchten, F.J. Leij, and L.J., Lund. pp. 115-124 (1992).

Arya L.M., and Paris J.F., A physicoempirical model to predict the soil moisture characteristic from particle-size distribution and bulk density data. *Soil Sci. Soc. Am. J*. **45**, pp. 1023-1030 (1981).

Aziz, K., and A. Sattari. (1979). "Petroleum reservoir simulation." *Applied Science Publishers*, London.

Ballestero T.P., Fritz, R.F., and Nancy, E.K. An investigation of the relationship between actual and apparent gasoline thickness in a uniform sand aquifer. *Groundwater*, **32**, pp. 708-718 (1994).

Bashir K. Quantifying crude oil spill volume in homogeneous and layered porous media from product thickness in monitoring wells. M.S. Thesis, King Fahd Univ. of Petroleum and Minerals, Saudi Arabia (1997).

Bear J., Ryzhik, V., Braester, C., and Entov, V. On the movement of an LNAPL lens on the water table. *Transport in Porous Media*, **25**, pp. 283-331 (1996).

Blake S.B. and Fryberger J.S., Containment and recovery of refined hydrocarbons from ground water. In: *Proceedings of the conference on Ground Water and Petroleum: Prevention Detection and Restoration*, PAEC, Toronto, Ontario (1983).

Blake S.B., and Hall R.A., Monitoring petroleum spills with wells: Some problems and solutions. In: *Fourth National Symposium and Exposition on Aquifer restoration and Ground Water Monitoring*, National Water Well Assoc., Columbus, OH. pp. 305-310 (1984).

Blunt M., Zhou D., and Fenwick D., Three phase flow and gravity drainage in porous media. *Transport in Porous Media*, **20**, pp. 77-103 (1995).

Borden R.C., and Kao C.M., Evaluation of groundwater extraction for remediation of petroleum contaminated aquifers. *Water Environ. Res.,* **64**, pp. 28-36 (1992).

Brooks, R. H. and A. T Corey. 1964. "Hydraulic Properties of Porous Media." *Hydrology Paper No. 3,* Colorado State Univ. 27 pp.

Brooks, R. H. and A. T. Corey (1966). "Properties of porous media affecting fluid flow." *J. Irrig. and Drain. Div., ASCE,* v. 92, pp.61-88.

Busby R.D., Lenhard, R.J., and Rolston, D.E. An investigation of saturation-capillary pressure relations in two-and three-fluid systems for several NAPLS in different porous media. *Groundwater*, **33**, pp. 570-578 (1995).

Chaffee W.T. and Weimar R.A., Remedial programs for groundwater supplies contaminated by gasoline. In *Pro. Of the 3rd Nat. Symp. On Aquifer Restoration and Groundwater Monitoring*, May 23-25, Columbus, Ohio, pp. 39-46 (1983).

Charbeneau R.J., Johns R.T, Lake L.W., and McAdamsIII M.J., Free-product recovery of petroleum hydrocarbon liquids. *Ground Water Mon. Rev.*, Summer 2000, pp. 147-158. (2000).

Charbeneau R.J., Wanakule N., Chiang C.Y., Nevin J.P., and Klein C.L., A two layer model to simulate floating free product recovery: Formulation and applications. In: *Proc. Conf. on Petroleum Hydrocarbons and Organic Chemicals in Groundwater: Prevention, Detection, and Restoration,* Natl. Ground Water Assoc., Dublin, OH, pp. 333-345 (1989).

Chiang C., Gary R. and Clint D., The relation ship between monitoring wells and aquifer solute concentration. *Groundwater*. **33**, 718-726 (1995).

Cohen R.M., Bryda A.P., Shaw S.T., and Spalding C.P., Evaluation of visual methods to detect NAPL in soil and water. *Ground Water Mon. Rev*., **12**, pp. 132-141 (1992).

CONCAWE., *Revised inland oil spill clean-up manual*. Concawe Report No. 7/81, The Hague, Netherlands (1981).

Conrad S., Hogan E., and Wilson J., Why are residual saturation of organic liquids different above and below the water table. *Presented at the Petroleum Hydrocarbons in Groundwater Conf*., May, 1987, Houston (1987).

Corapcioglu M.Y., Tuncay K., Lingam R., and Kambham K.K.R., Analytical expressions to estimate the free product recovery in oil-contaminated aquifers. *Water Resour. Res*., **30**, pp.3301-3311 (1994).

Corey A. T. *Mechanics of immiscible fluids in porous media*. Water Resources Publishers, Littleton, Colo. (1986).

Corey A. T., Rathjens C. H., Henderson J. H., and Wyllie M. R. J., Three-phase relative permeability. *Trans. Am. Inst. Min. Metall. Pet. Eng*., **207**, 349-351 (1956).

Corey, A. T. 1986. "Mechanics of immiscible fluids in porous media." *Water Resources Publishers*, Littleton, Colo.

Cote P. and Lipski C., Use of pervaporation for the removal of organic contaminants from water. *Environ. Progress*, **9**, pp. 245-261 (1990).

Darnault C.J.G., DiCarlo D.A., and Bauters T.W.J., Measurement of fluid contents by light transmission in transient three-phase oil-water-air systems in sand. *Water Resour. Res*., **37**, pp. 1895-1868 (2001).

de Pastrovich I.L., Barthel Y., Chiarelli A., and Fussell D.R., *Protection of groundwater from oil pollution*. CONCAWE Report No. 3/79, Den Haag, Netherlands (1979).

DeAngelis D., *Quantitative determination of hydrocarbons in soil, extraction-infrared adsorption method*. Appendix B-3, in: Manual of Sampling and Analytical Methods for Petroleum Hydrocarbons in Ground Water and Soil." API Publication no. 4449, API Washington, D.C., pp. 167-170 (1987).

DEQ., Department of Environmental Quality, Michigan, USA. http://www.michigan.gov/ (2005).

Domenico P.A. and Schwartz F.W., *Introduction to contaminant hydrology. Physical and chemical hydrology*. 1st edition, Singapore: John Wiley and Sons, Inc. pp. 573-627 (1990).

Dragun J., *The soil chemistry of hazardous materials*. Hazardous Material Control Research Institute Publications, Silver Springs, Maryland (1988).

Durnford D., Brookman J., Billica J., and Milligan J., LNAPL distribution in a cohesion less soil: A field investigation and cryogenic sampler. *Ground Water Mon. Rev*., **11**, pp. 115-122 (1991).

Eckberg D. and Sunada D.K., Nonsteady three-phase immiscible fluid distribution in porous media. *Water Resour. Res*., **20**, pp. 1891-1897 (1984).

EPA (United States Environmental Protection Agency)., *Underground storage tank corrective action technologies*. Rep. EPA/625/6-87-015. Cincinnati, OH: Hazardous Waste Engineering Research Lab. (1987).

EPA, *Leak Detection Methods for Petroleum underground storage tanks and piping*. www.leak.ust.pdf, pp.1-32 (1997),

EPA, *Operating & maintaining UST systems*. Practical help & check lists. 510, B-00-008 www.epa.gov/scrust1/pubs/ommanual.pdf. (2000).

Essaid H.I., Herkelrath W.N., and Hess K.M., Simulation of fluid distributions observed at a crude-oil spill site incorporating hysteresis, oil entrapment, and spatial variability of hydraulic properties. *Water Resour. Res*., **29**, pp. 1753-1770 (1993).

Farr A. M., Houghtalen R. J., and McWhorter D. B., Volume estimate of light nonaqueous phase liquids in porous media. *Groundwater.* **28**, pp. 48-56 (1990).

Faust C.R., Guswa J.H., and Mercer J.W., Simulation of three dimensional flow of immiscible fluids within and below the unsaturated zone. *Water Resour. Res*., **25**, pp.2449-2464 (1989).

Faust C.R., Transport of immiscible fluids within and below the unsaturated zone: AS numerical model. *Water Resour. Res*., **21**, pp. 587-596 (1985).

Ferrand L.A., Milly P.C.D., and Pinder G.F., Experimental determination of three-fluid saturation profiles in porous media. *J. Contam. Hydrol*., **4**, pp. 373-395 (1989).

Ferrand L.A., Milly P.C.D., Pinder G.F., and Turrin R.P., A comparison of capillary pressure pressure-saturation relations for drainage in two-and three-fluid porous media. *Adv. Water Resour.*, **13**, pp. 54-63 (1990).

Fetter C.W., *Contaminant hydrogeology*. Macmillan Publishing Company, New York. (1992).

Fiedler F.R. An investigation of the relationship between actual and apparent gasoline thickness in a uniform sand aquifer. M.S. Thesis, Univ. of New Hampshire, Durham, NH. (1989).

Forsyth P.A., and Sudicky E.A., Discrete wellbore simulations of pump-and-treat stretegies for remediation of LNAPL-contaminated aquifers. *J. Contam. Hydrol.*, **31**, pp.57-81 (1998).

Gruszczenski T.S. Determination of a realistic estimate of the actual formation product thickness using monitoring wells: A field bailout test. In: *Proceedings of the conference on Petroleum Hydrocarbons and Organic Chemicals in Ground Water: Prevention Detection and Restoration*, November 17-19, Dublin, Ohio: National Ground Water Well Association, pp.143-156 (1987).

Gupta S.C., and Larson W.E., Estimating soil water retention characteristics from particle size distribution, organic matter percent, and bulk density. *Water Resour. Res*. **15**, pp. 1633-1635 (1979).

Hall P.L., and Quam H., Countermeasures to control oil spills in western Canada. *Groundwater*, **14**, (1976).

Hall R.A., Blake S.B., and Champlin, Jr S.C., Determination of hydrocarbon thickness in sediments using borehole data. In: *Proceedings of the 4th National Symposium on Aquifer Restoration and Ground Water Monitoring*, National Water Well Assoc, Worthington, Ohio, pp. 300-304 (1984).

Hampton D.R. Laboratory and field comparison between actual and apparent product thickness in sands. In: *Fall meeting, AGU*, San Francisco, CA, December 5-9, Abstract in EOS, **69**, pp. 1213 (1988).

Hampton D.R., and Miller P.D.G., Laboratory investigation of the relationship between actual and apparent product thickness in sands. In: *Environmental Concerns in the Industry*, S.M. Testa, ed., Pacific Section, Amer. Assoc. Petrol. Geo., Palm Springs, CA, pp. 31-55 (1988a).

Hampton D.R., and Miller P.D.G., Laboratory investigation of the relationship between actual and apparent product thickness in sands. In: *Proceedings of the conference on Petroleum Hydrocarbons and Organic Chemicals in Ground Water: Prevention Detection and Restoration*, November 9-11, Dublin, Ohio: National Ground Water Well Association, pp. 157-181 (1988b).

Hampton D.R., Heuvelhorst H.G., Adams T.V., Greer S.J., and Hartenberger B.E., What can wells tell us about the location of immiscible fluids in aquifers? *EOS Trans*. AGU, **71**, pp. 500 (1990a).

Hampton D.R., Wagner R.B., and Huevelhorst H.G., A new tool to measure petroleum thickness in shallow aquifers. In *proceedings of Fourth National Outdoor Action Conference on Aquifer Restoration,* Groundwater Monitoring and Geophysical Methods. Dublin, Ohio: National Ground Water Well Association, May 14-17 (1990b).

Han W., Reddi L.N., and Banks M.K., Modelling of the effects of cyclic water table fluctuation on fate of NAPL gan-glia. In: *Proceedings of Conference on*

Hazardous Waste Research, May 20-22, Kansas State University, College of Engineering, Manhattan (1997).

Hardisty P.E. Behaviour of light immiscible liquid contaminants in fractured aquifers. *Geotechnique*, **48,** pp. 747-760 (1998).

Hardisty, P.E., and Ozdemiroglu, E. 2004. *The Economics of Groundwater remediation and Protection: A Tool for Decision Makin*g. CRC Press, NY.

Hardisty, P.E., Wheater, H.S., Birks, D., and Dottridge, J. 2003. "*Characterization of LNAPL in Fractured Roc*k." Q.J. Eng. Geol & Hydrgeol. Vol 36, pp. 343-354.

Haskell P. A., Use of surrogate compounds to monitor non-aqueous phase liquid removal during a cosolvent flood. MS Thesis. Clemson, SC: Clemson University (1997).

Haverkamp R., and Parlange J.Y., Predicting the water retention curve from particle size distribution: Sandy soils without organic matter. *Soil Sci*. **142**, pp. 325-399 (1986).

Hawk R.N. Non-aqueous phase hydrocarbon saturations and mobility in fine-grained, poorly consolidated sand stone. Unpub. M.Sc. Thesis, San Diego State Univ. (1993).

Hess K.M., Herkelrath W.N., and Essaid H.I., Determination of subsurface fluid contents at a crude-oil spill site. *J. Contam. Hydrol*., **10**, pp. 75-96 (1992).

Hoag G.E., *Belltown Sunoco gas spill., East Hampton, CT.* Technical report submitted to Continental Insurance Company, Underwriters Adjusting Company (1982b).

Hoag G.E., *Belltown Sunoco gasoline spill., East Hampton, CT*. A report submitted to Connecticut, Department of Environmental Protection, Sept. 15 (1982a).

Hoag G.E., Marley and M.C., Gasoline residual saturation in unsaturated uniform aquifer material. *J. Environ. Eng.*, **112**, pp. 586-604 (1986).

Hoag G.E., *Subsurface gasoline contamination in Whitman, MA.* A report of the State of Massachusetts, Department of Environmental Quality Engineering (1983).

Hocott C. R. Interfacial tension between water and oil under reservoir conditions. *AIM Petroleum Trans*., **132**, pp. 184-190 (1938).

Hofstee C., Dane J.H., and Hill W.E., Three-fluid retention in porous media involving water, PCE and air. *J. Contam. Tran*. **25**, pp. 235-247 (1997).

Holzer T.L. Application of ground water flow theory to a subsurface oil spill. *Groundwater*, **14**, pp. 138-145 (1976).

Huges J.P., Sullivan C.R., and Zinner R.E., The occurrence of hydrocarbon on an unconfined aquifer and implications for liquid recovery. In: *proceedings of Conference on Petroleum Hydrocarbon and Organic Chemicals in Ground Water: Prevention, Detection, and Restoration*. Dublin, Ohio: National Ground Water Well Association. (1988).

Huling S.G., and Weaver J.W., *Dense nonaqueous phase liquids, Ground Water Issue.*, EPA/540/4-91-002, U.S. EPA, R.S. Kerr Environ. Res. Lab., Ada, OK, pp. 21. (1991).

Hult M.F., Non-disruptive measurements of organic fluid thickness in the shallow subsurface. In: *Conf. Petroleum Hydrocarbons and Organic Chemicals in Ground Water*, NWWA, Houston, TX. (1984).

Hunt W. T., Wiegand J. W., and Trompeter J. D., Free gasoline thickness in monitoring wells related to groundwater elevation change. Proc: *Conference on New Field Techniques for Quantifying the Physical and Chemical Properties of Heterogeneous Aquifers*. National Water Well Assoc., Dublin, OH. pp. 671-692 (1989).

Huntley D., Hawk R.N., and Corley H.P., Non-aqueous phase hydrocarbon in a fine-grained sand stone: 1. Comparison between measured and predicted saturations and mobility. *Groundwater*.**32**, pp. 626-634 (1994a).

Huntley D., Wallace J.W, and Hawk R.N., Non-aqueous phase hydrocarbon in a fine-grained sandstone: 2. Effect of local sediment variability on the estimation of hydrocarbon volumes. *Groundwater* **32,** pp. 778-783 (1994b).

Huyakom P.S., Wu Y.S., and Panday S., A comprehensive three-dimensional numerical model for predicting the fate of petroleum hydrocarbons in the subsurface. In: *Proc. Conf. on Petroleum Hydrocarbons and Organic Chemicals in Groundwater: Prevention, Detection, and Restoration*, Natl. Ground Water Assoc., Dublin, OH, pp.239-253 (1992).

Jaynes D.B., Estimating hysteresis in the soil water retention function. In: *Proceeding of the international Workshop on indirect Methods for Estimating the Hydraulic*

Properties of Unsaturated Soil, Riverside, California, October 11-13, 1989. Edited by M. Th. Van Genuchten, F.J. Leij, and L.J., Lund. pp. 219-230 (1992).

Johnson P.C., Kemblowski M.K., and Colthart J.D., Quantitative analysis for the cleanup of hydrocarbon contaminated soils by in-situ soil venting. *Groundwater*, **28**, pp.413-429 (1990).

Johnson T.E., and Kreamer D.K., Physical and mathematical modelling of diesel fuel liquid and vapour movement in porous media. *Groundwater.* **32**, 551-560 (1994).

Kaluarachchi J.J. and Parker J.C., An efficient finite element method for modelling multiphase flow in porous media. *Water Resour. Res*., **25**, pp. 43-54 (1989).

Kaluarachchi J.J. and Parker J.C., Multiphase flow with simplified model for oil entrapment. *Transport in Porous Media*., **7**, pp. 1-14 (1992).

Kaluarachchi J.J. Effect of subsurface heterogeneity on free-product recovery from unconfined aquifers. *J. Contam. Hydrol*., **22**, pp.19-37 (1996).

Keach D.A. Hydrocarbon thickness on groundwater by dielectric well logging. In: *Proceedings of the conference on Petroleum Hydrocarbons and Organic Chemicals in Ground Water: Prevention Detection and Restoration*, November 9-11, Dublin, Ohio: National Ground Water Well Association, pp.275-290 (1988).

Kemblowski M. W. and Chiang C. Y., Analysis of measured free product thickness in dynamic aquifers. Proc: *Conference on Petroleum Hydrocarbons and Organic Chemicals in Ground Water: Prevention, Detection and Restoration*. November 9-11, Dublin, Ohio: National Ground Water Well Association. pp. 183-205 (1988).

Kemblowski M. W. and Chiang C. Y., Hydrocarbon thickness fluctuations in monitoring wells. *Groundwater*. **28**, pp. 244-252 (1990).

Kemblowski, M. W. and C. Y. Chiang. 1990. "Hydrocarbon thickness fluctuations in monitoring wells." Ground Water. v. 28, pp. 244-252.

Kessler A., and Rubin H., Relation between water infiltration and oil spill migration in sandy soils. *J. Hydrol.*, **91**:pp. 187-204 (1987).

Kim J, and Corapcioglu M.Y., Sharp interface modelling of LNAPL spreading and migration on the water table. *Environ. Eng. Sci*., **18**, pp. 359-367 (2001).

Kimberlin D.K., and Trimmell M.L., Utilization of optoelectronic sensing to determine hydrocarbon thickness within confined aquifers. In: *Proceedings of the conference on Petroleum Hydrocarbons and Organic Chemicals in Ground Water: Prevention Detection and Restoration*, November 9-11, Dublin, Ohio: National Ground Water Well Association (1988).

Kramer W.H., Groundwater pollution from gasoline. *Ground Water Mon. Rev.*, **2**, (1981).

Krumbein W.C., and Monk G.D., Permeability as a function of the size parameters of unconsolidated sand. *Trans. Am. Inst. Min. Metall. Eng*., **151**, pp. 153-160 (1942).

Land, C.S., (1968). "Calculation of imbibition relative permeability for two and three phase flow from rock properties." Soc. Pet. Eng. J., pp. 149-156.

Lebedeff A. F. The movement of groundwater and soil waters. In: *Proc., Internat. Cong. Soil Sci.,* **1** (1972).

Lenhard R. J. and Parker J. C., Discussion of estimation of free product hydrocarbon volume from fluid levels in monitoring wells. *Groundwater*. **18**, pp. 57-67 (1990b).

Lenhard R. J. and Parker J. C., Estimation of free product hydrocarbon volume from fluid levels in monitoring wells. *Groundwater*. **28**, pp. 57-67 (1990a).

Lenhard R. J. and Parker J. C., Experimental validation of the theory of extending two-phase saturation-pressure relations to three-fluid phase systems for monotonic drainage paths. *Water Resour. Res*. **24**, pp. 373-380 (1988).

Lenhard R. J., Measurement and modelling of three-phase saturation-pressure hysteresis. *J. Contam. Hydrol*. **9**, pp. 243-269 (1992).

Lenhard R.J., and Parker J.C., Measurement and prediction of saturation-pressure relations in three-phase porous media system. *J. Contam. Hydrol*., **1**, pp. 407-424 (1987).

Leverett M. C., and Lewis W. B., Steady flow of gas-oil-water mixtures through unconsolidated sands. *Trans. Am. Inst. Min. Metall. Pet. Eng*., **142**, 107-116 (1941).

Liao B. Analytical and numerical analysis of LNAPL migration and LNAPL thickness estimation in unconfined aquifers. PhD Thesis, School of Civil and Environmental Engineering, Georgia Institute of Technology (1999).

Liao B. and Aral M., Interpretation of LNAPL thickness measurements under unsteady conditions. *J. Hydrologic Eng*., **4**, pp. 125-134 (1999).

Lowry M.I., and Miller C.T., Pore-scale modelling of nonwetting-phase residual in porous media. *Water Resour. Res.*, **31**, pp. 455-473 (1995).

Lundegard P. D. and Mudford B.S., LNAPL volume calculation: Parameter estimation by nonlinear regression of saturation profiles. *Groundwater*, **3**, pp. 88-93 (1998).

Lyman W.J., and Noonan D.C., *Assessing UST corrective action technologies: Site assessment and selection of unsaturated zone treatment technologies*. EPA/600/2-90/011, U.S.EPA, Risk Red. Eng. Lab., Cincinnati, OH, pp. 107 (1990).

Marinelli F. and Durnford D. S., LNAPL thickness in monitoring wells considering hysteresis and entrapment. *Groundwater.* **34**, 405-414 (1996).

Matis J.R. Petroleum contamination of groundwater in Maryland. *Groundwater*, **9** (1971).

Mayer A.S., and Miller C.T., The influence of porous media characteristics and measurement scale on pore-scale distributions of residual nonaqueous phase liquids. *J. Contam. Hydrol.*, **11**, pp. 189-213 (1992).

McBride J.F., and Miller C.T., *Entrapment of non-aqueous-phase liquids in NAPL-water porous media: the residual-funicular NAPL saturation relation*. CMR, Centre for Multiphase Research News, Dept. of Env. Sci. and Eng., Univ. of North Carolina Chapel Hill, **3**, pp. 1-6 (1997).

McKeey J.E., Laverty F.B. and Hertel R.M., Gasoline in groundwater. *J. Water Pollu. Control Federation (JWPCF),* **44** (1972).

Mercer J.W., and Cohen R.M., A review of immiscible fluids in the subsurface: Properties models, characterization and remediation. *J. Conta. Hydrol*., **6**, pp. 107-163 (1990).

Miller C.T., Christakos G., Imhoff P.T., McBride J.F., Pedit J.A., and Trangenstein J.A., Multiphase flow and transport modeling in heterogenous porous media: Challenges and approaches. *Adv. Water Resour*., **21**, pp. 77-120 (1997).

Mishra S., Parker, J.C. and Singhal, N. Estimation of Soil Hydraulic properties and their uncertainty from particle size distribution data. *J. Hydrol.* **108**, pp. 1-18 (1989).

Mohanty K.K., Davis H.T., and Scriven L.D., *Physics of oil entrapment in water-wet rock*. Paper SPE 9406, presented at 1980 SPE Annual Tech. Conf. and Exhib., Dallas, TX. (1980).

Mualem Y., Modelling the hydraulic conductivity of unsaturated porous media. In: *Proceeding of the international Workshop on indirect Methods for Estimating the Hydraulic Properties of Unsaturated Soil*, Riverside, California, October 11-13, 1989. Edited by M. Th. Van Genuchten, F.J. Leij, and L.J., Lund. pp. 15-36 (1992).

Mull R., Calculations and experimental investigations of the migration of oil products in natural soils. In: *Int. Symp. On Ground Water Pollution by Oil Hydrocarbons*, Proc. Of Int. Assoc. of Hydrogeologists, Pargue, June 5-7, pp. 167-181 (1978).

Nakornthap K., and Evans R.D., Temperature-dependent relative permeability and its effects on oil displacement by thermal methods. *Soc. Pet. Eng. J.*, **26**, pp. 230-242 (1986).

Newell C.J., Acree S.D., Ross R.R., and. Huling S.G., *Light Nonaqueous phase liquids. Ground Water Issue, U.S.*, Environmental Protection Agency, Office of Research and Development, and Office of Solid Waste and Emergency Response, EPA/540/S-95/500 (1995).

Nimmo J.R. Akstin K.C., and Mello K.A., Improved apparatus for measuring hydraulic conductivity at low water content. *Soil Sci. Soc. Am. J.*, **56**, pp. 1758-1761 (1992).

Nodak, *Protecting your groundwater through farmstead assessment*. AE-1078. www.ext.nodak.edu/extpubs/8w.html (1998).

Oak Ridge National Laboratory, *Transportation Energy Data Book*: Edition 7. Report ORNL-6050, Prepared for the office of Vehicle and Engine Research and Development, Department of Energy (1983).

Osgood J.O. Hydrocarbon dispersion in groundwater: Significance characteristics. *Groundwater*, **12**, (1974).

Ostendorf D.W., Richards R.J., and Beck F.P., LNAPL retention in sandy soil. *Groundwater*, **31**, pp. 285-292 (1993).

Parcher M. A., Johnson J.A., and Parker J.C., Effects of soil types on separate phase hydrocarbon recovery under fluctuating water table conditions. In: *Proc. Petrol.*

Hydrocarbons and Org. Chems. In Ground Water, NGWA, Houston, Nov. 29-Dec 1. pp. 439-450 (1995).

Parker J. C., Lenhard R. J., and Kuppusamy T., A parametric model for constitutive properties governing multiphase flow in porous media. *Water Resour. Res*. **23**, pp. 618-624 (1987b).

Parker J. C., Lenhard R. J., and Kuppusamy T., Measurement and estimation of permeability-saturation-pressure relations in multiphase porous media systems. in porous media." *Impact of Physico-Chemistry on Study, Design and Optimization of Processes in Natural Porous Media,* Presses Universitaires de Nancy, France.. **23**, pp. 618-624 (1987a).

Parker J.C. and Lenhard R.J., A model for hysteretic constitutive relations governing multiphase flow, 1. Saturation-pressure relations. *Water Resour. Res*., **23**, pp. 2187-2196 (1987).

Parker J.C. and Lenhard R.J., Determining three phase permeability-saturation-pressure relations from two phase system measurements. *Geoderma* (1988).

Parker J.C. and Lenhard R.J., Vertical integration of three phase flow equations for analysis of light hydrocarbon plume movement. *Transport in Porous Media,* **5**, pp. 187-206 (1989).

Parker J.C., Zhu J.L., Johnson T.G., Keremesec V.J., and Hockman E.L., Modelling free product migration and recovery at hydrocarbon spill sites. *Groundwater*, **32**, pp. 119-128 (1994).

Reddi L.N., Han W. and Bank M.K., Fate and transport pf LNAPL under fluctuating water table conditions. *Geoenvironmental Eng*, pp. 264-271 (1997).

Reddi L.N., Han W., and Banks M.K., Moss loss from LNAPL pools under fluctuating water table conditions. *J. Environ. Eng*., **124**, pp. 1171-1177 (1998).

Reid S. The flow of three immiscible fluids in porous media. Ph.D. Thesis, Dep. Of Chem. Eng., Univ. of Birmingham, England (1956).

Rubin H, Narkis N. and Carberry J.B., Overview of NAPL contamination and the reclamation. *Soil and Aquifer Pollution Non-Aqueous Phase Liquids Contamination and Reclamation*, Springer Publisher, pp. 3-17 (1998).

Ryan R.G., and Dhir V.K., The effect of interfacial tension on hydrocarbon entrapment and mobilization near a dynamic water table. *J. Soil Contam*., **5**, pp. 9-34 (1996).

Ryan R.G., and Dhir V.K., The effect of soil particle size on hydrocarbon entrapment near a dynamic water table. *J. Soil Contam.*, **2**, pp. 59-92 (1993).

Saltelli, A., K. Chan, and E. M. Scott August. Sensitivity Analysis, John Wiley and Sons, Inc. p. 504 (2002).

Scheidegger, A. E. 1974. "Physics of flow through porous media." *Univ. of Toronto Press,* Toronto, Ontario.

Scheinfield R.A., John B.R. and Todd G.S. Underground storage tanks monitoring: Observation well based system. *Ground Water Mon. Rev*. **6**, pp. 49-55 (1986).

Schiegg H.O. Consideration on water, oil, and air in porous media. *Water Sci. and Technol*., **17**, pp. 467-476 (1985).

Schiegg H.O., and McBride J.F., Laboratory setup to study two-dimensional multiphase flow in porous media. In: *Proceedings of the conference on Petroleum Hydrocarbons and Organic Chemicals in Ground Water: Prevention Detection and Restoration*, Dublin, Ohio: National Ground Water Well Association, pp.371-398 (1987).

Schuckman L., Banks M.K, and Reddi L.N., Effect of fluctuating water levels on biodegradation of NAPLS in soil. In:. *Proceedings of Conference on Hazardous Waste Research*, May 20-22, Kansas State University, College of Engineering, Manhattan (1997).

Seagren E.A., and Moore T.O., Nonaqueous Phase Liquid Pool Dissolution as a Function of average pore water velocity. *J. Environ. Eng.*, **129**, pp. 786-799 (2003).

Sharma R. S. and Gray A.J., Modelling and remediation of non-aqueous phase liquids in unsaturated zones. *Proc. Int. Conf. On Geoenvironment*, Muscat, pp. 424-435. (2000).

Sharma R. S. Migration of non-aqueous phase liquids in subsurface. *Proc. Int. Conf. On Geoenvironment*, Muscat, pp. 571-583 (2000).

Sleep B.E., Sehayek L., and Chien C.C., A modelling and experimental study of light Nonaqueous phase liquid (LNAPL) accumulation in wells and LNAPL recovery from wells. *Water Resour. Res*., **36**, pp. 3535-3545 (2000a).

Sleep B.E., Sehayek L., and Chien C.C., Modeling wells in variably saturated soil with well bore fluid gravity segregation. *Adv. Water Resour*., **23**, pp. 689-697 (2000b).

Steffy D.A., Barry D.A. and Johnston C.D. Influence of antecedent moisture content on residual LNAPL saturation. *J. Soil Cont*., **6**, pp. 113-147 (1997).

Steffy D.A., Johnston C.D., and Barry D.A. Numerical simulations and long-column tests of LNAPL displacement and trapping by a fluctuating water table. *J. Soil Cont*, **7**, pp. 325-356 (1998).

Steffy D.A., Vertical immiscible displacement and entrapment of an LNAPL by a fluctuating water table. A field, laboratory and numerical study. Ph.D. Thesis, UWA, Australia (1997).

Stegemeier G.L. Mechanisms of entrapment and mobilization of oil in porous media. In: *American Institute of Chemical Engineers Symposium on Improved Oil Recovery by surfactant and Polymer Flooding*, Kansas City, Academic Press, pp. 55-91 (1977).

Stone H.L. Estimation of three phase relative permeability and residual oil data. *J. Pet. Technol*. **12**, pp. 53-61 (1973).

Stone H.L. Probability models for estimating three phase relative permeability, *J. Pet. Technol*., **249**, pp. 214-218 (1970).

Su, C., and R. H. Brooks. 1980. "Water retention measurement for soils." *J. Irrig. Drain. Div. Am. Soc. Civ. Eng.,* 106 (IR2), 105-112.

Sullivan C.R., Huges J.P., and Zinner R.E., Two techniques for determining the true hydrocarbon thickness in an unconfined aquifer. In *proceedings of Conference on Petroleum Hydrocarbon and Organic Chemicals in Ground Water: Prevention,*

Detection, and Restoration. Dublin, Ohio: National Ground Water Well Association, pp. 291-314 (1988).

Testa S.M. and Paczkowski M.T., Volume determination and recoverability of free hydrocarbon. *Ground Water Mon. Rev*. **9**, pp. 120-128 (1989).

Testa S.M. and Winegardener D.L., *Restoration of petroleum contaminated aquifers*. Lewis Publishers, Chelsea, Michigan (1991).

Trimmell M.L., Installation of hydrocarbon detection wells and volumetric calculations within a confined aquifer. In: *Proceedings of the conference on Petroleum Hydrocarbons and Organic Chemicals in Ground Water: Prevention Detection and Restoration*, Dublin, Ohio: National Ground Water Well Association. (1987).

Van Dam J. The migration of hydrocarbons in a water bearing stratum. In: *Hepple, Peter, ed. The Joint Problems of the Oil and Water Industries*: The Institute of Petroleum Symposium. Brighton, London, Jan 18-20. pp. 55-96 (1967).

Van der Waarden M., Bridie A.L.A.M., and Groenewoud W.M., Transport of mineral oil components to groundwater. I, *Water Res*., **5**, pp. 213-226. (1971).

Van Dijke M.I.J., and Van der Zee S.E.A.T.M., *Horizontal one-dimensional redistribution of oil and water with hysteresis due to oil entrapment*. Modeling. Analysis and Simulation, Report Centrum voor Wiskunde en Informatica, MAS-R9806, May 31 1998. Kruislaan, Amsterdam. (1998).

Van Duijn Cc.J., Molenaar J., and De Neef M.J., The effect of capillary forces on immiscible two-phase flow in strongly heterogeneous porous media. *Transport in Porous Media*, **21**, pp. 71-93 (1995).

Van Geel P.J. and Roy S.D., A proposed model to include a residual saturation NAPL saturation in a hysteretic capillary pressure-saturation relationship. *J. Contam. Hydrol*., **58**, pp. 79-110 (2002).

Van Geel P.J., and Sykes J.F., Laboratory and model simulations of a LNAPL spill in a variably-saturated sand, 2, Comparison of laboratory and model results. *J. Contam. Hydrol*., **17**, pp.27-53 (1994).

Van Geel P.J., and Sykes J.F., The importance of fluid entrapment, saturation hysteresis and residual saturations on the distribution of a lighter-than-water non-aqueous phase liquid in a variability saturated sand medium. *J. Contam. Hydrol*., **25**, pp.249-270 (1997).

Van Genuchten, M. Th. 1980. "A closed form equation for predicting the hydraulic conductivity of unsaturated soils." *Soil Science Society of America Journal* 44, pp. 892-899.

Waddill D.W., and Parker J.C., A saemianalytical model to predict recovery of light Nonaqueous phase liquids from unconfined aquifers. *Groundwater*. **35**, pp. 280-290 (1997).

Wagner R.B, Hampton D.R., and Howell J.A., A new tool to determine the actual thickness of free product in a shallow aquifer. In: *Proceedings of the conference on Petroleum Hydrocarbons and Organic Chemicals in Ground Water: Prevention Detection and Restoration*, November 9-11, Dublin, Ohio: National Ground Water Well Association (1988).

Wagner R.B, Hampton D.R., and Howell J.A., A new tool to measure petroleum thickness in shallow aquifers. In *proceedings of Fourth National Outdoor Action Conference on Aquifer Restoration, Groundwater Monitoring and Geophysical Methods*. Dublin, Ohio: National Ground water Association, pp. 45-59 (1989).

Wallace J.W., Effects of local sediment variability on hydrocarbon volume estimation. Unpub. M.Sc. Thesis, San Diego State Univ. (1992).

Warrick A.W., Mullen G.J., and Nielsen D.R., Scaling field-measured soil hydraulic properties using similar media concept. *Water Resour. Res.*, **13**, pp. 355-362 (1977).

Weaver J.W., Charbeneau R.J., Tauxe J.D., Lien B.K., and Provost J.B., *The hydrocarbon spill screening model (HSSM)* Volume 1: User's Guide, EPA/600/R-94/039a, U.S. EPA, R.S. Kerr Environ. Res. Lab. Ada, OK, pp. 212 (1994).

White M.D., Lenhard R.J., Numerical analysis of a three phase system with fluctuating water table. In: *Proceedings of the Thirteenth Annual American Geophysical Union Hydrology* days, March 30-April 2. Colorado State University, Fort Collins, CO, pp. 219-236 (1993).

Wickramanayake G.B., Gupta N., Hinchee R.E., and Nielsen B.J., Free petroleum hydrocarbon volume estimates from monitoring well data. *J. Environ. Eng.,* **117**. pp. 686-691 (1991).

Wickramanayake G.B., Hinchee R.E., and Nielsen B.J., Evaluation of liquid and vapor monitoring devices for underground storage tank leak detection. In: *Proc.*

Petroleum Hydrocarbons and Organic Chemical in Ground Water, National Water Well Association, Dublin Ohio, **4**, pp.19-28 (1990a).

Wickramanayake G.B., Kittel J.A., Hinchee R.E., Voudrias E.,. Reichenbach N., Pollack A.J., and Bigelow T.L., *Testing of monitoring devices for JP-4 in subsurface*. US Air Force Report No. ESL-TR-89-97, ENGRG. And Services Ctr., Tyndall AFB, Fla. (1990b).

Williams D.E., and Wilder D.G., Gasoline pollution of a groundwater reservoir – A case history. *Groundwater*, **9**, pp. 50-56 (1971).

Wilson J.L., Conrad S.H., Hagan E., Mason W.R., and Peplinski W., The pore level spatial distribution and saturation of organic liquids in porous media. In: *Proceedings of the conference on Petroleum Hydrocarbons and Organic Chemicals in Ground Water: Prevention Detection and Restoration*, Dublin, Ohio: National Ground Water Well Association (1988).

Yaniga P.M., Discrimination between real and apparent accumulation of immiscible hydrocarbons on the water table: A theoretical and empirical analysis. In *proceedings of Fourth National Symposium and Expo. On Aquifer Restoration and Ground Water: Monitoring*, National Ground Water Association, Dublin, Ohio, pp. 311-315 (1984a).

Yaniga P.M., Hydrocarbon retrieval and apparent hydrocarbon thickness: Interrelations to recharging/discharging conditions. In *proceedings of NWWA/API Conference on Petroleum Hydrocarbon and Organic Chemicals in Ground Water:*

Prevention, Detection, and Restoration. Dublin, Ohio: National Ground water Association, pp. 299-329 (1984b).

Yaron B, Dror I., Graber E., Jarsjo J., Fine P., and Gerstl Z., *Behaviour of volatile organic liquid mixtures in the soil environment. Soil and Aquifer Pollution Non-Aqueous Phase Liquids Contamination and Reclamation*, Springer Publisher, pp. 37-58 (1998).

Zhu J.L., Parker J.C., Lundy D.A., Zimmerman et L.M., Estimation of soil properties and free product volume from bail-down tests. In *Proc. Petroleum Hydrocarbons and Organic Chemical in Ground Water*, National Water Well Association, Dublin Ohio, pp. 99-111 (1993).

VITA

MUHAMMAD SALEEM

PERSONAL DATA

Nationality : Pakistani
Status : Married (2 Sons)
Date of Birth : 14/12/1964

BUSINESS ADDRESS

King Fahd University of Petroleum & Minerals
P.O. Box # 398
Dhahran – 31261, Saudi Arabia
Tel: + 966-3-8601752
e-mail: i_am_saleem@yahoo.com

ACADEMIC ACHIEVEMENTS

B.E. Civil Engineering, NED University, Pakistan (1988)
M.Sc. Nuclear Engineering, Quaid-I-Azam University, Pakistan (1990)
M.Sc. Civil Engineering (Water resources & environmental engineering), KFUPM, Saudi Arabia (1997)

EMPLOYMENT HISTORY

Oct. 2001 to date **Research Engineer.**

Department of Civil Engineering, KFUPM, Dhahran, Saudi Arabia.

Feb. 98 to Oct. 2001 **Lecturer B.**

Department of Civil Engineering, KFUPM, Dhahran, Saudi Arabia.

Feb. 96 to Feb. 98 **Research Assistant**
Department of Civil Engineering, KFUPM, Dhahran, Saudi Arabia.

Oct. 88 to date **Senior Engineer**
Pakistan Atomic Energy Commission (PAEC), Pakistan.

Jan. 88 to Oct. 88 **Senior Civil Engineer**
ABM ENGINEERS Engineering Consultants Karachi, Pakistan.